5-2018

Biofluid Analysis with Novel Targeted Mass Spectrometry Methods

Karen E. Yannell
Purdue University

BIOFLUID ANALYSIS WITH NOVEL TARGETED MASS SPECTROMETRY METHODS

by

Karen E. Yannell

A Dissertation

Submitted to the Faculty of Purdue University

In Partial Fulfillment of the Requirements for the degree of

Doctor of Philosophy

Department of Chemistry

West Lafayette, Indiana

May 2018

THE PURDUE UNIVERSITY GRADUATE SCHOOL
STATEMENT OF COMMITTEE APPROVAL

Dr. R. Graham Cooks, Chair
Department of Chemistry
Dr. Peter T. Kissinger
Department of Chemistry
Dr. Matthew Tantama
Department of Chemistry
Dr. Julia Laskin
Department of Chemistry

Approved by:

Dr. Christine Ann Hrycyna
Head of the Graduate Program

To my mom, she always picks up.

ACKNOWLEDGMENTS

I am very grateful for the support from numerous people who shaped me into the individual and scientist that I am today. My successes have been made possible by all of them.

I would like to thank my advisor, Professor R. Graham Cooks. His guidance and support made this dissertation possible. He created a dynamic laboratory and learning environment that was fun, supportive, and challenging; all of which expanded my outlook, understanding, and capabilities with a triple quadrupole mass spectrometer. Moreover, in his laboratory I met many wonderful people and scientists whom taught me the value of collaboration and expanded my scientific network.

I would also like to thank my undergraduate advisor, Professor Lauren Benz. She was the first person to introduce me to academic research. She let me explore her lab and test new methods before I knew how to properly make dilutions. Working in her laboratory was one of the most influential experiences of my life.

To my committee members, Professor Peter Kissinger, Professor Matthew Tantama, and Professor Julia Laskin who provided me with their time and guidance at various stages throughout my graduate work. In particular, many of my projects seemed to evolve from conversations with Pete and Candice Kissinger. They both were constant supporters of applying paper spray to authentic samples and they have served as excellent ambassadors for the clinical chemistry field.

I am especially thankful for Brandy McMasters and all my fellow Astonites who were excellent sources of information and sounding boards for ideas as I grew to find my own scientific voice. You all made my graduate experience wonderful. In particular, many of my accomplishments were possible because of Dr. Valentia Pirro, Dr. Christina Ferreira, Dr. Alan Jarmusch, and Clint Alfaro.

My parents embraced my scientific curiosity, nurtured my growth in the sciences, and instilled in me a work ethic that helped me get to where I am today. To all my siblings who counseled me through all the stages of my life and career, I could not have done it without your guidance, wisdom, and honesty.

To my friends: Kara Martin, Heather Osswald, Issac Marks, Kinsey and Ryan Bain, Chis Pulliam, and Terry Villareal. Our game nights and culinary adventures provided a much

appreciated balance to graduate school. To my fur babies, whose semi-unconditional love made every day much softer and more joyful.

Finally, I would like to acknowledge the support I have always received from my husband, Michael. He has been my loudest cheerleader since the day I realized I wanted to be a chemist. He was there each day to hear about every failed experiment and celebrate each data point and milestone. He was sitting next to me when I opened my graduate school acceptance letter and I am proud to say that we will be sitting next to each other at our commencement ceremony from Purdue University. I wouldn't want to travel down this path with anyone else. I would marry him a fourth time, but I think we both agree that would be a bit much!

TABLE OF CONTENTS

LIST OF TABLES

LIST OF FIGURES

LIST OF ABBREVIATIONS

PS	Paper spray
MS	Mass spectrometry
ESI	Electrospray ionization
IMS	Ion mobility spectrometry
SPE	Solid phase extraction
LC	Liquid chromatography
OF	Oral fluid
DBS	Dried blood spots
W1	Whatman 1
W31	Whatman 31
VSC	Velox sample cartridge
PK	Pharmacokinetic
TAT	Turnaround time
Cal	Calibrator
QC	Quality control
QQQ	Triple quadrupole
MS/MS	Tandem mass spectrometry
MRM	Multiple reaction monitoring
CE	Collision energy
TL	Tube lens
Quant/Qual	Qualifier quantifier ratio
LOD	Limit of Detection
LOQ	Limit of Quantitation
RSD	Relative standard deviation
TIC	Total ion current
AUC	Area under the curve
Imb	Imatinib
N-DM-Imb	N-desmethyl-imatinib
Prec	Precursor
NL	Neutral Loss
HRMS	High resolution mass spectrometry
QTOF	Quadrupole time of flight
DI	Direct infusion
FI	Flow injection
AJS	Agilent jet stream
PLSDA	Partial least squares discriminant analysis
LinSVM	Linear support vector machine
CAD	Coronary artery disease

PAD	Peripheral artery disease
ROC	Receiver operating characteristic
MPP	Mass Profiler Professional
FC	Fold change
RT	Retention time
PC	Phosphatidylcholine
SM	Sphingomyelin
TAG	Triacylglyceride
PD	Parkinson’s disease
HC	Health control
CSF	Cerebrospinal fluid

ABSTRACT

Author: Yannell, Karen, E. PhD
Institution: Purdue University
Degree Received: May 2018
Title: Biofluid Analysis with Novel Targeted Mass Spectrometry Methods
Committee Chair: R. Graham Cooks

Mass spectrometry (MS) provides a high level of sensitivity and specificity to accurately and precisely identify and quantify analytes in a complex matrix. In clinical samples, this instrument is often used to quantify drugs or discover new biomarkers. However, existing workflows routinely use chromatography to separate the components of a sample. These methods lack speed and are expensive, neither of which are ideal characteristics for point of care or high throughput analysis.

Paper spray (PS) is an ambient ionization technique that combines the sample preparation and ionization steps, to directly spray a complex sample into a MS. The MS provides the specificity and sensitivity to quantify drugs at low ng/mL levels of detection. Described here are three PS-MS methods demonstrating PS for clinical research. First, a drug is measured for a pharmacokinetic study and demonstrates PS-MS utility for personalized medicine. Then, PS is used to measure whole blood samples collected in a low resource region, demonstrating its compatibility with in-field clinical trial samples. And finally, PS is multiplexed to measure 30 drugs in oral fluid, proving that this methodology can be used for large panels of analytes as traditionally done in the clinical environment.

Endogenous metabolites in biofluids can also be measured by MS without prior separation. Multiple reaction monitoring (MRM)- profiling rapidly measures a sample to create a metabolite profile for classifying diseased and healthy samples. This methodology targets biological functional groups in a pooled sample using a library of over 200 precursor (Prec) and neutral loss (NL) scans. All MS signals discovered in these experiments are transformed into ion transitions and are measured in a MRM method. In MRM mode, each transition can be measured on the millisecond time scale allowing for rapid screening of large sample sets. Using univariate and multivariate statistics the sample set can be classified with high accuracy. With diseased sample sets metabolite profiles can be found that classify samples based on signals related to the disease.

Since a large variety of functional groups are considered and all signal discovered is collected by MRM, this is considered an unsupervised biomarker discovery methodology.

MRM-profiling is described here and demonstrated with over 900 human plasma coronary artery disease samples. First, the metabolite signal was discovered with Prec and NL scans. Then, with a MRM method, the samples were screened in under five days. A metabolite profile was established from this data for the disease. The signals that comprised the MRM-profile were identified and found to be associated with coronary artery disease metabolism. This validates that the methodology generates a useful metabolite profile but is much faster than traditional methodologies. The same methodology is also performed with Parkinson's disease cerebrospinal fluid samples and discovered signal relevant to the diseased population.

PART 1: ADVANCES IN PAPER SPRAY IONIZATION: AUTOMATION, APPLICATIONS, AND METHODS

CHAPTER 1. PAPER SPRAY IONIZATION INTRODUCTION

1.1 Background

Paper spray (PS) is an ambient ionization technique that was first published in 2010.[1] It combines sample preparation and ionization steps to rapidly introduce complex samples into a mass spectrometer (MS).[1-4] The process utilizes no separation, instead it dries a complex matrix on a porous substrate (typically paper) which is cut to a sharp point. The analyte of interest is extracted from the dried spot with a solvent and when voltage is applied to the back of the paper the solvent is sprayed in an ESI like mechanism (Figure 1.1). The type of MS used with PS varies, however it provides enough sensitivity and specificity to quantify analytes with good accuracy and precision.[1]

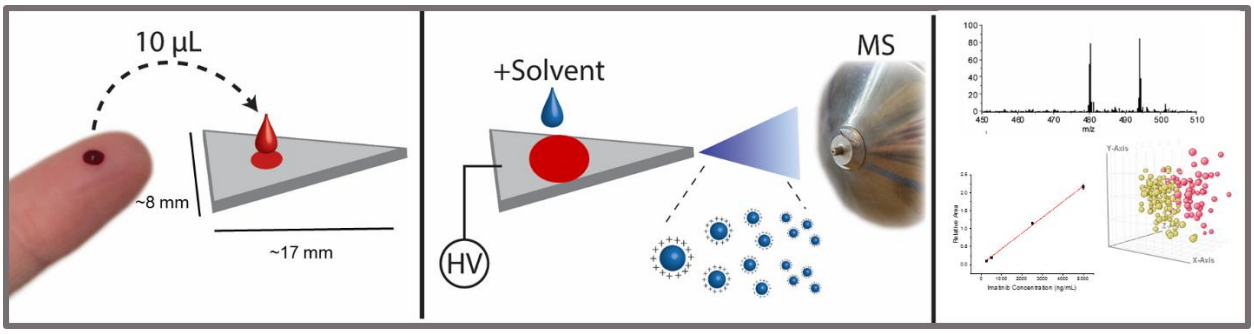

Figure 1.1 Paper spray ionization uses a small volume of sample (such as blood) that is pipetted onto a paper triangle (Panel 1). The triangle is placed in front of the MS inlet where a high voltage (3.5 – 5 kV) and solvent are applied to create an electrospray at the tip (Panel 2). PS can be used for full scan or targeted data acquisition for both quantitative and multivariate analysis (Panel 3).

Since its inception, a number of articles describing the fundamentals have been published.[2, 5-6] Early applications focused on drugs in whole blood.[1, 7] Although this is still a popular application, a wide range of fields utilize PS-MS for quantitative and qualitative analysis. These include clinical, forensics, toxicology, therapeutic drug monitoring, food and beverage analysis, explosives, and organic reactions.[3-4, 8-13] These are summarized further in a 2016 PS review.[14]

Advances in PS technology focus on two main points. (1) Automation, which is achieved with automatic PS sources like the Velox 360 (Prosolia Inc, Indianapolis, IN), allow for routine, non-expert use. (2) Combining PS with new instruments (IMS), novel devices (SPE or microfluidics), or novel substrates for improved sensitivity and specificity.[15-21] Point 2 is important for pushing the boundaries of PS, while automation makes PS more relevant to the fields described above, which entail routine analysis performed by non-experts.

Since 2010, the number of publications has increased exponentially [Figure 1.2]. However, the type of journal has not changed much to include non-chemical or engineering journals. This suggests it is not being applied in the intended fields. Specifically, when comparing the category of journals from 2010-2013 and 2014-2017, PS has only emerged in one new field while it decreased in another. One reason for this could be a lack of practical understanding of developing, optimizing, and validating a method. PS combines several steps of traditional LC-MS workflows into one step. This confounds method development, which aims to achieve low limits of detection and reproducible signal. Previous articles discuss the variables of PS but they lack a practical methodology for developing a PS method for easy understanding and straight forward implementation.[1, 15] The sections below describe the PS setup and optimization strategies used for methods in the following chapters. The variables that are traditionally evaluated in PS method development are described, and suggested optimization experiments are presented to serve as a practical guide for getting started.

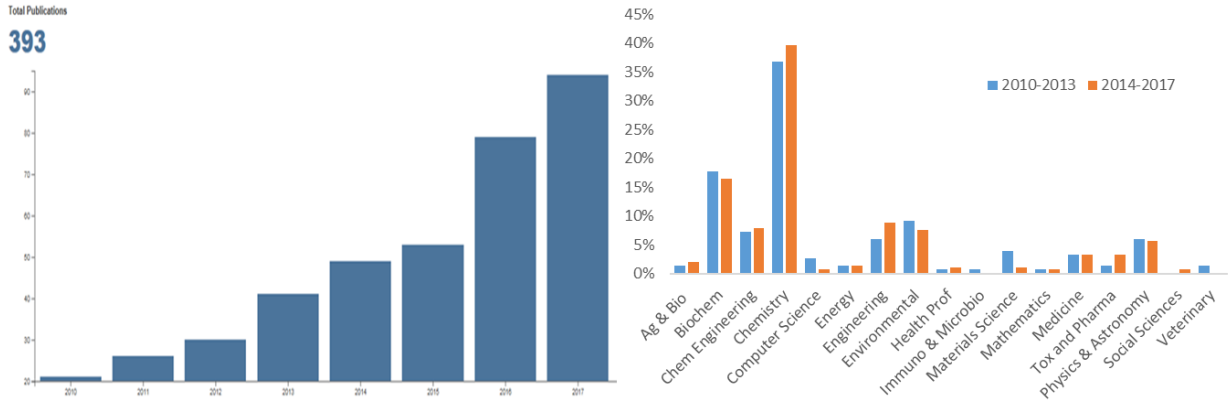

Figure 1.2 Number of PS publications by year from 2010 to 2017 (total of 393, left). Percent of PS journals published in various journal categories from 2010-2013 and 2014-2017. Data was gathered from a Scopus 'paper spray ionization' search on February 24, 2018.

1.2 PS Setup

1.2.1 Materials

Whatman 1 filter paper (W1) is purchased from Fisher Scientific (Waltham, MA) and Whatman 31 ET chromatography paper (W31) from GE Healthcare (Little Chalfont, UK). A Velox 360 paper spray ionization source (Prosolia Inc, Indianapolis, IN) and Velox sample cartridges (VSC) were used for the automated PS analysis.

A TSQ Quantum Access Max (Thermo Fisher Scientific, Waltham, MA) was used for all PS-MS experiments. Toothless copper clips were purchased from Muller Electric (Akron, OH). A high voltage cable and source override adapter were made custom for the TSQ by Purdue University's Amy Instrument Facility (JAFCI).

1.2.2 Manual PS

Manual PS was setup as shown in Figure 1.3 using the materials listed above. The Velox was used as suggested by Prosolia, Inc. To adapt the ion source to the TSQ, an extended ion transfer tube, provided by Prosolia, Inc, was used.

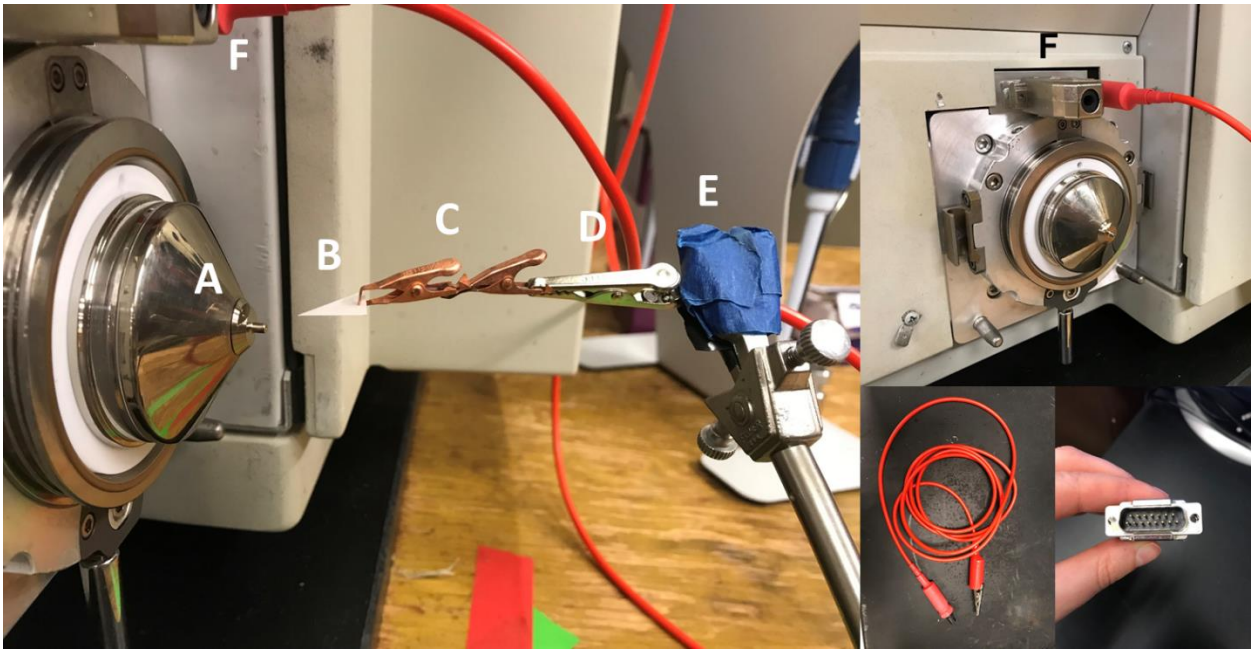

Figure 1.3 PS setup (left) used a clamp (E) to hold the high voltage cable (D) which in turn held the toothless copper clip(s). The PS substrate was secured by the toothless copper clip and was set in front of the MS inlet (A). The high voltage cable (F, bottom middle) was attached directly to the MS (F, top right) along with a source override adapter (F, bottom right).

Figure 1.4 shows how the PS substrate should be oriented for reproducible results. The PS substrate should be set directly in front of and perpendicular to the MS [Figure 1.4, A and B]. The substrate should be flat and not at an angle [Figure 1.4, D and E] because this causes solvent to pool at the tip or base of the substrate. Unless noted otherwise, solvent is applied slowly to the back of the paper [Figure 1.4 A]. The substrate should only receive enough solvent to wet the paper fully. It should not be overloaded with solvent such that a droplet forms on the paper [Figure 1.4 C].

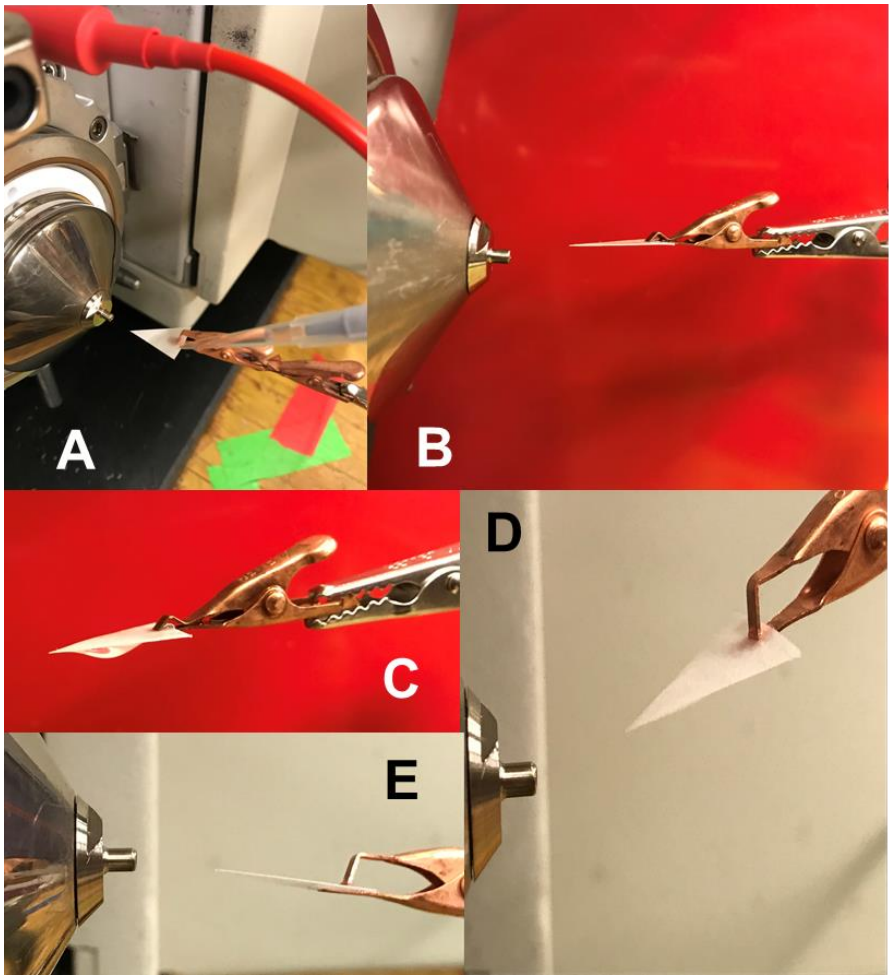

Figure 1.4 (A) The PS substrate correctly oriented in front of the MS inlet with solvent applied to the back of the substrate. (B) Another view of the substrate correctly oriented with solvent applied. (C) The substrate incorrectly overloaded with solvent. (D and E) The substrate incorrectly oriented at an angle to the MS.

1.3 Development and Optimization

This section discusses method development with a triple quadrupole (QQQ) MS and assumes ion transitions are known and stable for a multiple reaction monitoring (MRM) method. The experiments can be done with other MS filters or scans but using a MRM method offers a convenient assessment of improvements with each optimized variable.

Analysis of a complex sample by PS typically dries the sample to a porous substrate, uses a solvent to selectively dissolve the analyte of interest, leaving unwanted analytes and matrix on the substrate [Figure 1.1]. The solvent will transport that analyte to the tip of the paper. Next, the solvent must also spray, *i.e.* create a Taylor cone to generate microdroplets which evaporate to

ions that are transferred into the MS inlet.[5-6, 15] Analysis of wet matrices (*i.e.* not dried spots) should not be considered because sufficient matrix clean up does not occur and an excessive amount of material is deposited into the MS. This damages the MS and reproducible analysis cannot be achieved. Drying the sample is needed to achieve sample clean up with a complex matrix.

PS requires a porous substrate to be cut a sharp point. A previous study suggested a 90 degree angle gave the greatest signal intensity. However, sharper angles improve the electric field strength, which improves the spray.[4] Manually cut paper substrates were cut to a 60 degree angle in these experiments. Cellulose based filter paper is commonly employed but other commercially available substrates have been tested, *e.g.* from simple printer paper to various microfiber filters.[2, 15, 22] When considering a substrate, the chemistry of the surface is assessed since the analyte of interest and matrix bind to the substrate when dried.[2-3] Cellulose based paper may not be ideal for polar analytes that will adhere strongly to the cellulose hydroxyl groups. Other porous substrates may be substituted but must be evaluated for other issues (*e.g.*. reproducibility, chemical noise, retention of matrix). For example, the chemical background for commercially available substrates varies and should be evaluated for analyte suppression or interference [see Chp 3]. It is also possible to functionalize porous substrates with unique chemistry for a specific analyte.[15, 21]

One crucial aspect is that the substrate must hold the desired sample volume without having the sample spread to the tip or base. If the sample touches the tip, then the fibers necessary for ionization are damaged.[6] If the sample is touching the base, solvent cannot be easily applied. However, it is also important for sample to spread the entire width of the paper so that solvent is forced through the spot to collect the analyte [Figure 1.5]. W1 cannot hold a large volume of sample but it is easily obtained. An 8 x 17 mm W1 triangle can only hold ~1-2 µL of sample before the sample front meets the tip. W31 can hold more sample (~10-15 µL) and therefore might be preferred for those testing complex aqueous based matrices. The paper also should not be too large that it bends downward with solvent addition or has excess surface area. More surface area requires more solvent which in turn dilutes the analyte. However, the substrate should be large enough that it can be handled easily and reproducibly cut.

Cutting the substrate has been done manually with scissors or automatically with a die or laser. If using a laser, burnt edges should be kept to a minimum and evaluated for chemical interferences. If cutting with a die, a sharp tip must be created. Manually cutting is labor intensive and is not reproducible. However, it is a quick and cheap way to evaluate PS. Reproducibility,

with manual cutting, can be improved by using a template, *i.e.*. create a rectangular shape and cut it to a tip [Figure 1.5]. Note, pencil, not pen, can be used to mark substrates.

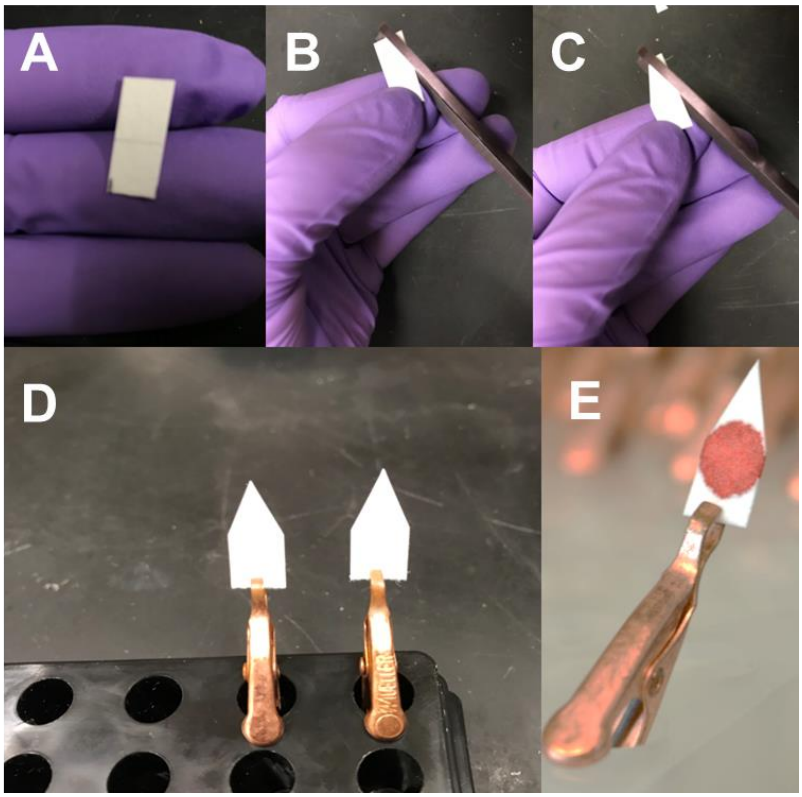

Figure 1.5 Using an 8 x 20 mm rectangle of W31 is a simple way to cut reproducible PS substrates manually (A-D). A PS substrate that is approximately 8 x 17 mm can hold 10-15 µL of sample. This spot should cover the entire width of the substrate while not interfering with the PS tip (E).

Solvent optimization is one of the most significant variables for achieving a sensitive and reproducible method. It should be done carefully and systematically for best results. Recommendations from published PS studies may work well and require no additional optimization. When a new class of analyte is being tested solvent optimization should achieve better reproducibility or sensitivity. This variable often has the greatest impact on improving method results.

Solvent and voltage are linked variables and should be evaluated in tandem.[5] A common question at this juncture is what distance to set the PS tip from the MS inlet. Distance is a separate variable and may be evaluated after solvent and voltage. For solvent and voltage experiments set it to a reasonable distance ~5-10 mm.[2] The orientation, or positioning, of the paper is important here to achieve reproducible measurements. The paper should be flat, and the tip and base centered to the MS inlet. It is preferred to have the tip offset and raised slightly above the MS inlet. There is some tolerance to this orientation but the ideal positions are shown in Figure 1.4 B.

Similar to LC-MS methods, a solvent system typically contains an organic solvent (majority), water, and modifier. To make clear conclusions about an optimal PS system, the variables must be separated further and evaluated by comparing the signal of a sample to the signal of a blank. This is due to the fact that background noise varies greatly with different solvent conditions (and PS substrates). The solvent systems in subsequent chapters were optimized as outlined in Figure 1.6.

Although PS has been achieved with high water percentages, it is believed that it is best to keep this between 5-20 %. Some water is needed to avoid rapid evaporation from the PS surface. Too much water requires higher voltages to spray and large wet droplets are formed.[5-6]

For each solvent system, the optimal voltage and volume for PS was determined in full scan mode. When optimizing the spray solvent and voltage, the spray and ionization capability should not be confounded by factors associated with a dried spot. Therefore, solvent systems doped with analyte should be used as samples here. For PS, the substrate needs to be saturated completely but not over saturated such that solvent pools on the paper (Figure 1.4 C) and the volume should achieve 30-60 seconds of stable spray. When using an automated PS system (*i.e.* Velox) this experiment was done in a manual fashion. A Velox Sample Cartridge (VSC) was set in front of the MS inlet using a ring stand and the voltage was applied from the voltage cable. This optimized the voltage and solvent volume needed for a cartridge quickly.

The next step was to determine the best application of solvent and determine if a priming solvent was needed. A sample and blank, both with IS, in complex matrix were used for these experiments. The application of solvent can be broken into three categories. (1) Solvent is applied to the back of the paper and it moves through the sample, captures the analyte, and sprays it. (2) If the solvent did not move through the sample then it was 'primed' by spotting ~10 µL of solvent directly on the dried spot then apply the remaining solvent to the back of the paper. The prime

solvent breaks the physical barrier of the dried spot more efficiently and enables the solvent applied to the back to move through the dried spot. If the required sensitivity was not achieved here it could be from the analyte adhering strongly to the matrix or PS substrate. (3) In this case, the prime solvent was altered (*i.e.* pure organic) to try to dissolve the analyte. The solvent optimized was used to transport the analyte to the tip and create spray. The optimal spot solvent can be experimentally determined but *a priori* knowledge about the solubility of the analyte or special conditions (*e.g.* cell lysis) is helpful here.

After optimization the method should spot and dry a sample on paper, dissolve the analyte into a solvent, transport the analyte to the paper tip, and create spray with an optimized voltage. If desired sensitivity were reached then no additional optimization is needed. If no reproducible or sensitive parameters were reached, the polarity and precursor ion formation (especially in the complex matrix) were reexamined. In some cases, the analyte may not be removed from the paper. The analyte in water methanol was tested to see if matrix was the issue or if the analyte adheres too strongly to the paper. If it cannot be removed from the paper when the matrix is water (or methanol) then consider another PS substrate. If it is a matrix issue then (1) ensure other adducts are not being formed with the complex matrix and/or try forcing the desired adduct, (2) test additional spot solvents to break it from the matrix, or (3) test sample clean up steps prior to spotting the analyte or online SPE.[16] Additional optimization steps are briefly described in Figure 1.6.

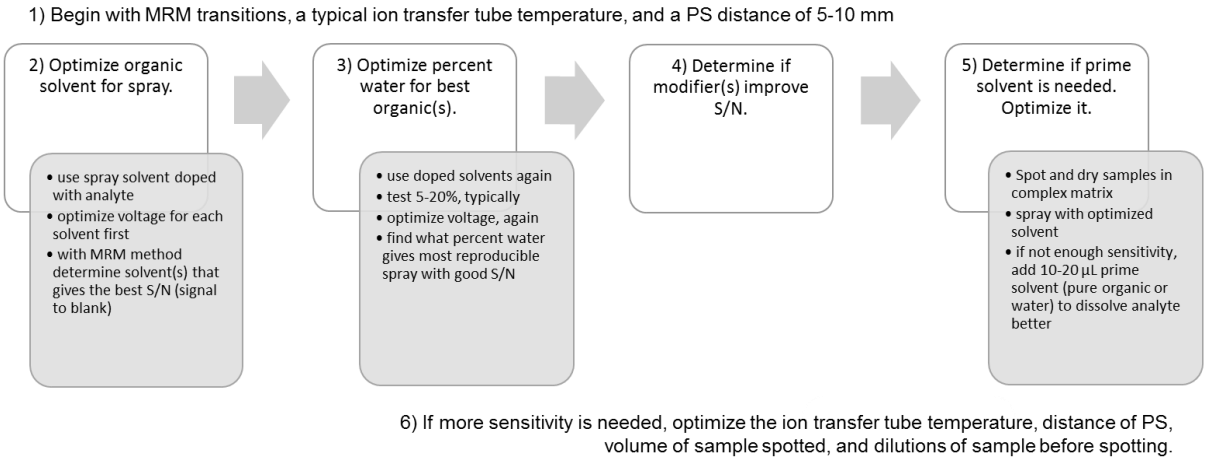

Figure 1.6 Optimization workflow used for developing methods in subsequent chapters. The development focuses on solvent conditions and solvent application for W1 or W31 PS substrates.

1.4 Validation Experiments

Validation experiments are often done prior to implementing a LC-MS assays into a lab. To the author's knowledge, these have not been done and/or published fully for a PS method yet. This is likely due to the economic and sample limitations of an academic laboratory. However, many publications have explored a few of the experiments traditionally done for validating a method.[10-11, 22] These are discussed in more detail below. As PS continues to be used and developed, experiments for validation procedures will need to be established. This is the first approach in discussing what should be included in PS validation and how parameters should be tested.

For reference the FDA Guidance document is available for LC-MS assays.[23] Because of many similarities between PS and LC-MS methods, experiments can be adopted as needed from this or similar guides. The FDA validation for LC-MS must have experiments demonstrating specificity, linearity, accuracy, precision, range, limit of quantitation (LOQ), and limit of detection (LOD).

Tandem mass spectrometry (MS/MS) and high resolution mass spectrometry (HRMS) experiments are specific. However, PS does not have a retention time (RT) from chromatography so analytes with the same molecular weight may interfere with the analysis. PS can ensure specificity by (1) picking transitions that do not have common losses (*e.g.* water) and (2) selecting a qualifier fragment to produce a qualifier and quantifier ratio (Qual/Quant) between 20% and

80%. The Qual/Quant should be stable in all calibrator (Cal) and quality control (QC) samples. In unknown samples that are positive for the analyte, this ratio should also be stable. If it is not, then the signal is not guaranteed to be the analyte and further analysis needs to be done on the sample. Qual/Quant ratios are demonstrated in subsequent chapters and are easily implemented with PS methods to gain additional specificity.

Linearity and range is often described with PS by noting the R^2 of the linear fit of a line to the calibration points. R^2s with PS are often >0.99 and must always be >0.95. This is acceptable manner of describing linearity with PS especially when the Cal curve is within the expected range of unknowns. Additional studies could be done to find concentrations where linearity fails or to check the accuracy of a sample with a concentration greater than the high. These are an evaluation of the MS used in the assay as much as it is a test of the ionization technique.

Accuracy and precision are demonstrated with Cal and QC samples and interday experiments. In the literature, PS often has accuracy and precision tested in some manner. But QCs are not always tested and replicates of standard samples are rare. As good analytical practice indicates, Cal and QC samples should be made from separated standards or stock solutions to check for preparation and standard solution errors. The QC calculated concentration to theoretical concentration should have no more than 20% error. For better statistical evaluation, a minimum of six replicates should be done if the resources are available. Relative standard deviation (RSD) of these replicates demonstrates precision. For quantitative methods, PS should match LC-MS standards here; RSD must be <15%, except Cal 1 may be <20%.

The LOD and LOQ are often reported with PS using the IUPAC definition: 3*(standard deviation of blank)/slope of the calibration line for LOD and 10*(standard deviation of blank)/slope of the calibration line for LOQ.[8] This concept is further described in a 1983 fluorescence paper which is often cited with the LOD and LOQ calculations for PS-MS.[24] This definition is a theoretical LOD and LOQ for PS-MS and assumes that the signal for a blank is zero and/or not stable. However, blanks with PS have varying chemical noise from different PS substrates and solvents. Additionally, with signal normalization using IS, the background (or blank) relative signal is very stable, therefore, the standard deviation of the blank is very small. An experimental way of determining the LOD and LOQ was done for all the following methods; dilutions of the analyte were analyzed and compared the blank matrix (noise).

Not listed in the FDA document but often required in assay validations are recovery and matrix effects studies. Both are not perfect aspects of any PS method. However, ion suppression, enhancement, or analyte loss is corrected with the use of a matching stable isotopically labeled IS or structural analog as an IS. Nevertheless, these validation experiments should be done for proper reporting and description of the assay performance. For matrix effects, comparison of the absolute signal from a sample prepared in water verses complex matrix is all that is needed (perform replicates to report error). For recovery, a sample in the matrix that is processed and acquired as the method stipulates should be compared to a blank sample processed in the same way but not sprayed with solution that contains the sample absolute quantity of analyte in the spray. This will compare the amount of analyte extracted and sprayed verses just sprayed. It also considers all the noise from the paper and matrix. Comparing PS to another ionization techniques (*e.g.* nESI) is not ideal as the ionization efficiency is different. Examples of these are in the following chapters.

1.5 Conclusions

PS is a fast methodology for analyzing a complex sample in a short period of time. As it increases in popularity standards for method development and validation should be established. These method development strategies were used for developing the methods in the following chapters. Many of the validation experiments are demonstrated as well.

Subsequent chapters describe methods that push the limits of PS and direct them further into hospital, clinical, and toxicology environments. First, PS in the clinical space is demonstrated with a proof of concept workflow designed to collect and analyze a small volume of blood for therapeutic drug monitoring. The workflow introduces PS coupled to automatic blood sampling device for better quality data than traditional blood sampling. In chapter three, in-field sample collection is performed and alternative dried blood spot devices are compared for compatibility with PS. Here an automatic PS source is demonstrated and improves analytical performance for PS over manual PS. Finally, multiplexing, which is commonly done with liquid chromatography (LC), is maximized in a PS method measuring 22 opioids, benzodiazepines, and illicit drugs in oral fluid (OF).

CHAPTER 2. AUTOMATIC BLOOD SAMPLE COLLECTION AND RAPID ANALYSIS BY PS-MS/MS: A PROOF OF CONCEPT WORKFLOW FOR IMPROVED DRUG MONITORING

2.1 Abstract

Optimizing drug dose in personalized medicine (where N=1) requires more reliance on temporal data in a variety of critical care situations. One solution, phlebotics (robotics and phlebotomy) coupled with paper spray mass spectrometry (PS-MS), enables drug monitoring in a few microliters of blood and in less than one minute per sample. This automated blood collection device combined with PS rapid analysis methodology facilitates the acquisition of quality data with reduced labor cost, more patient comfort, improved safety, and less wasted blood. A proof of concept pilot study is performed here using a healthy male subject (n=1) dosed with acetaminophen (Tylenol, N-acetyl-p-aminophenol). The subject's whole blood is collected automatically, processed, and acetaminophen was measured using PS-MS. In a hospital scenario, PS allows for rapid quantitative results aiding physician's diagnosis and prescribed therapies. The analytical methodology and figures of merit are given and a pharmacokinetic curve (PK) for acetaminophen is shown.

2.2 Introduction

There is an increasing demand to closely follow a patient's therapeutic response for improved healthcare and patient outcomes. [25-26] Clinical drug trials require more data for pharmacokinetic studies. Physicians rarely monitor drug concentration in critical patients, when the drug has a narrow therapeutic range, or when the metabolism of the drug is highly variable. Pediatric intensivists could benefit from quantitative guidance in dosing newborns. [27-29] This form of personalized medicine requires more frequent blood draws which, given current protocols, are not feasible. The blood waste and cost associated with traditional phlebotomy are challenges and current bioanalytical methods and testing procedures are, likewise, costly and slow.

Conventional blood draws and methods for analyzing the sample require vials of blood to be taken from the patient for each time point or test performed. Multiple needle sticks discomfort the patient and add stress to the subject which harms the patient and alters the data.[30-31] Blood

draws are imprecise in time and wasteful in volume. Furthermore, the multiple needle sticks and excess volume of blood can put the patients' health at risk (*e.g.* anemia, infection).[31-32] Lastly, each time blood is drawn manually, there are hazards to the healthcare professionals with handling of sharps and samples (*e.g.* needle sticks, blood borne pathogen exposure, etc.) and possibilities regarding the improper storage of the sample. When a blood draw for drug monitoring is deemed necessary, a large volume (milliliters) is required for the laboratory tests, mainly liquid chromatography mass spectrometry (LC-MS). This expensive testing has a poor turn round time (TAT) which is not ideal for critical care or point-of-care analysis.

Given all this, automated blood drawing with rapid analysis must replace existing protocols for personalized medicine to progress. One prototype automated blood drawing system, the Phlebot™ (Phlebotics , West Lafayette, IN) (Figure 2.1) has many proven advantages. The closed system automates the collection time and volume of a whole blood sample from a patient and properly stores it at an optimal temperature (4° C). Patient care is improved since they are stuck with a needle only once and they can sit comfortably as a small, precise volume of blood is automatically drawn and collected at specified time points. For the doctors and scientists, this leads to better data because the patient is not stressed and more control over the sampling and storage is provided. Furthermore, the Phlebot's design and automation improves hospital safety and lowers costs since healthcare professionals do not have to handle needles and blood for each time point taken. At present, the Phlebot is investigational use only (IVO) and will evolve toward clinical practice.

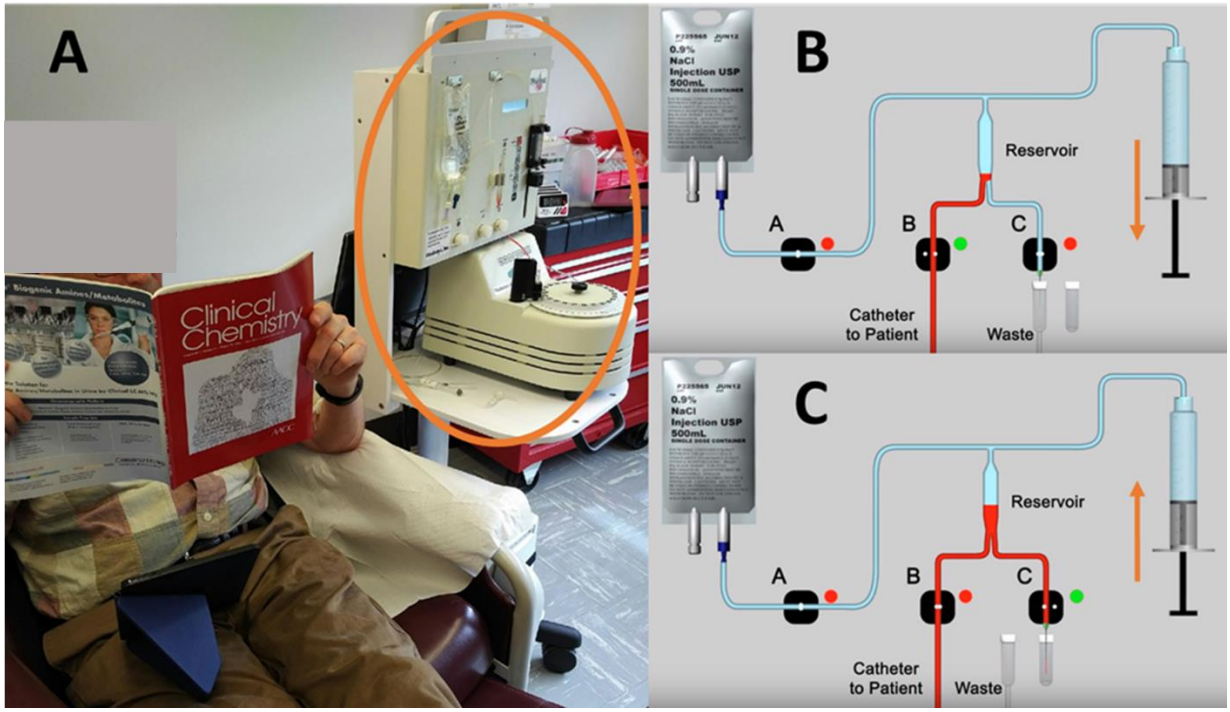

Figure 2.1 Schematic of the Phlebot. The Phlebot (A, circled) has a small footprint and painlessly draws multiple precisely timed aliquots of whole blood from an intravenous catheter and stores them at a controlled temperature (4° C). For sample collection, the blood fills the reservoir using a software controlled syringe to draw venous blood (B). A small portion of the sample goes to waste and the remaining is collected as a sample (C). Finally, blood remaining in the reservoir is returned to the patient with sterile saline.

PS tandem mass spectrometry (MS/MS) protocols are ideal to analyze samples collected by the Phlebot. The time scale of the sample analysis and volume of sample required for PS matches the Phlebot collection time and volume. When these two technologies are coupled together, there is potential for monitoring a patient in real time allowing for better, optimized dosing and ultimately improved patient outcomes. In critical care situations, these technologies can save lives by monitoring patient treatments while using only microliters of their blood. This pilot study demonstrates a new workflow for drawing, storing, and analyzing blood in a critical care setting. Using a model drug, Tylenol, a subject was dosed, blood drawn and stored by the Phlebot, and plasma measured by PS-MS/MS. The new protocol provides high quality data, improved comfort and care to the subject, reduced cost and medical hazards, and a reduction in

the sample and time required per test. While not demonstrated here, it is feasible, to draw blood from a sleeping subject.

2.3 Materials and Methods

2.3.1 Materials

All solvents were HPLC grade and were purchased from Signal Aldrich (St. Louis, MO). Analytical grade standards for acetaminophen and acetmoinophen-D_4 were purchased from Cerilliant (Round Rock, TX). Bovine plasma with sodium heparin was obtained from BioreclamationIVT (Hicksville, NY). The Phlebot was acquired from Phlebotics (West Lafayette, IN). All other PS materials are listed in Chapter 1.

2.3.2 Solution Preparation

Six acetaminophen Cals were made in bovine plasma with sodium heparin and human plasma with sodium citrate at 250, 500, 1000, 2500, 5000, and 10000 ng/mL. QCs were made at three different concentrations: 750, 3000, and 8000 ng/mL. Each sample was mixed with an IS solution (16,500 ng/mL acetaminophen-D_4 in water) at a 1:10 ratio (*i.e.* 4 µL IS and 40 µL sample) so that the final concentration of IS was 1,500 ng/mL. Six replicates of the Cal and QC solutions were analyzed with the method described below. Dilutions of Cal 1 and blank matrix samples with IS were ran in replicates of five to determine the LOD.

2.3.3 PS-MS/MS

W31 was precut with scissors to have a base of 8 mm and a height of 17 mm (Figure 1.5). Manual PS was setup as described in Chapter 1. Samples mixed with IS were pipetted onto the paper (10 µL) and allowed to dry for a minimum of 30 min at room temperature. Samples could be dried faster using a stream of nitrogen and heat. A prime solvent, 20 µL methanol, was added directly to the plasma spot and 70 µL of the spray solvent (95% methanol, 5% water, 0.1% formic acid) was added to the back of the paper. Two transitions for acetaminophen were measured and one for the IS (Table 2.1) using the instrument parameters found in Table 2.2.

For data analysis, the TIC for the quantifier transition was integrated and divided by the TIC area of the IS transition. This relative intensity was used for quantitation. The Qual/Quant was used for additional positive identification for the analyte. While not demonstrated here the IS can be dried in the blood collection vials to avoid a pipetting step. The Phlebot syringe is, in effect, a digital pipettor.

Table 2.1 Transitions used for MRM of acetaminophen. A tube lens value of 78 V was used for all analytes.

Analyte	Precursor Ion (*m/z*)	Product Ion (*m/z*)	CE (eV)
Acetaminophen Quantifier	152.1	110.2	16
Acetaminophen Qualifier	152.1	93.2	23
Acetaminophen- D_4	156.1	114.2	16

Table 2.2 TSQ parameters for data acquisition.

MS polarity	positive
Voltage (kV)	3.5
Acquisition time (s)	42
Scan time (ms)	250
Collision pressure (mTorr)	1.5
Ion transfer tube temperature (C)	300

2.3.4 Additional Studies

To study the matrix effects, the IS (16,500 ng/mL acetaminophen-D_4) was spiked 1:10 into pooled bovine plasma and water (n=5) and measure as described in the section above. An interday analysis of the calibration curve was performed by preparing and analyzing the Cal and QC samples on three separate days (n=3 on each day).

2.3.5 Phlebot Sample Collection

A healthy male subject took a single 500 mg dose orally of acetaminophen (Tylenol, Johnson and Johnson, New Brunswick, NJ). For 2.5 hours, a 250 µL whole blood sample was drawn every 5 min using a prototype Phlebot and dispensed into vials with sodium heparin and stored at 4 C. The blood sample was centrifuged and the plasma recovered. At this point, the plasma samples were randomized, blinded, and given to the analyst. This workflow can be accelerated for in-hospital analysis.

The plasma was mixed with IS (40 µL plasma and 4 µL IS) and prepared in the manner described above. A calibration curve using the subject's blank plasma (in sodium citrate) was used to quantify the samples. To make sure this anticoagulant gave the same results as the sodium heparin, a calibration curve and QC samples were analyzed with both matrices (n=4) and compared.

2.4 Results and Discussion

2.4.1 PS-MS/MS Figures of Merit

Based on signal to noise analysis of blank samples and Cal 1 dilutions (n=5) the LOD of acetaminophen is 50 ng/mL. This is higher than most analytes measured by PS due to the small mass to charge ratio and the noise in this region on the instrument used. Nonetheless, this LOD meets the needs of the assay and is well below the therapeutic range of the analyte.[33] For the Cal curve, the average relative intensity (n=6) under the curve was plotted against the concentration of the Cal solutions (Figure 2.2).

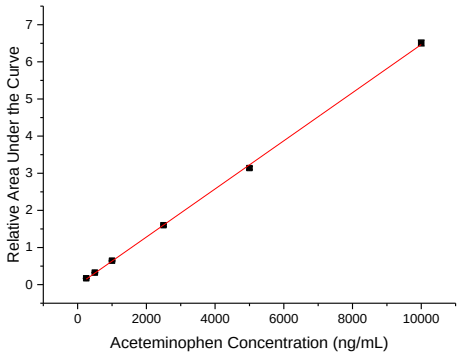

Figure 2.2 Calibration curve of acetaminophen. Line is not weighted, y = 0.00065x - 0.01474 and R^2 = 0.999. The error bars are one standard deviation of six replicates.

The RSD of the six replicates was <10% and often < 5%, indicating that the method is precise. To determine accuracy, the actual concentration of three QC samples was calculated using the line equation and found to have less than 5% error (Table 2.3). The Qual/Quant is an additional marker for positive identification of the analyte. Here, the Qual/Quant ratio is 26% for Cal 3 and all other Cal and QCs fall within 20% of this value demonstrating stable fragmentation above the cutoff value (Cal1).

Table 2.3 Acetaminophen Cal and QC sample concentrations (ng/mL) and the averaged performance of six replicates. The actual concentration of the QCs was calculated by the calibration curve in Figure 2.2.

Sample	Theoretical Conc. (ng/mL)	RSD (%)	Avg Qual/Quant (%)	Avg Actual Conc. (ng/mL)	QC Error (%)
Cal1	250	3%	29%	-	-
Cal2	500	2%	27%	-	-
Cal3	1000	2%	26%	-	-
Cal4	2500	2%	25%	-	-
Cal5	5000	1%	25%	-	-
Cal6	10000	1%	25%	-	-
QC1	750	3%	27%	773	3%
QC2	3000	9%	24%	3156	5%
QC3	8000	1%	25%	8282	4%

2.4.2 Matrix Effects, Recovery, and Interday Study of Paper Spray Mass Spectrometry

The absolute area under the curve for the five water and plasma IS replicates were averaged. The plasma sample had only 4% of the intensity of the water sample- 2.5 million counts for plasma sample and 56 million counts for water sample. This decrease in signal is due to both suppression and analyte recovery from the biological matrix. All suppression and recovery issues are corrected (normalized) by using an IS, demonstrated by the reproducibility and accuracy of the method (above results).

For the interday analysis, each curve produced the same slope and R^2 suggesting good day-to-day reproducibility. Additionally, the replicates on each day had <13% RSD and the QCs had <10% error. The results are summarized in Table 2.4.

Table 2.4 Summary of the interday calibration curves and QCs (n=3).

Day	R^2	Line Slope	RSD Range	Percent Error Range
1	0.999	0.0006	1-6%	1-3%
2	0.999	0.0006	1-13%	1-10%
3	0.999	0.0006	1-6%	1-2%

2.4.3 Pharmacokinetic Samples

The calibration curves made using different anticoagulants and blood sources gave the same slope, R^2, reproducibility, and accuracy (Table 2.5), suggesting either anticoagulant can be used in the study. For the analysis of the unknown samples, the subject's blank plasma in sodium citrate was used to calculate the acetaminophen concentration.

Table 2.5 Acetaminophen's summary of analytical performance when using two different anticoagulants and plasma sources.

Anticoagulant	Plasma Source	R^2	Line Slope	Qual/Quant Range	RSD Range	QC Error Range
Sodium Heparin	Pooled bovine	0.999	0.00057	24-34%	1-5%	4-11%
Sodium Citrate	Human Subject	0.999	0.00061	25-30%	1-9%	1-5%

Each positive sample collected from the subject had a stable Qual/Quant ratio just like the calibration curve (Table 2.6), which confirmed that the signal was solely from acetaminophen. The acetaminophen concentration for each time point is listed in Table 2.6 and plotted in Figure 2.3. The 0 - 10 min samples and the 85 min sample did not contain acetaminophen. Time points 0 – 10 min are before the acetaminophen was absorbed and the 85 min sample was not collected so water was measured in its place. The 15 min sample had trace acetaminophen (above LOD but below the cutoff). The sample concentration range was from 1246 – 8175 ng/mL which matches therapeutic ranges previously reported.[34]

Table 2.6 The calculated concentration, RSD, and Quant/Qual of acetaminophen in plasma samples using PS-MS/MS.

Time Point	RSD	Acetaminophen Concentration (ng/mL)	Qual/ Quant
0	43%	0	90%
5	18%	0	77%
10	22%	0	54%
15*	3%	232	29%
20	2%	1246	25%
25	5%	3176	25%
30	4%	4234	24%
35	3%	5585	25%
40	6%	7109	26%

Table 2.6, Continued

Time Point	RSD	Acetaminophen Concentration (ng/mL)	Qual/ Quant
45	4%	8039	25%
50	5%	8175	25%
55	4%	7838	25%
60	1%	6843	25%
65	1%	5642	24%
70	4%	5531	26%
75	8%	5763	26%
80	2%	5260	24%
85	11%	0	70%
90	2%	4551	25%
95	3%	4388	25%
100	1%	4523	25%
105	4%	4055	25%
110	2%	4270	25%
115	2%	3634	26%
120	2%	3666	25%
125	2%	3683	26%
130	1%	3666	25%
135	3%	3632	25%
140	2%	3488	25%
145	2%	3371	26%
150	3%	3348	24%

The pharmacokinetic (PK) curve was plotted showing the acetaminophen concentration in plasma over time (Figure 2.3). The PK curve (Figure 2.3) shows the absorption and excretion pattern of the drug in the subject. More data points are needed beyond 2.5 h to show the complete elimination of the drug. The time points were taken 5 minutes apart which is frequent for PK curves. This was done intentionally to demonstrate the precision of the collection and

measurement. Only one in thirty samples was missed by the Phlebot due to the subject moving his arm and temporarily pinching the capillary closed at the time of the blood draw (3% error rate).

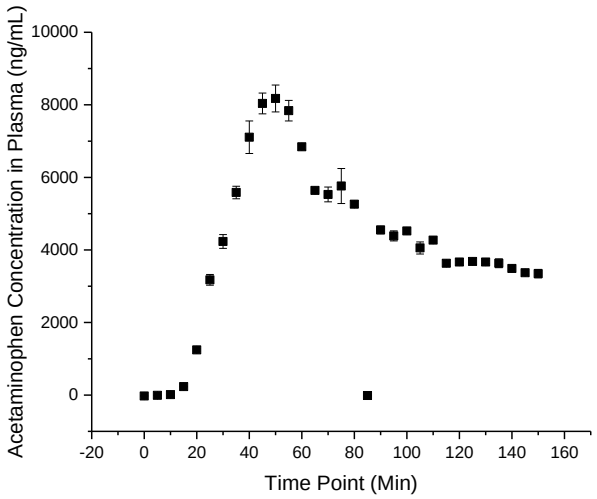

Figure 2.3 PK curve of acetaminophen in plasma when one healthy male takes a 500 mg dose of Tylenol. Error bars represent one standard deviation of three replicates of plasma samples measured by PS-MS. Time point 85 min was not collected.

This protocol automatically collects and stores a patient's blood sample. The subject felt no sensation while the sample was being drawn and sat comfortably during the collection. Because of the speed, automation, and ease of the sampling and analysis, this workflow has the potential for a single sample, or time point, to be collected, analyzed, and reported before the next time point is collected- the ultimate real time analysis protocol for drug monitoring.

2.5 Conclusion

This proof of concept study shows that the Phlebot collection device takes more time points in a better manner for the patients' health, staff safety, and hospital costs. With one needle stick, it collects many time points with less blood waste and high time point accuracy in a more comfortable manner for the patient. Coupled to an inexpensive rapid analysis technique, PS-MS, it is possible for the physician to receive blood analysis with faster turnaround time to ensure drug

dosing is effective but not toxic to the patient. In critical care or neonatal situations this saves lives. Overall, it is possible to adopt modern blood collection and analysis technologies to improve patient care and improve patient outcomes. Future studies need more subjects to submit to this or similar protocols. There is also the potential for near patient monitoring in near real time with miniaturized mass spectrometers, which have been demonstrated for many drug assays without the Phlebot component.[35-36]

CHAPTER 3. EVALUATION OF DRIED BLOOD SPOT DEVISES FOR IN-FIELD COLLECTION OF CLINICAL SAMPLES AND PS-MS/MS ANALYSIS

3.1 Abstract

PS is an ambient ionization technique capable of quantifying analytes from dried whole biofluid samples. In-field sample collection for clinical studies could benefit from the capability to use capillary blood from a finger prick to measure analytes. The collection technique is simple, requiring only a lancet, ensuring low cost and rapid collection time. This approach can be used in remote areas such as field stations in areas without lab access. In this study, three different dried blood spot (DBS) devices are used with PS and tested for rapid quantification of imatinib and N-desmethyl-imatinib. These devices were compared to two traditional PS methods. For all methods, when the sample is coupled directly to a QQQ, analytes are detected with high sensitivity. Analytical figures of merit for the four devices are compared and it is concluded that several of the novel devices successfully deploy DBS with PS and yield similar results to traditional PS methods. Clinical samples collected from patients in a remote resion of Southeast Asia were analyzed as a successful proof of concept for in-field blood collection and subsequent rapid laboratory analysis.

3.2 Introduction

DBS analysis by MS is a widely used technique that involves analyte extraction from the dried blood matrix followed by chromatographic separation and transfer into a mass spectrometer.[37-40] DBS cards are a common way to collect and analyze drugs and exogenous analytes in whole blood while using only microliters of the biofluid.[37-38] The cards are applicable to point of care studies and in-field or remote sample collection since they are easily stored, handled, and shipped.[37-39] Due to their increased popularity, more commercially available DBS devices are being developed and they promise better results, improved sample collection, and simpler overall protocols.[39]

For clinical trials involving in-field sampling, DBSs are appealing because they only require a small sample of blood obtained from a finger prick rather than an intravenous blood draw.[39, 41]

This allows multiple replicates to be taken relatively painlessly. Furthermore, storing samples as DBSs facilitates in-field blood collection because the sample is stable, easy to ship, non-infective, and conventional field requirements such as refrigeration of a liquid sample are unnecessary.[39, 41-42] However, many DBS methodologies place an unknown amount of blood or blood with varying hematocrit. Furthermore, when the blood spot is removed in the laboratory, some sample is often left on the card. This can cause highly variable results. For quantitative results, an accurate volume of blood should be added to the card, using a disposable micropipette or by using a collection device that controls the sample volume, and the entire spot should be analyzed.[37-38, 43] Extracting the entire DBS or a consistent fraction from the card (or related device) is necessary for accurate and precise results.[37-39]

Although DBS analysis by MS measures analytes of interest in small samples of blood, traditional DBS-MS methodologies require a significant amount of time and material (*e.g.* solvent) for the offline extraction and separation (by LC).[37-38, 40] This backend sample workup makes DBS-MS relatively time consuming, material consuming, expensive, and less desirable for the analysis of a large numbers of clinical samples. PS provides a means of DBS analysis directly from the dried blood spot, with no additional sample preparation, no offline analyte extraction, and no chromatography.[1-2, 7]

To maintain an appropriate blood concentration and avoid unwanted side effects, therapeutic drug monitoring is necessary for many regularly administered drugs. In the case of the tyrosine kinase inhibitor imatinib (Gleevec®, Novartis), toxicity occurs at relatively low levels so it is particularly important to maintain in vivo concentrations in the narrow therapeutic window.[44] Furthermore, the concentration of the drug and metabolite vary greatly with the individual patient.[44] As discussed in Chapter 1 and 2, PS is a rapid analysis technique that can provide clinicians pharmacokinetic and therapeutic drug monitoring information from a complex sample. PS is an excellent method to measure these drugs in a patient using only 10 µL of blood from a finger prick.

Although multiple published studies show the range of PS-MS applications using filter paper, chromatographic paper, or another porous medium, the technology would benefit from an understanding of its performance when using commercially available DBS cards (or other devices) to collect the blood spots and analyze them with PS-MS.[2-3, 7] One major requirement for PS is that the blood sample is applied directly to the triangle used as the spray emitter. This limits the use of

commercially available DBS devices to those designed for PS or to those which can be cut to a point. These limited options may not meet the specifications for studies that require a device with special features such as blood filtration or precise volume measurement of the sample. This restriction can be overcome by either extracting the analyte from the dried blood spot offline, which is time consuming and expensive, or by integrating the DBS device with PS-MS.[45] With this latter approach, the DBS device may be superimposed on a paper triangle to perform PS or the DBS device may be cut to a point and used as the PS source itself. In this way, PS analysis becomes applicable to a wide range of DBS devices including recently marketed collection devices.

In this study, imatinib (Imb) and its major active metabolite, N-desmethyl-imatinib (N-DM-Imb), were measured in whole human blood by PS-MS/MS using multiple DBS devices integrated into the PS platform.[46] Note that only DBSs were analyzed in this study, because agreement between the quantitative results of PS analysis of DBS and whole blood sample analysis by LC-MS/MS has been demonstrated previously.[47] Three commercially available DBS devices, namely Whatman FTA cards, TomTec PDMS-4 cards, and Novilytic Noviplex blood filtration cards were tested using unique direct extraction and ionization methods by PS-MS/MS. The data obtained were compared to traditional PS measurements using W31 and the automated Prosolia Velox 360 PS source with VSCs (Chapter 1).

FTA cards are a commonly used DBS collection device that hold up to four DBSs. Among the various FTA cards, the DMPK-C card carries minimal amounts of chemicals from the production process (as seen in the mass spectrum) and is therefore the best choice for PS analysis as interferences and additives causing ion suppression should be avoided.[39] Similar to FTA DMPK-C cards, TomTec PDMS-4 is a cotton based DBS collection device. The TomTec card contains nine laser cut circular disks held in place by small bridges of paper that break easily allowing a disk containing the entire blood sample to be removed. This product is unique since it is aimed at improving recovery of a blood spot over traditional DBS cards by retaining the entire sample for analysis. The Novilytic device filters a whole blood sample (~25 µL) and dispenses precisely 2.5 µL plasma onto the collection disk. This technology removes the centrifugation step previously required to obtain a dried plasma spot. To be clear, this device only measures the plasma fraction of the drug in whole blood.

Any of these devices may be used for in-field sample collection but the DBSs are typically punched out and the analyte is extracted before MS analysis.[42] In this study, the above devices were used with PS for rapid data collection. Although these were not fully validated assays, specific analytical figures of merit were compared between the DBS devices and the success of PS implementation are discussed. In addition to these comparative measurements, capabilities for in-field collection and PS analysis were tested. Field samples from patients dosed with Imatinib were spotted on W31 and VSCs. These samples were collected in a remote, low resource clinic, shipped back to the lab, and measured using methods described below. These preliminary clinical results represent a proof of concept test of in-field DBS collection and analysis by PS-MS/MS.

3.3 Materials and Methods

3.3.1 Reagents and Instruments

LC-MS grade solvents and formic acid (99%) were purchased from Sigma Aldrich (St. Louis, MO). Imatinib, N-desmethyl-imatinib, and their D_8 isotopically labeled IS were purchased from AlsaChim (Illkirch-Graffenstaden, France). Whole human pooled blood with K_2EDTA was purchased from BioreclamationIVT (Hicksville, NY). SafeTec Microsafe® disposable micropipettes were purchased from SafeTec LLC (Ivyland, PA).

Whatman FTA DMPK-C DBS cards were purchased from GE Healthcare Life Sciences (Chicago, IL). Noviplex cards were obtained from Novilytic (West Lafayette, IN) and PDMS-4 cards were obtained from TomTec Life Sciences (Hamden, CT). Additional PS materials from Chapter 1 were used.

3.3.2 Instrumental Parameters

Thermo Fisher Xcalibur software was used for data acquisition and analysis. All instrument and method parameters are listed in Table 3.1. The MRM transitions and parameters are listed in Table 3.2. Full scan analysis was performed in positive mode using 0.5 s scan time from *m/z* 100 - 800.

Table 3.1 TSQ Xcalibur acquisition parameters in MRM mode.

MS Polarity	Positive
Acquisition time (s)	33
Scan Time (ms)	150
Scan Width (*m/z*)	0.01
Peak Width (FWHM)	0.70
Collision Gas Pressure (mTorr)	1.5
Ion Transfer Tube Temperature (C)	300

Table 3.2 MRM transitions and parameters for Imb and N-DM-Imb and their deuterated IS.

Analyte	Precursor Ion $[M+H]^+$ (*m/z*)	TL (V)	Quantifier Fragment (*m/z*)	CE (eV)	Qualifier Fragment (*m/z*)	CE (eV)
Imb	494.3	106	394.1	24	217	23
N-DM-Imb	480.2	98	394.1	23	203.1	24
Imb-D_8	502.3	129	394.1	25	-	-
N-DM-Imb-D_8	488.3	100	394.1	24	-	-

3.3.3 Data Analysis

The relative area for each sample was calculated by dividing the TIC area for the quantifier fragment by the TIC area of the corresponding IS. LODs were determined from serial dilutions of the lowest calibrator; where signal to blank (noise) equaled to three. All calibration curves were generated by plotting the concentration of the sample against the relative area. The calibration curves were not weighted and the origin was ignored unless noted otherwise. The Quant/Qual were calculated by dividing the qualifier TIC area by the quantifier TIC area.

3.3.4 Solution Preparation

Cal and QC solutions were prepared from separate stock solutions. For each Cal or QC, a 20X concentrated solution of Imb and N-DM-Imb was prepared in methanol/water (1:1), then diluted 20X into blank pooled whole human blood and mixed well. If IS was to be incorporated into the liquid sample, it was spiked into the solution at this point. Otherwise, an IS stock solution, made in methanol, was spiked directly onto the paper (2 µL) and dried for 10 minutes. When IS

was mixed into the sample the final concentration was 1500 ng/mL for Imb-D_8 and 500 ng/mL for N-DM-Imb-D_8. When the IS was spiked onto the paper, the IS concentration in methanol was 7500 ng/mL for Imb-D_8 and 2500 ng/mL for N-DM-Imb-D_8. Cal concentrations for Imb were 250, 500, 2500 and 5000 ng/mL with QCs at concentrations of 350 and 2000 ng/mL. The concentrations for N-DM-Imb Cals were 75, 150, 750 and 1500 ng/mL and the QCs had concentrations of 105 and 600 ng/mL. The calibrator concentrations are a reflection of the therapeutic range and not of the LOD and Cal 1 serves as the cutoff value for calculating concentration in unknown samples.[39] The Novilytic calibrators and QCs were higher for N-DM-Imb; they were prepared at 300, 600, 3000 and 6000 ng/mL and the QCs were 420 and 2400 ng/mL in whole blood.

3.3.5 PS Setups

W31 PS setup from Chapter 1 was used here. For this method, 10 µL of blood was spotted on W31, dried for 2 hours, then manually cut and attached to a copper clip (Figure 3.1 A). To spray the sample, 3500 V was applied to the copper clip and 45 µL of a spray solvent (95% methanol, 5% water and 0.1% formic acid) was pipetted to the back of the paper. This voltage and solvent were used throughout the study unless otherwise noted.

Whatman FTA DMPK-C cards were used in a similar manner to the W31 paper. Internal standard was prespotted on the card followed by a 10 µL blood spot addition. After drying, the spots were manually cut out, attached to a copper clip and voltage and solvent were applied (Figure 1C).

The TomTec cards were also prespotted with IS followed by a 10 µL blood spot addition. Once dry, the TomTec disk was punched out and secured to the top of a precut W31 triangle with a copper clip (Figure 3.1 B). The sample disk was primed with 30 µL of methanol by applying the solvent to the top of the disk and allowing it to flow through the disk onto the W31 paper below. Next, 30 µL of spray solvent was added to the top of the disk and a high voltage was applied. Again, it is important that the top of the disk is in direct contact with the W31 paper surface for efficient analyte extraction.

Each Novilytic card was spotted with approximately 25 µL of whole blood sample until the card's QC indicator turned red signifying enough sample had been added. The filtration layers were peeled away after 3 min as specified by the product instructions and the remaining plasma

spot was allowed to dry in open air for 15 min. The Novilytic card is a plasma collection device manufactured with multiple layers of filter materials which are secured on top of a sample disk. The collection disk is covered by the filtration system and therefore does not allow for an application of IS to the collection disk prior to adding the whole blood. Consequently, IS was added to the plasma collection disk after the filtration occurred and when the plasma was dry. The plasma disk spotted with IS was then placed on top of a W31 triangle, primed with 20 µL methanol and sprayed with 20 µL of the spray solvent (Figure 3.1 D).

For the automated Velox analysis, VSCs were prespotted with IS. Next, 10 µL of the blood sample was spotted on the center of the VSC covering the IS spot (Figure 3.1 E). As mentioned in Chapter 1, the blood must spread horizontally to touch both edges of the VSC. The spots were allowed to dry for two hours. Each VSC received 9 µL methanol (Pump A) as the Sample Solvent (prime solvent, applied directly to the spot) and 120 µL of the 95% methanol, 5% water and 0.1% formic acid (Pump B) as the Cartridge Solvent (spray solvent, added to the back of the cartridge). A voltage of 5000 V was applied to generate spray.

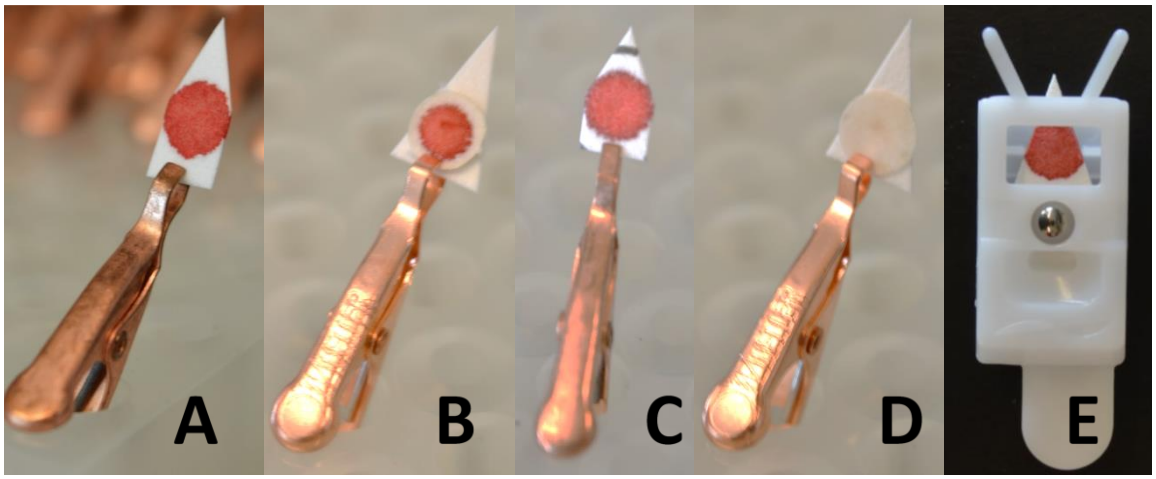

Figure 3.1 DBS devices and modifications made to couple the device to PS methodology. A) W31, B) TomTec, C) FTA, D) Novilytic and E) VSC. A, B, C, and E contain 10 µL of whole blood while D used approximately 25 µL and the disk capture 2.5 µL plasma.

3.3.6 Internal Standard Study

Three different methods of introducing IS were tested using a QC sample and W31 methods described above. First, IS was mixed into the blood sample prior to spotting 10 µL. Second, IS was prespotted onto the paper and dried before the blood sample was added. When IS was prespotted, a small pencil mark was made onto the W31 paper to indicate the center position. The solvent front was also circled with a pencil to indicate the IS spot clearly. For this, 2 µL of IS was spotted followed by a 10 µL spot of whole blood sample. This way the diameter of the IS spot was approximately half the size of the diameter the blood spot and the pencil marks helped ensure all the IS would be covered by the sample and captured in the analysis. The third method spotted 2 µL IS in the center of a DBS. Each condition was analyzed in triplicate. The last two methods of introducing IS are important for in-field blood spot collection where it is difficult to mix the whole blood with an IS solution. As described in the PS Setup section, all DBS devices studied here use a method of pre or post spotting IS to mimic the environment which the devices will be used.

3.3.7 Additional Studies

For all whole blood devices, 10 µL of a blank blood sample was added. The samples were measured in full scan mode to evaluate the background of the devices. A blank plasma sample was evaluated for the Novalytic device.

To evaluate the matrix effects from the blood sample, the DBS devices were spotted with the internal standard solution. On top of the IS spot, either blank whole blood or DI water was spotted (10 µL). These samples were prepared in triplicate and analyzed with MRM methods.

Finally, to validate the use of the SafeTec Microsafe® pipettes, a QC sample was spotted in triplicate onto W31 paper using either a SafeTec pipette or a single channel pipette. The sample contained IS prior to spotting, was measured as describe in the methods above, and reproducibility between the two compared.

3.3.8 Vietnam Sample Collection

A 3 inch by 4 inch piece of W31 paper was prespotted with four separate IS spots. Pencil was used to circle the IS solvent front to mark where the blood spot should go. The paper was set between cardboard to maintain the shape and sealed in an aluminum-coated bag containing

desiccant and a humidity card. The W31 paper was shipped to field clinics in the Hướng Hóa district of the Quảng Trị province in Vietnam. For five consecutive days, three patients were dosed with 400 mg Imb and one patient with 600 mg. From each patient a blood sample was taken five days in a row, two hours after the dose was administered. Each sample was taken by cleaning the patient's finger, pricking it with a lancet, discarding the first blood drop, and collecting the second drop with a 10 µL SafeTec Microsafe® disposable micropipette. Each pipette measured precisely 10 µL of blood from the patient. Then the blood was dispensed onto the W31 paper on top of the IS spot. Four samples per time point were collected. After drying the samples for 2 hours, they were sealed with desiccant, stored at room temperature, and shipped back to Purdue University for analysis. In addition to four W31 samples, one VSC was spotted for analysis using the Velox. The samples were collected over a one month period and stored as described above for three months before analysis. Calibration curves and QC samples were analyzed using the methods described above followed by the samples collected in-field.

Patients provided written, informed consent before entering the study. The study was conducted in accordance with Good Clinical Practice guidelines and the Declaration of Helsinki, and was approved by Vietnamese Ministry of Health and Purdue University IRB approval: 1507016329 (Clinicaltrials.gov identifier: NCT02614404).

3.4 Results

The reproducibility of PS-MS data depends on the method used to introduce the IS into the sample.[7] This study, necessitating in-field blood handling, required that the IS be spotted before or after the sample was spotted. The best reproducibly for the QC was achieved when the IS and blood were mixed prior to spotting the sample on paper; the RSD for a QC sample analyzed in triplicate was less than 2% with this methodology. However, as an acceptable alternative for in-field sample collection, prespotting the IS solution followed by the blood sample yielded a RSD of less than 6%. The prespotting method was better than spotting the IS to an already dried blood spot, which gave a RSD greater than 20%. Additional methods as described by Abu-Rabie et al. may help overcome the poor reproducibility shown when IS was added to a dried blood spot and they should be investigated in the future.[48]

Table 3 summarizes all figures of merit for the DBS devices. Results for all the devices were compared to those for traditional manual PS methodology in which blood and IS were mixed then spotted and dried onto W31 paper. The W31 samples were manually cut out and sprayed. When the IS and blood were premixed, the method yielded a LOD of 5 ng/mL for Imb and 6 ng/mL for N-DM-Imb. Both analytes had linear curves for Imb and N-DM-Imb (Figures 3.2 A and 3.3 A) with high precision- < 3% and 6% RSD for Imb and N-DM-Imb, respectfully (Table 3.3). The QC samples yielded an accuracy of 106% and 99% for Imb and 93% and 105% for N-DM-Imb- for the low and high QCs, respectively, demonstrating that the method is accurate. Overall, these data suggest a high performing PS-MS/MS method with good precision, accuracy, and linearity. One reason for this is that the blood and IS are mixed homogenously before spotting. Furthermore, any blood sample lost in the cutting process is lost in approximately the same ratio as the IS which allows for highly reproducible and accurate results even if small portion of the sample is removed.

A qualifier fragment ion intensity was measured along with a quantifier fragment for each analyte as an additional step towards positive identification. The Qual/Quant was determined for each Cal. For Imb the Qual/Quant was between 17% and 20%, and for N-DM-Imb the ratio was between 19% and 25%. The variation was no greater than 20% across all Cals and QC samples, which suggests that these fragmentation processes can be used to positively identify the analytes in blood by PS-MS/MS.

Table 3.3 Summary of figures of merit for the DBS devices investigated.

Imatinib						
Device	W31	W31	FTA	TomTec	Novilytic	VSC
Internal standard:	mixed in	prespotted	prespotted	prespotted	postspotted	prespotted
LOD (ng/mL):	5	5	5	2.5	60	10
RSD (%):	3	18	37	16	25	13
QC low, accuracy (%)	106	111	79	105	100	108
QC high, accuracy (%)	99	90	101	95	110	99
N-desmethyl-imatinib						
Device	W31	W31	FTA	TomTec	Novilytic	VSC
Internal standard:	mixed in	prespotted	prespotted	prespotted	postspotted	prespotted
LOD (ng/mL):	6	6	6	6	100	25
RSD (%):	6	9	29	12	27	9
QC low, accuracy (%)	93	105	86	89	83	100
QC high, accuracy (%)	105	85	89	92	114	110

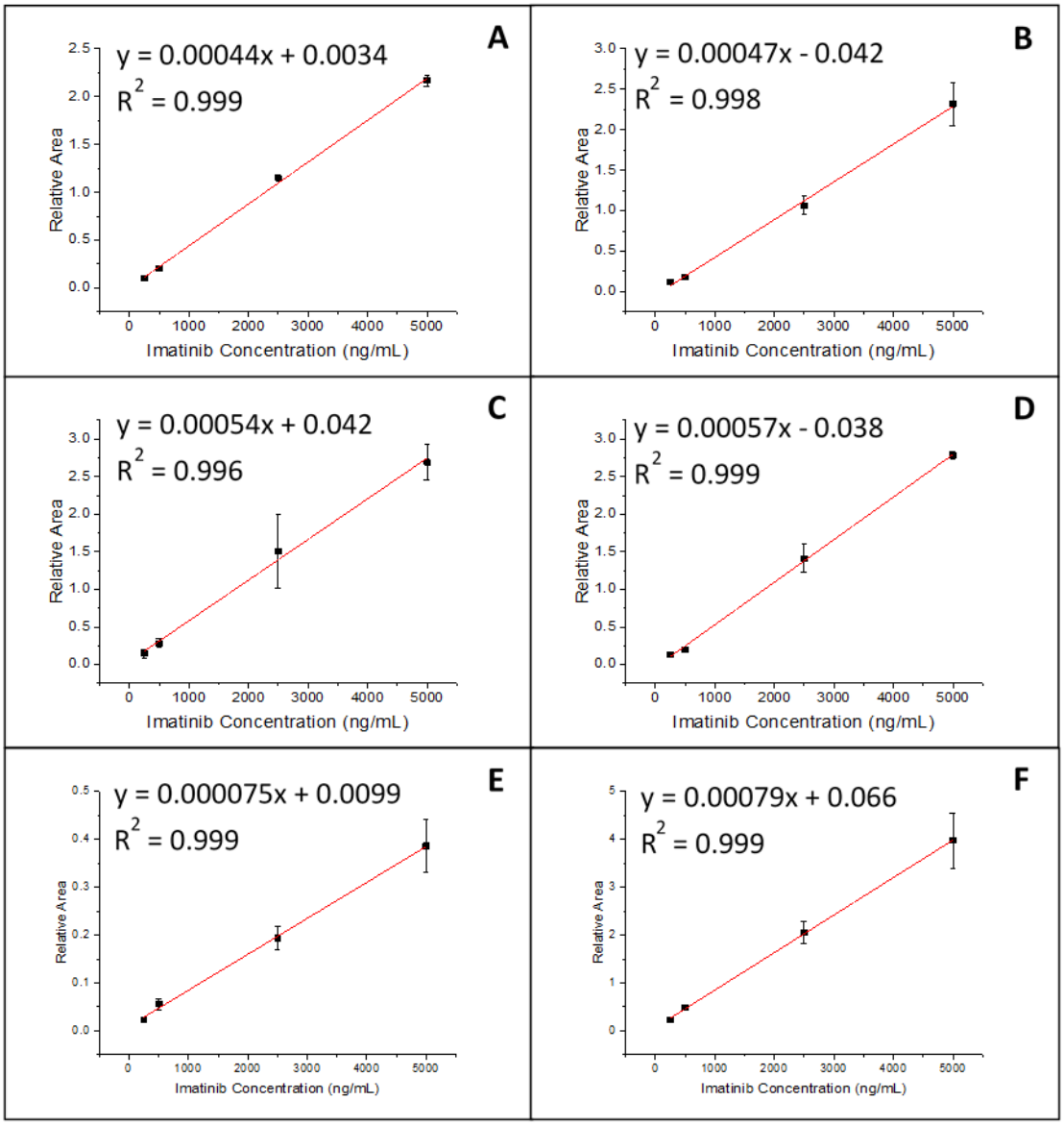

Figure 3.2 (A) Imatinib Cal curves for W31 blood spot analysis when IS and blood are premixed, (B) W31 with prespotted IS, (C) FTA cards with prespotted IS, (D) TomTec cards with prespotted IS, (E) Novilytic cards with postspotted IS and (F) VSC with prespotted IS . Error bars equal 1 sigma (n=3, VSC n=6). The curves are not weighted and the origin is ignored. Fits and R^2 values are displayed in the plot.

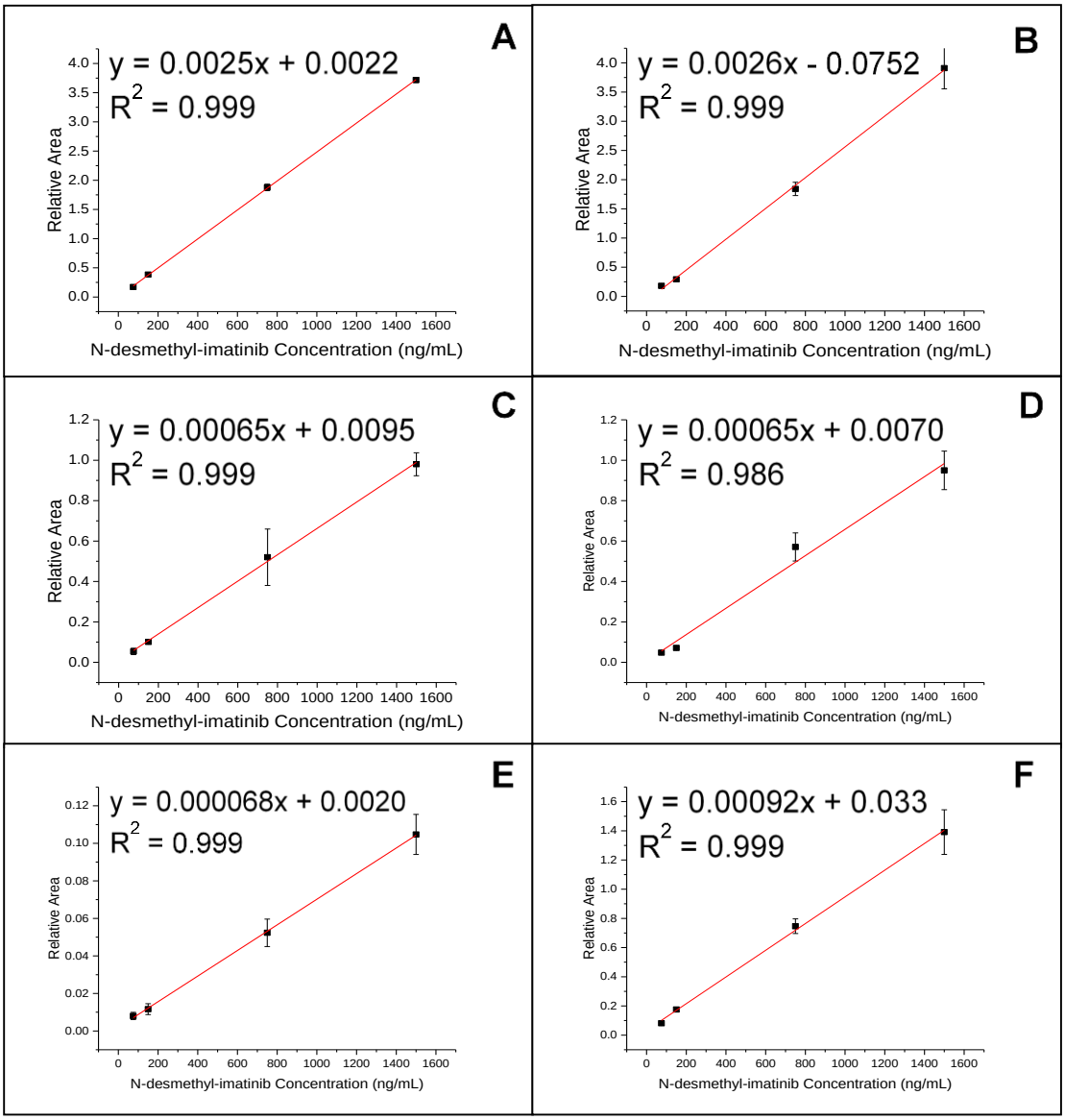

Figure 3.3 (A) N-desmethyl-imatinib Cal curves for W31 analysis when IS and blood are premixed, (B) W31 with prespotted IS, (C) FTA cards with prespotted IS, (D) TomTec cards with prespotted IS, (E) Novilytic cards with postspotted IS, and (F) VSCs with prespotted IS. Error bars equal 1 sigma (n=3, VSC n=6). The curves are not weighted and the origin is ignored. Fits and R^2 values are displayed on the plot.

When the IS was prespotted to the paper, the performance was similar compared to when the IS was mixed into the sample (Figures 3.2 B and 3.3 B). However, the calibrator RSDs of the prespotting method were a little greater: <18% for Imb and <9% for N-DM-Imb (Table 3.3). This additional error was likely due to some of the blood spot being cut off in sample analysis while the

IS remained unchanged. The QC accuracy was still acceptable with 111% and 90% for the low and high Imb QCs and 105% and 85% for the low and high N-DM-Imb QCs.

The FTA card had the same LODs as W31, with 5 and 6 ng/mL for Imb and N-DM-Imb, respectively. The device also gave a linear response for both analytes (Figures 3.2 C and 3.3 C). However, the Cal reproducibility with this device was poor - RSDs were between 9% and 37% for the Imb Cals and between 6% and 29% for N-DM-Imb Cals. The QCs were not as accurate either, 79% and 101% for Imb QCs and 86% and 89% for N-DM-Imb QCs. The poor reproducibility and accuracy were likely due to a number of factors. First, the full scan spectra of blank blood showed a higher background signal (10^8 counts) for the FTA cards when compared to the other devices tested (Figure 3.4). This background was significantly higher than that observed in other devices. The FTA card paper is also composed of a different material than the W31 paper, and the tip created with the FTA cards is more rounded than and not as sharp as the tip made with W31 paper which can also negatively impact the spray quality.[49] Finally, similar to the W31 paper, the RSD was likely increased due to the IS prespotting method combined with sample loss from the cutting process.

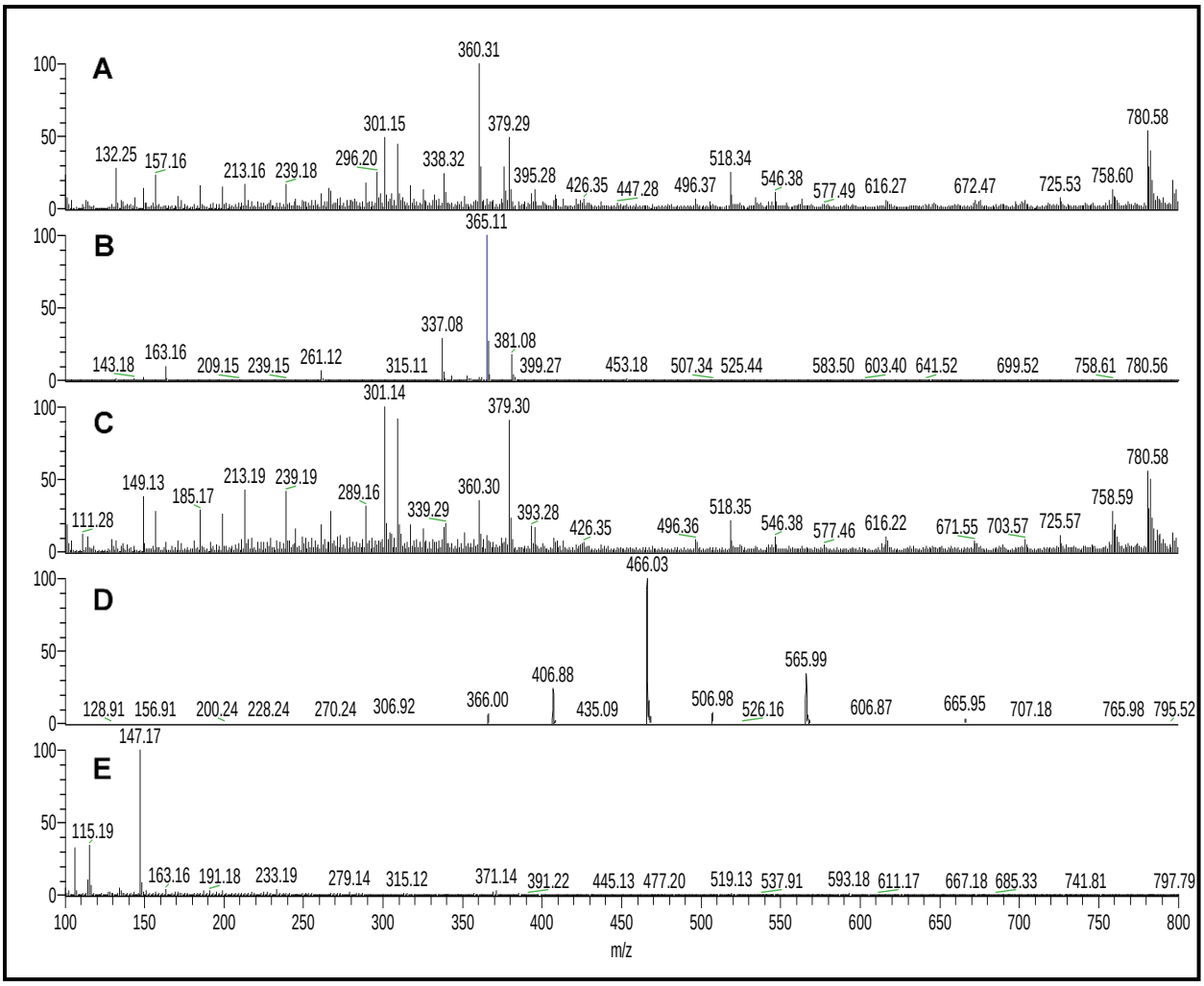

Figure 3.4 Full scan spectra of human blank blood on (A) W31, (B) FTA cards, (C) TomTec cards, (D), plasma from the Novilytic cards and (E) blood using the Velox cartridges. The relative intensity of W31 is $3x10^6$, FTA is $1x10^8$, TomTec is $3x10^6$, Novilytic is $8\ x10^7$, and $8x10^6$ for the Velox.

The TomTec device was simple and easy to use. The LODs were similar to W31 paper, 2.5 ng/mL for Imb and 6 ng/mL for N-DM-Imb. Additionally, the TomTec method yielded curves with linear responses for both analytes (Figures 3.2 D and 3.3 D), and the Cal reproducibility was acceptable with a RSD ≤16% for Imb and ≤12% for N-DM-Imb. Furthermore, the TomTec device demonstrated good accuracy: 105% and 95% for Imb QC low and high and 89% and 92% for N-DM-Imb. Based on the slopes obtained from the Cal curves and the relative area of the signal, the

sensitivity of the TomTec analysis matched that of the W31 analysis (Figures 3.2 B and 3.2 C). This suggests that the extraction of the drug and transfer to the triangle paper placed underneath it was as efficient as the extraction of the drug using the traditional W31 PS methodology.

When analyzing plasma with the Novilytic device, the free drug is the only material being measured.[50] Whereas in whole blood analysis by PS, the free and protein bound fractions contribute to the signal. This study found that, after filtration of the whole blood calibrators, the PS signal using the Novilytic device was linear (Figures 3.2 E and 3.3 E). However, this device had a higher LOD, 60 ng/mL for Imb and 100 ng/mL for N-DM-Imb, and a smaller slope by an order of magnitude. The deviation of the LOD and sensitivity of the method, when compared with the W31 analysis, can be attributed to two main features of this methodology. First, a smaller sample volume was measured, 2.5 µL plasma verses 10 µL for whole blood. Second, only a fraction of the drug that was spiked into the whole blood Cal samples was able to contribute to the MS signal. The QC values were accurate with 100% and 110% for Imb low and high QCs and 83% and 114% for N-DM-Imb QCs. However, the reproducibility of the Novilytic card was poor (between 11% and 25% for Imb and 9% and 27% for N-DM-Imb calibrators), likely due the addition of the IS after the plasma had been filtered, collected, and dried on the disk. As demonstrated earlier, the IS spiking study suggested that the reproducibility suffers when IS is added after the biofluid has been dried. The reproducibility could also be affected by variations in the plasma fraction or variation in the volume measured by the device. Future studies aimed at improving the reproducibility of this method may benefit from spiking the IS onto the plasma collection disk prior to the assembly of the filtration device. Furthermore, plasma Cals and QCs along with whole blood QCs should be utilized in future studies to determine whether the IS addition is the only source of error. Nonetheless, this method could benefit studies that require observation of unbound, available portion of drug in patient plasma and for studies that measure the rate of drug release from the bound form to the unbound form.

The VSCs allow for automated PS analysis with the Velox 360 source which is convenient to use for high throughput analysis. The analytical results from the VSCs were very good, with LODs similar to those of obtained from manual PS, 10 ng/mL for Imb and 25 ng/mL for N-DM-Imb. The calibrators produced a linear response (Figures 3.2 F and 3.3 F). The RSD was low, < 13% for Imb and <9% for N-DM-Imb. The QCs were accurate with 108% and 99% accuracy for both Imb low and high QCs, respectively, and 100% and 110% for N-DM-Imb QCs. The higher

performance of this device is likely a result of the use of laser cut paper rather than the manually cut paper; the latter cutting consistently yields the same tip angle and size ensuring optimal ionization. Additionally, precut paper enables the capture and analysis of the entire blood sample with no sample loss from cutting the spot out. The only two drawbacks of the VSCs were related to the cartridge itself. The VSCs are bulkier than other devices and this must be taken into consideration in field studies. The VSC tip must also remain protected (see Vietnam sample results below). If it is damaged, it is difficult to obtain stable spray ionization from the paper. Therefore, proper handling and storage is essential with this device. However, for some studies, the analytical benefits of automated ionization may outweigh the drawback of ensuring proper shipping and storage of the cartridges.

To analyze the effect that whole blood matrix has on the Imb signal the IS signal with a whole blood sample was compared to the IS signal with a water samples. The average absolute intensity of the IS (n=3) was measured for each sample matrices. For W31, FTA, TomTec, Noviplex and VSC the whole blood IS signal was 9% 91%, 30%, 88% and 91%, respectively, compared to the IS signal with a water sample. The lower overall signal for the IS in whole blood is caused by ion suppression and from recovering less sample due to the physical barriers on the paper from the matrix (*e.g.* dried cells). This, however, is not detrimental to the assay performance because recovery is sufficient and the IS normalizes the signal to yield high reproducibility. Noviplex and VSCs appear to extract the analyte while retaining the matrix in the most efficient and reproducible manner. FTA cards are efficient but not reproducible.

For in-field collection of blood samples, a cheap, disposable, and accurate pipette must be used for devices that do not measure the sample volume. Fitting these criteria, SafeTec Microsafe® pipettes were used to measure the blood samples and proved to be as precise and accurate as a single channel pipette. QC samples pipetted onto W31 with these micropipettes had RSDs and percent errors comparable to QCs spotted with a single channel pipette (Table 3.4). Thus, these micropipettes are acceptable in-field devices to collect small blood samples from finger pricks.

Table 3.4 SafeTec micropipette comparison to single channel pipette.

Sample	Imatinib		N-DM-Imatinib	
	RSD	% Diff	RSD	% Diff
Single Channel Pipette, QC1	9%	11%	12%	15%
SafeTec, QC1	19%	18%	14%	16%
Single Channel Pipette, QC2	14%	3%	18%	0%
SafeTec, QC2	9%	3%	11%	4%

To verify this collection method and analysis, twenty patient whole blood samples were collected on site in Vietnam using the SafeTec Microsafe® pipettes, transferred onto prespotted W31 paper or VSC, air dried for 2 hours, and then stored under desiccant at room temperature until shipped to the laboratory. As with most drugs, Imb has been shown to be stable in a DBS under these conditions.[42] The W31 samples were analyzed by manual PS (n=3). Only three of the W31 replicates were measured and one was retained for reanalysis, if necessary. The single VSC was analyzed with the Velox 360.

Cal curves were run the day of the clinical sample analysis and the curve equation was used to calculate the concentration Imb and the metabolite N-DM-Imb in each clinical sample (Table 3.5). The QCs were accurate (<15% error) and the RSD of three replicates was less than 21%. The concentrations of the analytes were plotted over a five-day period to show the blood concentration of Imb and its metabolite in patients throughout the dosing regimen (Figure 3.5). Although the IS concentration was fairly consistent between the Cals, QCs, and samples, much higher error was seen in the patient samples than the Cal or QCs; average RSD for Imb in patients was 31%. This additional error was caused from inconsistent and non-uniform spotting of the blood followed by manually cutting the paper. All Qual/Quant ratios of positive samples were within 20% of the Cal 3 ratio, which is additional data that the sample was positive for Imb.

The most unexpected source of error was from imprecise dispensing of blood onto the W31 paper. In the laboratory, a clean circle was made over the circled IS spot but, in the field the sample was, at times, dispensed in an uneven shape missing part of the IS spot. For this reason, the in-field use of a devices like the TomTec cards or the VSCs should reduce error in the future since they capture the whole sample without introducing manual sources of error. Nonetheless, even with this error, the dosing trend and drug metabolism followed expected results as can clearly be seen in Figure 3.5. Additionally, the results supported the clinical study by Low et al (unpublished).

Table 3.5 Vietnam sample results from W31 PS (n=3). Values marked with an asterisk are below the cutoff value (Cal 1). The Cal curve had a line fit of y=0.00106x for Imb and y=0.00103x for N-DM-imb. Both curves had R^2 >0.99.

Patient & Day	Imatinib		N-Desmethyl-Imatinib	
	Concentration (ng/mL)	RSD	Concentration (ng/mL)	RSD
TA005 Day1	1721	21%	214	23%
TA005 Day2	3102	13%	666	17%
TA005 Day3	3043	21%	652	18%
TA005 Day4	2841	40%	708	32%
TA005 Day5	5702	7%	1086	6%
XY001 Day1	593	19%	90	29%
XY001 Day2	337	52%	79	47%
XY001 Day3	1691	17%	249	11%
XY001 Day4	915	40%	150	32%
XY001 Day5	205*	37%	64*	24%
XY003 Day1	3583	37%	374	41%
XY003 Day2	4653	72%	1335	90%
XY003 Day3	5513	8%	814	15%
XY003 Day4	4376	24%	917	27%
XY003 Day5	4392	22%	601	18%
XY004 Day1	1145	36%	115	38%
XY004 Day2	1672	59%	540	62%
XY004 Day3	1462	29%	393	26%
XY004 Day4	2020	48%	444	50%
XY004 Day5	2259	27%	373	20%

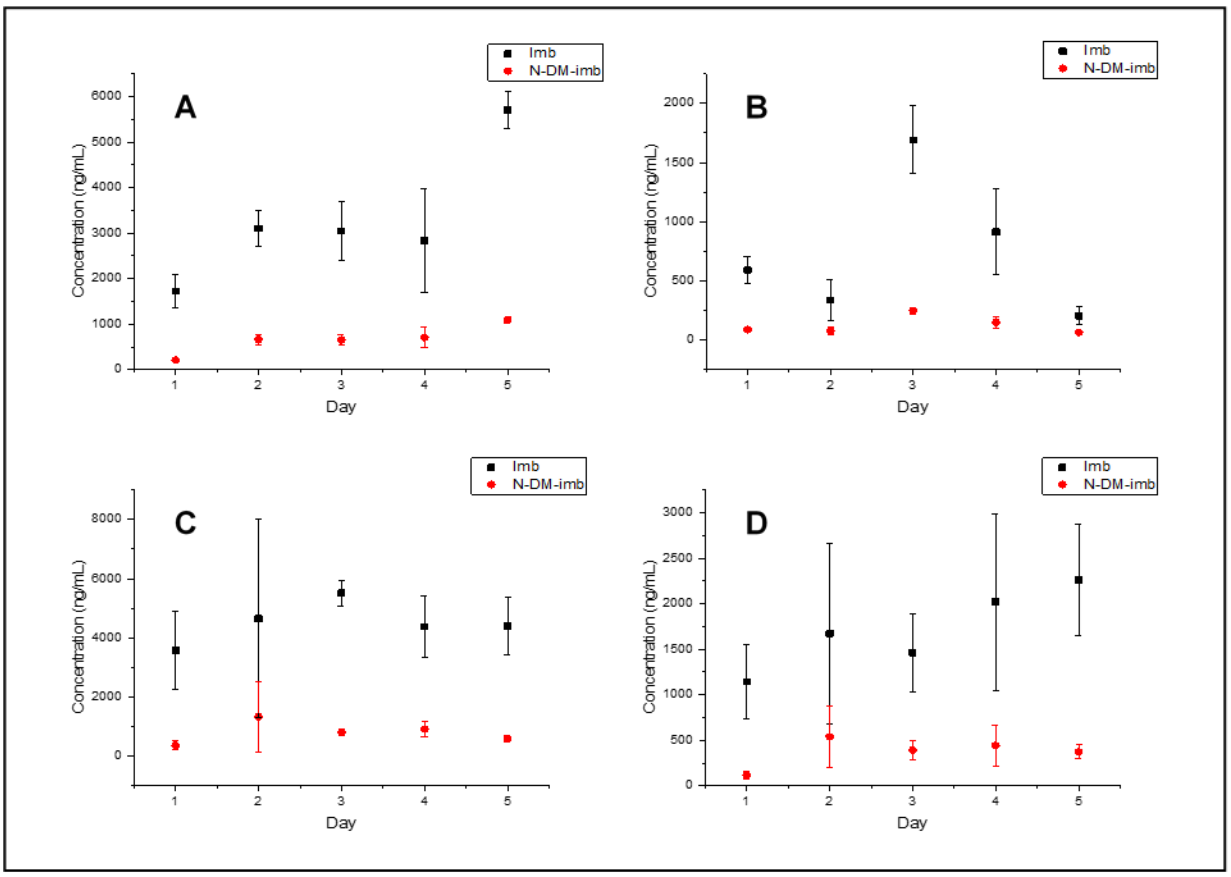

Figure 3.5 Longitudinal depiction of drug concentration in patient samples (n=3). Patient TA005 (A) received 600 mg dose, patient XY001 (B) received 400 mg dose, patient XY003 (C) received 400 mg dose and patient XY004 (D) received 400 mg dose. Error bars are 1 standard deviation.

Many VSC cartridges were either damaged by the tip being bent or smashed and/or improperly spotted *i.e.* spot not spread the width of the paper (Figure 3.6). In total 13 of 23 cartridges sustained considerable damage to the tip. Many of the damaged tips were salvaged as best as possible via flattening with the tips of tweezers however, some still did not yield any signal. The patient data was too inconsistent for clear conclusions and data is not shown. More care should be given to storing the cartridges carefully. Improved tip guards or individual cartridge caps for spray tip protection may help with this. Additional training of nursing and phlebotomy staff would also be beneficial. This was a new technique, not previously deployed in any field trial.

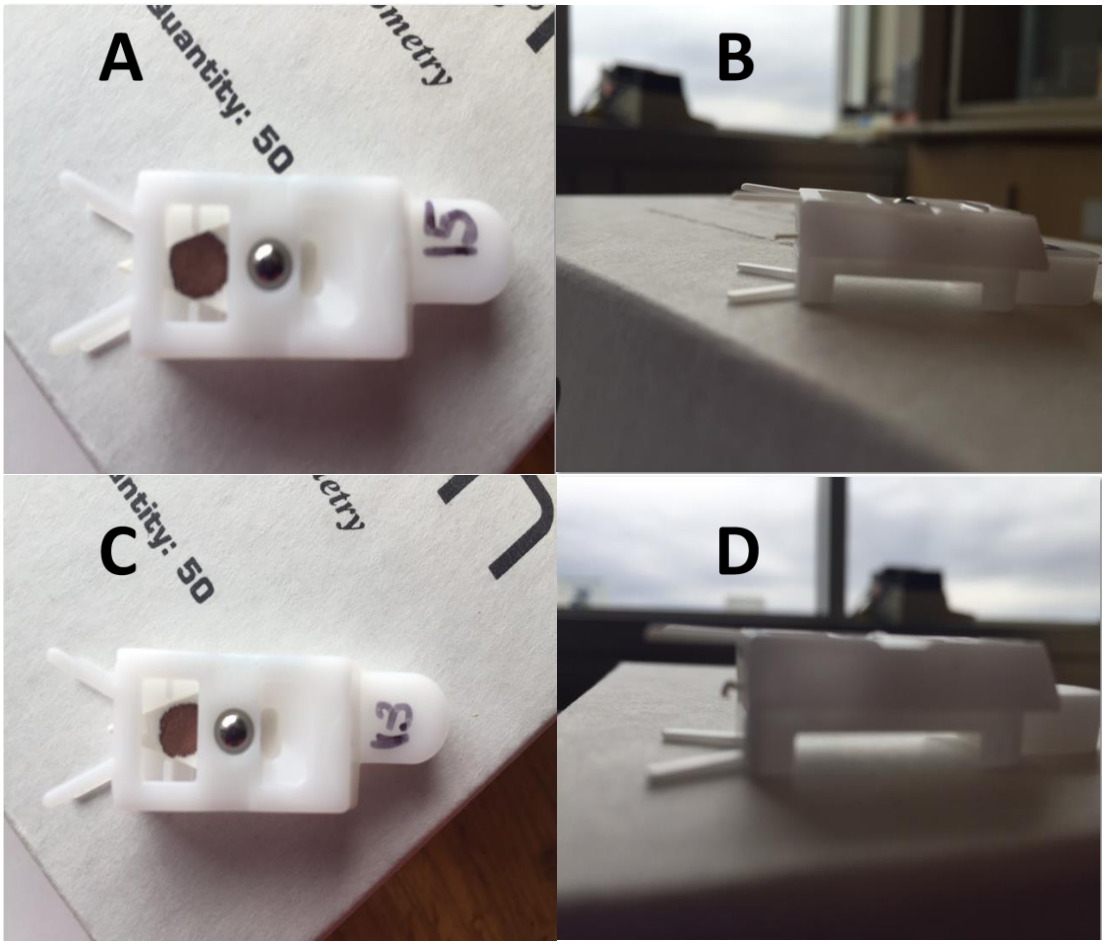

Figure 3.6 VSCs from Vietnam (A) properly spotted (B) intact tip (C) improperly spotted (D) damaged tip.

3.5 Conclusions

A variety of commercially available DBS devices can be used with PS-MS for the quantitation of drugs in human blood to support clinical trials. The novel methods of coupling the collection devices to the PS source are easy to implement and optimize, allowing fast turn around and quick determination of figures of merit. In this study, all four devices and the W31 exhibited linear results. All but the Novilytic plasma device yielded the same slope for the calibration curve suggesting the same sensitivity across these devices and coupling strategies. In some cases, *i.e.*. the FTA and Novilytic devices, reproducibility needs to be improved before it can be used in the field.

As it stands, the most successful devices allow material, such as IS, to be introduced onto the collection device before the addition of the biofluid. The reproducibility is best in devices that can collect and measure the whole sample with no need to tamper with the DBS, such as cutting it out. With the FTA cards and W31, error was introduced with imperfectly spotted DBS's and when cutting the spot from the whole device. On the other hand, the VSCs and TomTec cards can capture the whole sample. Automation also improved the analysis; every VSC is laser cut in a precise shape preventing error introduced with manually cutting paper as required with other types of devices. In addition, the fact that analysis of the VSC is part of an automated system reduces human error. Automation would likely improve the PS method for the other DBS devices and should be investigated. However, W31 paper is reasonably priced, simple, and was effective both in the lab and during field studies, for manual PS-MS. In the future, error can be reduced with the field samples by collecting and analyzing the whole samples with a methodology that utilized an automated system.

Overall, drug concentrations present in human biofluids can effectively be quantified using PS ionization with commercially available DBS devices. This method enables more flexibility in the manner of sample collection and analysis which benefits a successful, low cost clinical study.

CHAPTER 4. MULTIPLEXING PAPER SPRAY IONIZATION FOR TESTING OPIOIDS AND PRESCRIPTION DRUGS IN ORAL FLUID

4.1 Introduction

There are many situations in which professionals need information on the drugs in a person's system. In the clinical field, physicians in offices and emergency departments (ED) send out urine, blood, and oral fluid (OF) samples for analysis to labs for immunoassay screening and conformational testing by LC-MS/MS. The TAT associated with this testing harms patient care by preventing the physician from treating the patient quickly and providing new prescriptions. In-office testing by large clinics is becoming more common, however, the in-office tests still have long TATs. During roadside stops, a driver's impairment must be assessed with high accuracy while not requiring a blood draw. All of these tests are done routinely and they require a large volume of sample, time for chromatography, and are expensive. Immunoassays are a common point of care (POC) alternative but these are not as sensitive or selective for analytes as a MS assay.[51]

Previous chapters establish that PS-MS/MS allows for the analysis of drugs in biofluids. PS allows for fast acquisition and analysis while significantly lowering the sample volume and TAT of results compared to chromatographic assays. However, PS-MS/MS has not achieved a high level of quantitative multiplexing that is given by LC-MS/MS methods, which clinical and forensic fields are accustomed to. The objective is to utilize this technology to develop a multiplexed method for the quantitation of drugs in oral fluid (OF) using less sample and time than conventional techniques. This method is proof of concept for the multiplexed quantitation ability of PS and can be deployed to specific settings for demonstrating the workflow utility.

Many PS methods focus on whole blood analysis but OF is also a good match. OF is non-invasive, exchanges metabolites with the blood stream, is in good agreement with concentrations of other biofluids, and is used routinely for drug testing.[52-54] Additionally, it is more difficult for the patient to tamper with the sample. [55-57] However, there are many disadvantages to OF testing. For a typical LC-MS/MS OF assay, a large volume of sample (*c.a.* 2 mL) is required which can be difficult for many patients using drugs to provide.[57] Collection devices are often absorbent pads and drug recovery from these is poor.[56-57] A smaller volume of unbuffered OF (<10 µL) is all that is needed for PS and is collected easily for routine screening or in an emergency situation. PS-

MS/MS methods are significantly less expensive than LC methods which lowers healthcare costs of routine tests like these. In a laboratory a Velox 360 may be used to achieve high throughput analysis and an IMS may be integrated for an additional level of specificity for isobaric drugs. Alternatively, a mini mass spectrometer may be used for roadside screenings.

This multiplexed method is less than three minutes injection to injection has the capability of adapting too many different fields and biofluids. However, it is especially suited to yield rapid drug quant in OF for point of care testing. This method demonstrates the quantitative capability of 30 opioids, benzodiazepines, tranquillizers, illicit substances and their metabolites in oral fluid by PS-MS/MS. Initial validation data is given, as well.

4.2 Materials and Method

HPLC grade solvents and 99% pure formic acid were purchased from Signal Aldrich (St. Louis, MO). The following analytical grade standards were purchased from Cerilliant (Round Rock, TX): 6-monoacetylmorphine, alprazolam, amitriptyline, amphetamine, benzoylecogonine, buprenorphine, clozapine, cocaine, codeine, desipramine, diazepam, EDDP, fentanyl, fluoxetine, haloperidol, JWH 018, ketamine, MDMA, meprobamate, methadone, methamphetamine, morphine, norbuprenorphine, nordiazepam, O-desmethyl-cis-tramadol, oxycodone, paroxetine, propoxyphene, tramadol, venlafaxine, 6-monoacetylmorphine-D_3, alprazolam-D_5, amitriptyline-D_3, amphetamine-D_5, Benzoylecogonine-D_3, buprenorphine-D_4, Clozapine-D_4, codeine-D_3, Codeine-D_3, Desipramine-D_3, diazepam-D_5, EDDP-D_3, fentanyl-D_5, Fluoxetine-D_6, Haloperidol-D_4, JWH 018-D_{11}, Ketamine-D_4, MDMA-D_5, meprobamate-D_3, Methadone-D_3, Methamphetamine-D_5, morphine-D_3, norbuprenorphine-D_3, nordiazepam-D_5, O-desmethyl-cis-tramadol-D_6, oxycodone-D_3, Paroxetine-D_6, propoxyphene-D_5, tramadol-^{13}C, D_3, and Venlafaxine-D_6. Human negative oral fluid was purchased from BioreclamationIVT (Hicksville, NY). All additional PS materials are listed in Chapter 1.

A TSQ Quantum Access Max and Xcalibur software was used for data acquisition. All instrument parameters are listed in Table 4.1. Two transitions for most analytes were detected (Table 4.2) and one transitions per IS (not listed, transition matched quantifier ion). A few analytes gave only one fragment.

Cal and QC samples were prepared from separate stocks by diluting a 20X sample of the drugs into OF (20X dilution) and then IS was added at a 1:10 ratio. Cal and QC concentrations are in Table 4.3.

Table 4.1 TSQ Xcalibur acquisition parameters in MRM mode.

MS Polarity	Positive
Acquisition time (min)	1.8
Scan Time (ms)	75
Scan Width (*m/z*)	0.01
Peak Width (FWHM)	0.70
Collision Gas Pressure (mTorr)	1.5
Ion Transfer Tube Temperature (C)	300

Table 4.2 MRM transitions and parameters for the analytes.

Compound	Precursor Ion (m/z)	TL	Quantifier Product Ion (m/z)	CE	Qualifier Product Ion (m/z)	CE
6-Monoacetylmorphine	328.1	120	165.1	36	211.1	25
Alprazolam	309	120	281	25	206	23
Amitriptyline	278.1	81	233.1	16	191	25
Amphetamine	136.2	61	91.2	17	119.2	6
Benzoylecogonine	290.1	82	168.1	18	105.1	29
Buprenorphine	468.2	130	55.3	49	187	38
Clozapine	327.1	85	270	22	192	42
Cocaine	304.2	83	182.1	19	82.2	29
Codeine	300.1	100	215	25	165.1	39
Desipramine	267.1	80	72.3	16	208.1	22
Diazepam	285	91	193	32	154	25
EDDP	278.2	82	234.1	30	249.1	24
Fentanyl	337.3	87	188.1	22	105.1	34
Fluoxetine	310.1	103	44.4	13	-	-
Haloperidol	376.1	90	123	35	165	23
JWH 018	342.2	107	155	24	127.1	41
Ketamine	238.1	77	125.1	28	179	16
MDMA	194.1	73	163.1	12	135.1	20
Meprobamate	219.1	76	158.1	7	55.3	23
Methadone	310.2	61	265.1	15	105.1	28
Methamphetamine	150.1	92	119.2	10	91.2	19
Morphine	286.1	107	201.1	24	165.1	36
Norbuprenorphine	414.2	100	187	36	101.2	35
Nordiazepam	271	100	140.1	26	165	27
O-desmethyl-cis-tramadol	250.2	64	58.3	17	-	-
Oxycodone	316.2	92	298.1	18	241	28
Paroxetine	330.1	85	192.1	20	178.1	23
Propoxyphene	340.3	61	266.1	5	58.3	20
Tramadol	264.2	61	58.3	16	-	-
Venlafaxine	278.2	68	260.1	11	121.1	29

Table 4.3 Cal and QC concentration for the drugs measured in OF.

Compound	Cal1	Cal2	Cal3	Cal4	Cal5	Cal6	QC1	QC2
6-Monoacetylmorphine	5	10	50	100	250	500	15	125
Alprazolam	5	10	50	100	250	500	15	125
Amitriptyline	5	10	50	100	250	500	15	125
Amphetamine	10	20	100	200	500	1000	30	250
Benzoylecogonine	10	20	100	200	500	1000	30	250
Buprenorphine	100	200	1000	2000	5000	10000	300	2500
Clozapine	1	2	10	20	50	100	3	25
Cocaine	1	2	10	20	50	100	3	25
Codeine	25	50	250	500	1250	2500	75	625
Desipramine	1	2	10	20	50	100	3	25
Diazepam	5	10	50	100	250	500	15	125
EDDP	1	2	10	20	50	100	3	25
Fentanyl	1	2	10	20	50	100	3	25
Fluoxetine	1	2	10	20	50	100	3	25
Haloperidol	1	2	10	20	50	100	3	25
JWH 018	10	20	100	200	500	1000	30	250
Ketamine	5	10	50	100	250	500	15	125
MDMA	1	2	10	20	50	100	3	25
Meprobamate	5	10	50	100	250	500	15	125
Methadone	1	2	10	20	50	100	3	25
Methamphetamine	10	20	100	200	500	1000	30	250
Morphine	25	50	250	500	1250	2500	75	625
Norbuprenorphine	25	50	250	500	1250	2500	75	625
Nordiazepam	1	2	10	20	50	100	3	25
O-desmethyl-cis-tramadol	1	2	10	20	50	100	3	25
Oxycodone	5	10	50	100	250	500	15	125
Paroxetine	10	20	100	200	500	1000	30	250
Propoxyphene	5	10	50	100	250	500	30	200
Tramadol	1	2	10	20	50	100	3	25
Venlafaxine	1	2	10	20	50	100	3	25

PS was performed manually. W31 was precut as described in Chapter 1 and attached to a copper clip. The OF Cal and QC samples (7 µL) were pipetted and dried for 15 minutes. The solvent (75 µL, 95% methanol, 5% water, and 0.1% formic acid) was added throughout the data acquisition to maintain spray for 1.8 minutes.

The data analysis was automated in a MatLab program but can also be analyzed with Xcalibur. The TIC for the quantifier transition was integrated and divided by the TIC area of the IS transition. This relative intensity was plotted against the calibrator concentration to build a curve (Figure 4.1) or used to determine the concentration of a QC (Table 4.4). The Qual/Quant was calculated for each sample for each analyte.

Six replicates of Cals and QCs were acquired. Blank samples were tested after the high Cal and QCs to assess carryover. A matrix effect study was done by comparing IS signal of samples prepared in OF to those prepared in methanol. An interference study was performed by testing other drugs at high concentrations to assess specificity of the ion transitions with other common drugs.

4.3 Results and Discussion

All tested compounds were selectively detected down to the ng/mL range. LODs for all analytes are clinically relevant to drug cutoffs and most are within an order of magnitude of POC testing requirements (Table 4.4).[51, 54]

A summary of the performance is in Table 4.4 and example Cal curves is in Figure 4.1. The statistical results of the method showed precision, accuracy and linearity. All analytes but one had an average RSD of less than 20% for six replicates. Mebrobamate was the exception here and it was likely due to a low internal standard concentration that caused inconsistent normalization. A few of the analytes had higher RSDs for the Cal 1. This is expected at lower concentrations but may be improved with a more sensitive QQQ. The QCs had an error less than 20% showing the accuracy of this method. The low QC error had more error but was still <20%.

The qualifier quantifier ratio of the transitions is a further way to check for specificity. This ratio must be stable (within 20% from calibrator 3) throughout the calibration curve range and the ratio must be met (within 20%) in unknown samples for a positive identification. The RSD of this ratio is reported in Table 4.4. For most analytes the ratio is stable however, some analytes do not have two selective *and* sensitive transitions which causes the ratio to be lost on the low end. A more sensitive QQQ could correct this low end sensitivity problem or the MRM acquisition parameters can be adjusted for the qualifying transition by monitoring the quantifier mass with a CE that achieve a Qual/Quant ratio.

Table 4.4 Results summary from the PS-MS/MS method.

Compound	LOD (ng/mL)	Cal Curve R^2	Average RSD	QC Low Error	QC High Error	Qual/Quant RSD
6-Monoacetylmorphine	< 5	0.9997	10%	3%	4%	15%
Alprazolam	< 5	0.9987	16%	12%	6%	9%
Amitriptyline	1	0.9997	9%	20%	3%	3%
Amphetamine	5	0.9999	6%	19%	3%	18%
Benzoylecogonine	5	1	4%	8%	3%	7%
Buprenorphine	< 100	0.9999	7%	12%	2%	26%
Clozapine	< 1	0.9998	9%	14%	9%	10%
Cocaine	< 1	0.9999	7%	2%	7%	3%
Codeine	10	0.9934	15%	15%	12%	10%
Desipramine	< 1	0.9997	8%	15%	4%	8%
Diazepam	< 5	0.9995	7%	7%	3%	2%
EDDP	< 1	0.9996	8%	6%	6%	4%
Fentanyl	< 1	0.9999	5%	2%	8%	11%
Fluoxetine	< 1	0.9992	15%	8%	5%	-
Haloperidol	< 1	0.9999	5%	10%	14%	2%
JWH 018	5	0.9999	7%	15%	4%	2%
Ketamine	< 5	0.9998	4%	0%	1%	7%
MDMA	< 1	0.9998	7%	10%	16%	17%
Meprobamate	< 5	0.9997	22%	17%	1%	96%
Methadone	< 1	0.9999	3%	18%	0%	5%
Methamphetamine	5	1	5%	5%	9%	2%
Morphine	10	0.9998	9%	2%	10%	8%
Norbuprenorphine	10	0.9993	11%	3%	3%	2%
Nordiazepam	< 1	0.9999	12%	16%	2%	16%
O-desmethyl-cis-tramadol	1	0.9997	4%	3%	3%	-
Oxycodone	1	0.9999	8%	9%	0%	35%
Paroxetine	5	0.9998	13%	8%	8%	23%
Propoxyphene	< 1	0.9996	12%	12%	0%	16%
Tramadol	< 1	0.9999	7%	6%	0%	-
Venlafaxine	5	0.9995	7%	1%	4%	5%

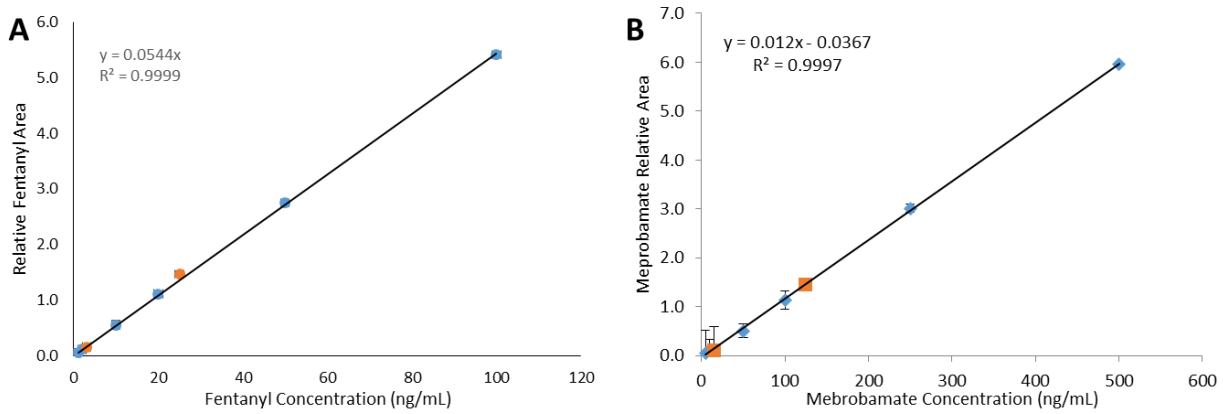

Figure 4.1 Two Cal curve examples (blue) with their QC sample results (red). Each point is the average signal of six replicates and the errors bars represent one standard deviation. (A) Fentanyl is one of the best performing analytes and (B) meprobamate is one of the worst.

Carryover studies showed no contamination after high concentration samples. Some matrix suppression is occurring. There is on average 21% absolute signal for the OF sample compared to a methanol sample. Quantification is still possible due data normalization with the use of quality stable isotope internal standards. Interferences did occur with isobaric compounds (*e.g.* hydromorphone and morphine). This yields false positives within the compound class. Unfortunately, the structure of some compound classes are too similar that specific transitions for these do not exist. For absolute quantitation of these analytes, IMS can be employed for additional specificity. Otherwise, it can be used for a qualitative screening.[58]

4.4 Conclusions

This PS-MS/MS methodology demonstrates a proof of concept for rapidmultiplexed drug analysis of intact oral fluid. The limits of detection were relevant to existing immunoassay cutoffs. More sensitivity is needed to reach the cutoff of all LC-MS/MS assays but they are near the cutoff values in this assays.[51, 53] A more sensitive MS could be used to lower the cutoffs in this assay even further. This would improve the Qual/Quant ratio as well. The reproducibility of standard solutions was often below 15% RSD and percent error of the QC samples was below 20%.

PS-MS/MS significantly lowers sample volume requirements for OF testing in comparison to chromatographic assays, and reduces TAT for quantification of target drugs. The assay was

rapid, collecting quantitative data on 30 analytes in under three minutes. Additional multiplexing can be achieved with a faster MS and more resources for standards. The increased speed and reduced sample volume are important for clinical and ED toxicological OF testing, where time is critical and a large volume of OF is difficult to provide. Other biofluids are invasive (blood) or maybe tampered with (urine). However, this method must be automated with the Velox 360 PS source for this application. Additionally, the MS should be coupled with an IMS to achieve more selectivity for drugs with similar ion transitions. In a forensic setting, this method would be more applicable with a miniature MS that has a PS interface for POC analysis. For this application, low detection limits are important but a drug screening method maybe all that is needed.

PART 2: MRM-PROFILING: RAPID SCREENING AND CLASSIFICATION OF SAMPLES BASED ON A MOLECULAR PROFILE

CHAPTER 5. MRM-PROFILING OF HUMAN PLASMA FOR CORONARY ARTERY DISEASE BIOMARKER DISCOVERY

5.1 Background

Metabolite profiling for biomarker discovery is an important aspect to improve disease diagnostics and make new therapeutic advancements. Metabolites are characteristic of an organism's phenotype and include information on the organism's diet, environment, genetics, and health.[59-60] When investigated appropriately, a metabolomics study uncovers biomarkers that are specific for a disease state. These can then be used for understanding a disease mechanism, designing new drugs, or diagnosing a disease. [59, 61]

Metabolomic studies often employ MS for its sensitivity and specificity in both an untargeted and targeted fashion. Targeted methodologies use MS/MS or MRM to analyze specific analytes that are known in a sample.[60, 62-63] These can be quantitative and may require standard solutions and stable isotopically labeled internal standards for signal normalization. Targeted methods require *a priori* knowledge of analytes or pathways affected by a disease.[60] These methods do not discover new analytes for a disease. Rather, they focus on quantifying known analytes, observing changes in different populations of compounds, and determining if any can serve as a biomarker. It is challenging for these methods to take into account heterogeneity of diseases where multiple pathways can be affected.[63-64]

High resolution instruments are often utilized to collect full scan or product ion scan data for untargeted methods. HRMS provides accurate mass for formula generation and resolves analytes with similar monoisotopic masses.[65-66] These scans are data dependent, are not based on biological understanding of the disease, and do not require prior knowledge about the disease metabolism or pathways.[60] Many utilize algorithms which fragment peaks over a certain threshold (counts). Therefore, these methods are often biased toward peaks with the highest intensity, which causes lower intensity peaks to not be analyzed and data lost. Ignoring such data is not a good strategy for identifying new biomarkers. If 2D data domain screening (product ion scans over a large mass range) is performed, then a large amount of sample is used to collect what may be an excessive amount of data, much of which may not be biologically relevant.[64, 67] Practically, HRMS systems require daily maintenance to prevent MS shifts and their data files are very large, requiring expensive data storage solutions and management considerations.

Both targeted and untargeted metabolomics methodologies typically employ chromatographic separation (*e.g.* LC). This is time consuming (*c.a.* 30 min/sample), error prone (*e.g.* RT shifts), and subjected to pump malfunctions and column clogs.[59, 68] Furthermore, columns and mobile phases are expensive and drive up the cost of a project. Lastly, chromatography does not measure an intact sample. Sample prep is often required before injection onto a column and analytes that may be of interest could be lost in this process. These steps bias analytes on polarity and charge.[59]

Advances in traditional metabolomics methodologies tend to scale up resolution and scan speed of MS systems. The field needs a new approach of interrogating an intact sample with a biological purpose for metabolite profiling, sample classification, and biomarker discovery. MRM-profiling is a rapid, semi-targeted metabolomics methodology that can accomplish all of these.[69] It searches a few pooled samples for ion transitions using precursor (Prec) and neutral loss (NL) scans that are specific for biological functional groups, especially groups likely to be associated with the subject samples.[70] The discovered ion transitions are then placed into a MRM method which can scan each transition on the millisecond time scale for rapid acquisition of metabolite signals. A thousand samples takes just days to acquire all the data.

Omics data analysis workflows analyze data that contains a number of factors and is ideal for processing MRM-profiling data. Univariate statistics, *e.g.* t-test and fold change (FC), are applied so only significant transitions remain. Then, multivariate statistics, *e.g.* partial least squared discriminant analysis (PLSDA), is used to build classification models and determine the specificity, sensitivity, and accuracy of the MRM-profile.[65, 71] In this way, the net interactions of all affected metabolites create a metabolite profile, by comparing many metabolites that are either up or down regulated in a disease population. These changes classify an unknown sample. A schematic of the MRM-profiling discovery and screening phases is presented in Figure 5.1.

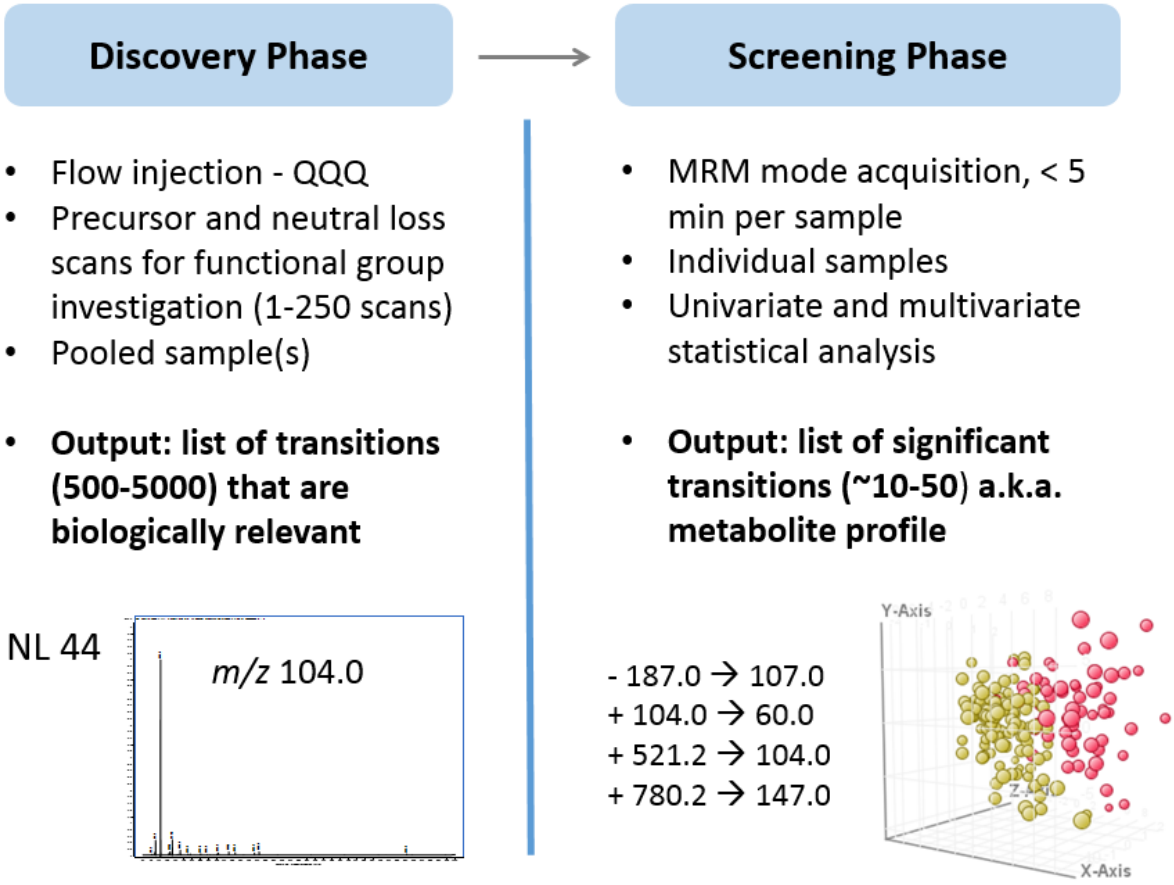

Figure 5.1 Workflow diagram of MRM profiling experiments showing a specific case of NL 44 amu. Discovery and screening phases produce a metabolite profile for a disease which can be used for classification of samples.

MRM-profiling is much more high-throughput than LC-MS metabolomics methods because it directly introduces a diluted sample or simple extract into the MS. No time or materials are required for chromatography. Instead, with direct infusion (DI) or flow injection (FI) techniques, in lieu of LC, the user saves time and money and they also analyze an intact or near intact sample. No complex sample pretreatment is needed, just a simple dilution. Therefore, DI or FI can measure many analytes with varying chemical properties.[59, 72] This is a move closer to universal analysis of the metabolome.[59-60]

For MRM-profiling, a QQQ is utilized for MS/MS experiments. Rather than performing full scan or product ion scan experiments, a pooled sample is explored with a biological purpose.

Prec and NL scans, selected to measure known and/or common functional groups, facilitates discovery of the biologically significant signals. The Prec and NL scans cover a wide variety of functional groups and classes of molecules. When all are employed in a study, metabolites are interrogated in an unsupervised fashion and the methodology aims to impose no bias of what metabolites are discovered. After the discovery, the Prec and NL signals are converted into ion transitions and MRM mode is used to collect data for only the targeted set of signals for each sample. Thus, unnecessary data collection of background noise or non-biological, unimportant signal is eliminated and the speed of screening large sample sets is increased.

Selectivity is achieved with fragmentation. However, without high resolution or chromatography isobaric analytes still exist. Even though a single ion transition may measure multiple analytes, significant alterations can still be found in the metabolite profile [ref Fernanda]. Additionally, ion suppression or enhancement is embraced here and thought of as an intrinsic feature of the sample which adds information rather than losing it. Since the signal is analyzed as relative signal intensity modulation by the matrix does not interfere with the analysis. However, only a relative, not quantitative, understanding of how an analyte is fluctuating is known. Finally, data analysis workflows are simpler than LC and HRMS methods since no RT or mass correction is necessary.

So far, all MRM-profiling methods have required minimal amounts of sample, often <20 µL of biofluid, making them ideal for analyzing a drop of blood from a finger prick. It is thus conservative of precious samples. Previously, MRM-profiling has been demonstrated with cerebrospinal fluid analysis for Parkinson's disease, follicular fluid analysis for polycystic ovarian syndrome, and diet alterations in humans amongst other studies.[69, 73-74] These studies were successful at discovering ion transitions that could separate different populations.

As interest grows in this methodology, it is desirable to confirm that this workflow improves biomarker discovery and allows discovery of metabolite signals related to the disease. This is tested as described below by studying a sample set of a well characterized disease, screening a large sample set (N>900) quickly, relating the MRM signal profile to biomarkers that are biologically relevant, and confirming their identity by LC-MS. Coronary artery disease (CAD) is a well-studied and highly prevalent disease. In the US alone, over 90 million people suffer from some form of cardiovascular disease and one in three deaths in the US were attributed to CAD.[75] Worldwide, escalations and complications from CAD caused 7.4 million deaths in 2015.[76]

Currently, generic blood panels and physical examinations are performed for initial screening followed by invasive stress testing and imaging to confirm the diagnosis.[77] New molecular biomarkers for diagnosing CAD and evaluating a prescription or lifestyle therapy could benefit this ever growing patient population and reduce healthcare costs related to CAD.

The 900 plus plasma samples studied here are characterized as either case (CAD) or control. The metabolite signal is discovered by MRM-profiling then investigated by traditional methods to demonstrate that the MRM-profiling signal is related to CAD metabolism. Also discussed in this chapter are method development considerations for MRM-profiling and an example of method optimization for the CAD project is given so that new laboratories can quickly adopt this methodology for biomarker discovery.

5.2 Materials

5.2.1 Instrumentation and Software

An Agilent 1290 Infinity series pump and a 6470 QQQ were used for MRM-profiling (Santa Clara, CA). For sample preparation, an Agilent Bravo Automatic Liquid Handling Platform was used for pipetting, a Thermo Fisher Scientific SpeedVac was used for drying the samples, and an Agilent PlateLoc was used for sealing 96-well plates. An Agilent 6545 QTOF was used for HRMS acquisition. MassHunter Acquisition (B.08.00), Qualitative (B.08.00), and Quantitative (B.08.00) software were used for MRM-profiling and LC-MS experiments. For the univariate and multivariate statistics, Metaboanalyst 3.0 (metaboanalyst.ca, accessed 08/2017-09/2017) and Mass Profiler Professional (B.14.8) were used.

5.2.2 Chemicals

Agilent HPLC vials with 200 µL glass sample inserts were used for single sample analysis. Deep and shallow poly propylene 96 well plates were used for high throughput sample preparation. HPLC grade acetonitrile, methanol, and chloroform were all used for sample preparation and analysis. Millipore ultra-pure water (18.2 MOhm) was procured from a house system. Analytical grade formic acid, ammonium formate, and reserpine were from Sigma Aldrich. Alprazolam-D_5 (0.1 mg/mL) was purchased from Cerilliant. Plates were sealed with an Agilent PlateLoc using the

foil seal. An Agilent ZORBAX Eclipse Plus RRHD C18, 2.1 × 150 mm, 1.8 µm column was used for separation.

5.2.3 Samples

Human plasma samples (1081) were provided to Dr. Tommy Sors, Discovery Park, Purdue University from the Fairbanks Institute for Healthy Communities (Indianapolis, IN) and stored at -80 C. Some clinical data was also provided for each sample (*e.g.* case/control, gender, age, medical history, lab results). This data is expansive but incomplete for many samples.

5.3 Method Development

Considerations for implementing MRM-profiling and parameters for optimization are discussed below. Specifically, a FI-MRM-profiling method optimization for studying CAD is described. These experiments can be adopted for DI methods or projects with other samples.

5.3.1 System Setup and Sample Introduction

As mentioned above, MRM-profiling uses a QQQ which very fast, reproducible, and does not require much maintenance as the experiment is in progress (*i.e.* no cleaning or calibration during a multi-day experiment). Without chromatography, errors associated with separation (*e.g.* RT shift) are avoided. Overall, with proper method development, robust data collection is easy.

For ionization, ESI has been employed the most with MRM-profiling. However, the mode of introducing the sample into the source has varied. Some methods have used a glass syringe and syringe pump to directly infuse (DI) sample into the ionization source. Other methods, like the one described in this chapter, used a HPLC pump for flow injection (FI) analysis.[72-73] Careful consideration of DI and FI benefits and limitations must be made before beginning a project. FI is automatic and carries a small volume of diluted sample or extract (20 -40 µL plug of sample) to the ESI source through LC pump lines with the solvent flow. However, as seen with this CAD method and elsewhere, it can be more time consuming since the sample must travel to the source and more time is required for cleaning the solvent lines.[78] DI methods continuously introduce sample into the MS. These methods may require a larger volume of diluted sample (>200 µL) and

are difficult to automated. However, they are much faster since they require nearly no time to reach the source and minimal cleaning. Another methodology not yet explored with MRM-profiling is nano-infusion. [59-60] This is similar to DI but it uses a very small amount of sample 5-20 µL diluted sample and requires no time for cleaning since the nozzles are single use. This is automated in the NanoMate® and is therefore amenable to high throughput analysis. [12] However, the method is sensitive to high salt content so not every biological sample may work with this setup. Ambient ionization methods could also be used but have been developed minimally with MRM-profiling. Briefly, PS is limited by the time it can spray the sample, can have high background noise, and, similar to chromatography, some analytes can be retained on the paper and not analyzed. DI and nano-infusion methods continuously introduce sample to the MS. This is advantageous in measuring large transition sets (>500 transitions) in a MRM-profiling method. As demonstrated below, FI methods have a discrete amount of time the sample is introduced and may require more than one injection to collect data for all the ion transitions. This adds significant time to the method.

Because of the large sample set, automation was necessary for this project. A NanoMate® was not available so FI was chosen. An Agilent 6470 QQQ with a 1290 pump was used for this project. For FI, the pump was connected using the shortest tubing that had the smallest inner diameter available. A 20 µL sample loop was initially used and switched to a 40 µL sample loop as needed. Since a column was not used, the sample was sent directly from the auto sampler to the Agilent Jet Stream (AJS) source, by-passing the MS switching valve and sample filter for time savings. A low flow rate (<0.1 mL/min) was desired to maximize the number of scans collected during one injection. To create enough back pressure on the pump, restrictive tubing was placed on the pump prior to the auto sampler switching valve. The addition of multiple lines of restrictive tubing did not achieve the required pressure (>30 bar) so a short C18 column was added prior to the injection port. This column was intended to only build pressure, not for separation. Future systems should investigate a NanoMate®, nanoLC, or alternative tubing to avoid adding a column.

5.3.2 Sample Preparation

Dilute and shoot sample preparation is encouraged for MRM-profiling so that no metabolites or potential biomarkers are lost in complex sample preparation phase. Another MRM-profiling project described in Chapter 8 utilized a simple dilution of cerebrospinal fluid and

achieved reproducible analysis. However, dilute and shoot of human plasma does not give acceptable reproducibility. Therefore, a modified Bligh Dyer extraction procedure was used to extract lipids and small metabolites.[73, 79] For high throughput sample preparation, several of these steps were automated by using a Bravo liquid-liquid handler (Table 5.1) and 96-well plates were employed. Given more time for development the whole workflow could be automated.

Table 5.1 Modified Bligh-Dyer sample preparation procedures of human plasma for MRM-profiling.[a]

Step:	Addition of:	Volume (µL)	Manual/Bravo
1	Plasma	40	Manual
2	Chloroform	100	Bravo
3	Methanol	180	Bravo
4	Vortex, 30s		Manual
5	Chloroform	100	Bravo
6	Water	100	Bravo
7	Vortex, 60 s		Manual
8	Centrifuge, 60 m, 4000 RPM		Manual
9	Collect 75 µL top and bottom layer, place in new container		Manual
10	Dry down, SpeedVac, 50C, ~3hr		Manual
11	Solvent	300	Bravo
12	Sonicate, 10 m		Manual
13	Centrifuge, 5 m, 4000 RPM		Manual
14	Dilute 200X into solvent		Bravo

a. The addition of samples and reagents and their respective volumes are listed. Notes for if the step was performed manually or by the Bravo liquid-liquid handler and additional sample preparation details are given.

After step 8, three layers exist, a top aqueous and polar layer containing polar metabolites, a middle solid white layer of protein, and a bottom chloroform layer containing lipids. An inconsistent issue that arose during the project was that the protein layer interfered with the

collection of the lower layer if it was not centrifuged enough. This could be avoided in future experiments by (1) using less plasma and thus minimizing the protein layer or (2) using a higher speed rotor for centrifugation (20,000 rpm, not 4,000 rpm).

This final sample preparation procedure was used for every MRM-profiling experiment. During development, the sample preparation was often performed one sample at a time, not a 96 well plate format, or using alternative volumes. These differences are noted for each experiment in the sections below.

5.3.3 Solvent Evaluation and Source Conditions

The solvent and modifier conditions are influential parameters for this analysis and their development should be considered for every MRM-profiling project. For MRM-profiling the solvent and source conditions should aim to dissolve and ionize all analytes in the sample. Given the diversity of the analytes in a biological system this is difficult to achieve. If information is known about the analytes in the sample or of interest in the disease, a solvent can be tailored for those. In no information about what analytes are of interest, then optimization should aim at detection of as many different types of analytes as possible. For the CAD solvent optimization, tradeoffs in ionizing one class of molecules over another occurred. But by exploring different options with simple experiments, clear data was gathered as to which solvent was best.

A few solvents were tested with the plasma extract. These were known to give good signal for lipids, however, their performance with small metabolites was unknown.[73, 80] These solvents were used to reconstitute the dried plasma extracts (step 11, Table 5.1) and were used as the pump solvent.

A: 70% acetonitrile, 30% methanol, 10 ppm ammonium formate, 0.1% formic acid
B: 90% methanol, 10% chloroform, 10 ppm ammonium formate, 0.1% formic acid
C: 66% chloroform, 33% methanol, 10 ppm ammonium formate, 0.1% formic acid

Source conditions with the AJS needed to be optimized for each solvent system under consideration. This was done manually by optimizing the parameters in Table 5.2. The parameters were optimized in the order listed by injecting a reserpine standard diluted in the solvent and selecting the condition with the highest absolute signal intensity. This methodology worked well but could be improved by measuring analytes with varied chemical properties. Therefore, a

phosphotidylcholine (PC) lipid was added to the sample and conditions were re-optimized. The AJS parameters for solvent A and solvent B are in Table 5.2.

Table 5.2 AJS source parameters optimized with the ranges and steps tested. [b]

Parameter	Unit	Range	Step	Solvent A	Solvent B
Capillary voltage	V	2000-4000	500	2500	3500
Sheath gas temperature	C	50-300	50	150	200
Sheath gas flow	L/min	4-12	2	6	6
Gas temperature	C	50-350	50	300	350
Gas flow	L/min	3-13	2	7	11
Nebulizer	psi	20-60	10	25	60

b. Each parameter was tested individually by injecting a standard (n=3) and selecting the value with the highest MRM signal of the standard. AJS parameters optimized for solvent A and solvent B when using a flow rate of 0.05 mL/min are listed as well.

The nozzle voltage was not evaluated and this remained at 1500V for all experiments. These parameters were optimized using a flow rate of 0.05 mL/min. For any flow rate significantly different from this, source conditions may need to be reevaluated. Under these conditions, solvent A and B had pressures of 20 and 30 bar, respectively.

Solvent C is commonly used for lipid analysis. However, here it caused the ammonium formate to crash out in the source and continuously clogged the nebulizer regardless of the AJS source parameters. This solvent was therefore eliminated. With optimized AJS conditions, solvent A gave 100X greater signal for reserpine. Analysis of an undiluted plasma extract in solvent A gave very good results for a PC, positive mode, Prec 184 scan (Figure 5.2)

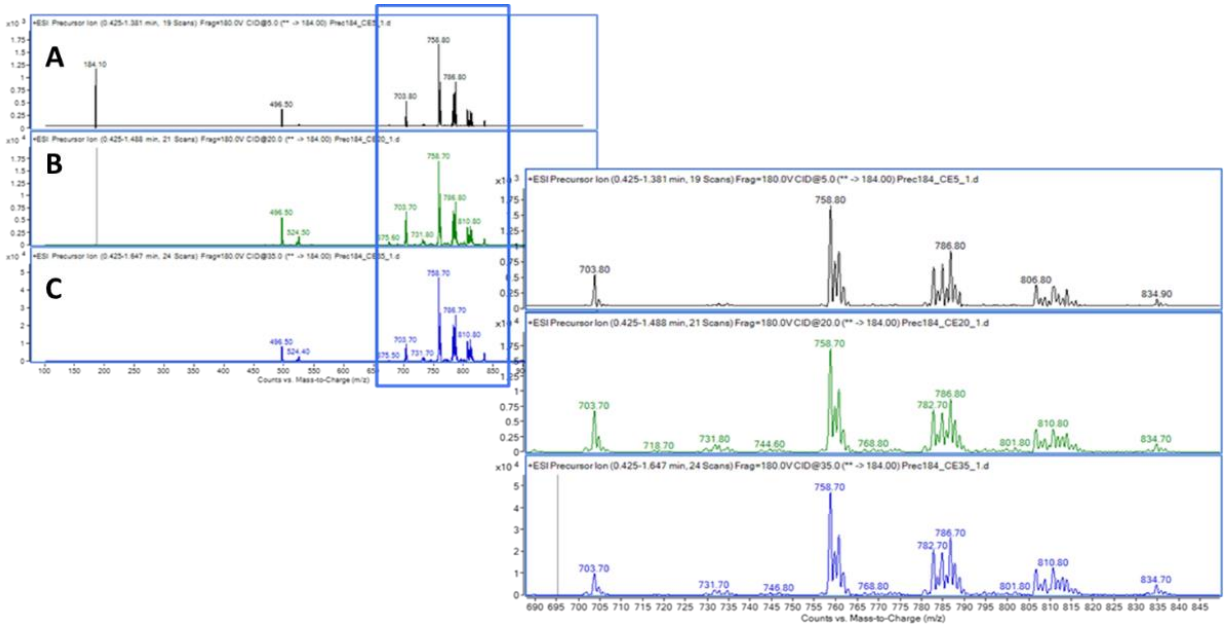

Figure 5.2 Positive mode, Prec 184 scan of sample extract in solvent A with no dilution at three different collision energies, 5 (A), 20 (B), and 35 (C) eV. Data was collected from *m/z* 100-1000 (left) and *m/z* 690-845 region is enhanced (right).

However, upon inspecting the negative mode, it was found that the solvent A did not dissolve and/or ionize the plasma extract sample well. Figure 5.3 shows negative mode full scan spectra of the lipid region, *m/z* 530-980. No negative mode peaks were seen with solvent A (Figure 5.3, A) but solvent B had distinct lipid signals (Figure 5.3, B). Solvent B was selected and evaluated for acid addition.

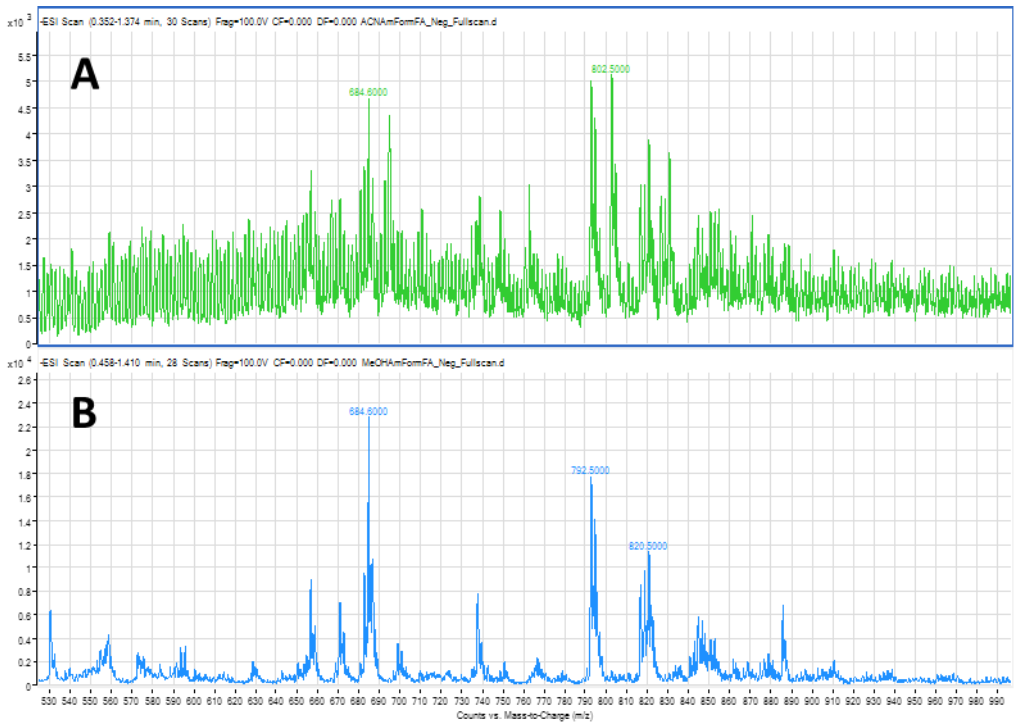

Figure 5.3 Negative mode, full scan spectra from *m/z* 530-990 of a human plasma extract reconstituted and injected with either (A) solvent A (70% acetonitrile, 30% methanol, 10 ppm ammonium formate, 0.1% formic acid, top) or (B) solvent B (90% methanol, 10% chloroform, 10 ppm ammonium formate, 0.1% formic acid, bottom).

Modifiers help create certain adducts but they should only be used if they do not impair compound ionization of other analytes. Figure 5.4 shows positive mode, Prec spectra of human plasma sample in solvent B prepared with (A) and without acid (B). The solvent with acid had 10^4 signal and many small metabolites below *m/z* 315 were only seen with this solvent. However, the peaks that appeared with no acid, namely *m/z* 369.1 and 426.0 were present at the same intensity in both solvents.

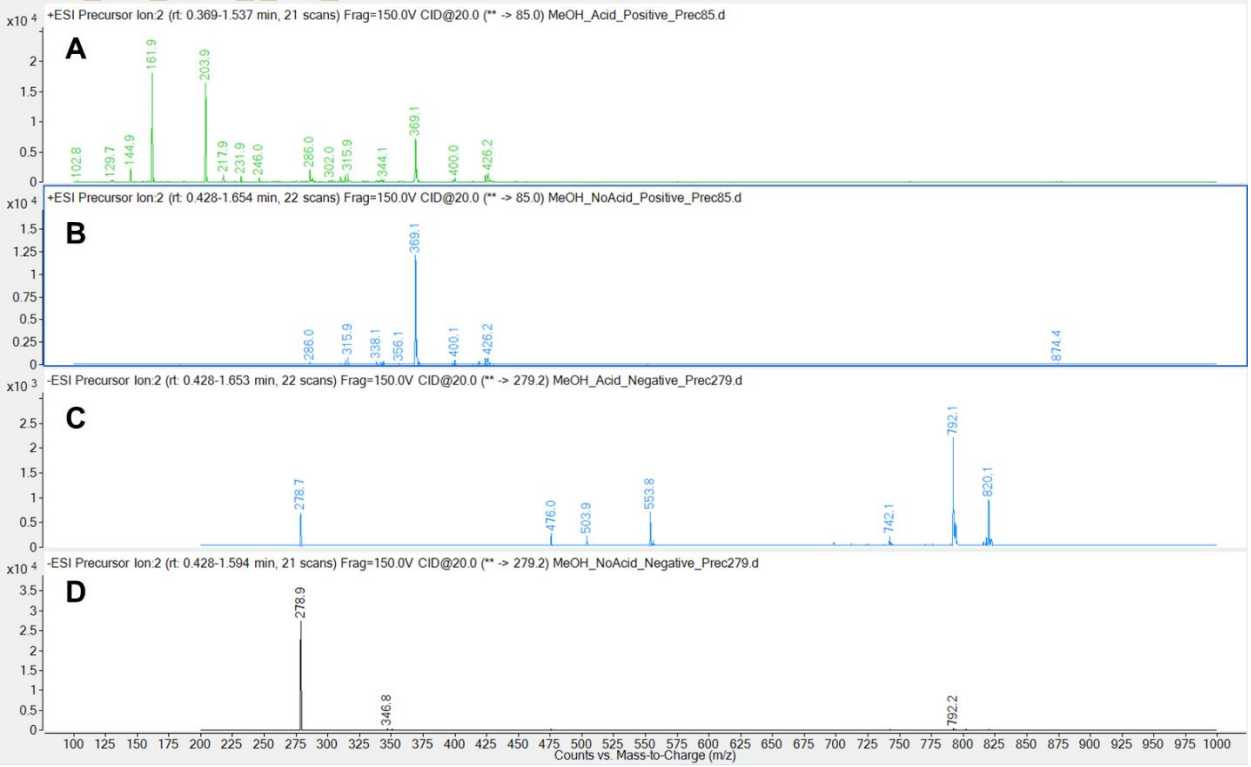

Figure 5.4 Positive mode, Prec 85 scan (CE 20) from *m/z* 100-1000 of plasma sample prepared and sprayed with solvent B with acid (A) and solvent without acid (B). Negative mode, Prec 279.2 scan (CE 20) from *m/z* 200-1000 of plasma sample prepared and sprayed with solvent B with acid (C) and solvent without acid (D).

Similar profiles are found for both solvents in the negative mode (Figure 5.4, C and D). A Prec 279.2 scan using solvent (C) which contains acid gave several additional peaks compared to solvent without acid (D). Because of the numerous additional peaks in both the positive and negative mode, the acidified solvent was better for this method than the solvent without modifier.

The use of the automated auto-sampler required a solvent for washing the needle that collected and injected the sample to prevent needle carryover. A 2:2:1 mixture of methanol: isopropyl alcohol: chloroform was selected to remove both polar and lipid material.

5.3.4 Prec and NL Scan Optimization

Initial Prec and NL tests were performed using a pooled plasma sample prepared with solvent A. Samples were treated as described in Table 5.1 except that 150 µL of the top and bottom

layers were collected, the sample was dried for a longer period of time at 36 C, and the sample was reconstituted in 400 µL solvent A. This sample was then tested with no further dilution and also with a 20X and 200X dilution of the reconstituted extract into solvent A.

For optimization a random selection of Prec and NL scans in both positive and negative mode were selected to be used for optimization of scan parameters. The goal was to create a method that was fast, reproducible, required one injection of sample, measured three or more collisions energies, and could easily be analyzed with MassHunter Qualitative software. The dilutions of the sample extract were also tested and carryover initially evaluated. Note, all Prec and NL scans covered the largest mass/charge range possible from *m/z* 50-1000 but certain NL scans were limited on the low end. Discovery scans for some MRM-profiling projects could go higher than this range.

Optimized scan speed and sample injection volume were key for obtaining good spectra in one injection for three CE values (5, 20, and 35 eV). Figures 7.5 and 7.6 show spectra collected at different scan speeds with a positive mode NL 32 and NL 299 scan, respectively. The NL 32 scan (Figure 5.5) is one that gives low single from this sample overall and it has the largest expected scan range of any of the scans in the discovery phase. If this scan can be improved it is assumed the data for all the other Prec and NL scans will also improve. The 200 ms scan speed (Figure 5.5, A) is too fast to measure any significant signal. The 500 and 1000 ms scans (Figure 5.5, B and C) show a higher *m/z* 126.9 peak but the 2000 ms scan (Figure 5.5, D) shows the highest intensity for *m/z* 126.9 and a clear *m/z* 318.9 peak.

The NL 299 scan in Figure 5.6 has a much higher signal overall from the human plasma extract. However, an improvement in peak shape can be seen in the *m/z* 820-920 region as scan time increases from 500 to 1000 ms (Figure 5.6 A, B). In both these examples, spectrum quality can be improved by increasing scan time and this parameter should always be evaluated for discovery phase experiments.

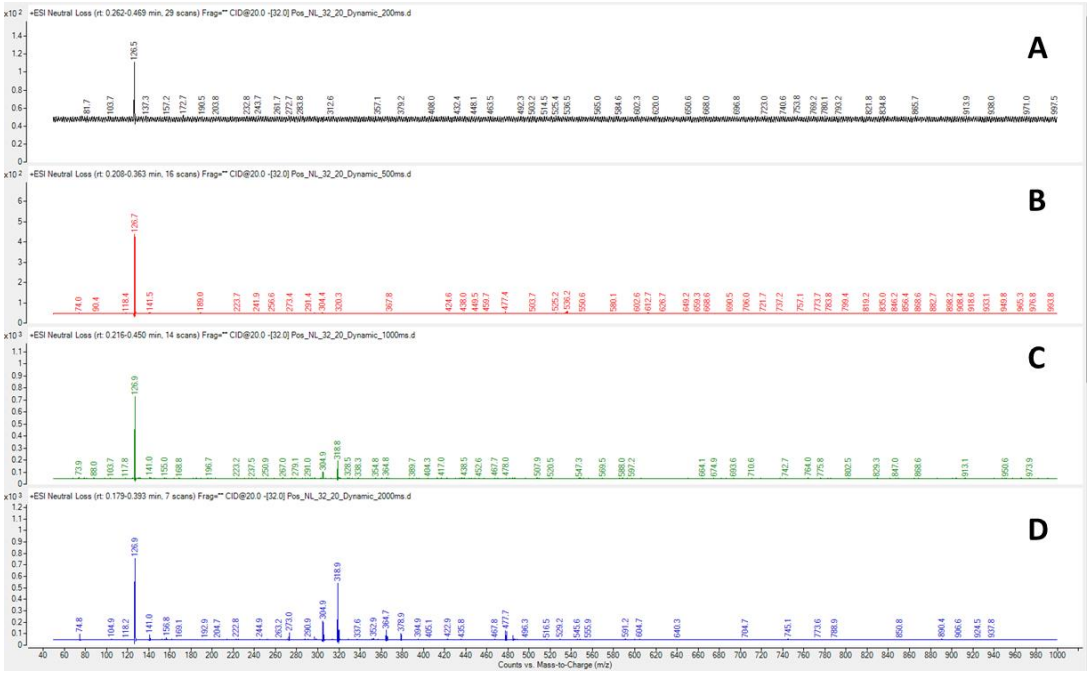

Figure 5.5 Positive mode NL 32 from *m/z* 50-1000 collected with four different scan times: 200 (A), 500 (B), 1000 (C), and 2000 (D) ms. This data was collected with a 200X diluted human plasma extract in solvent B.

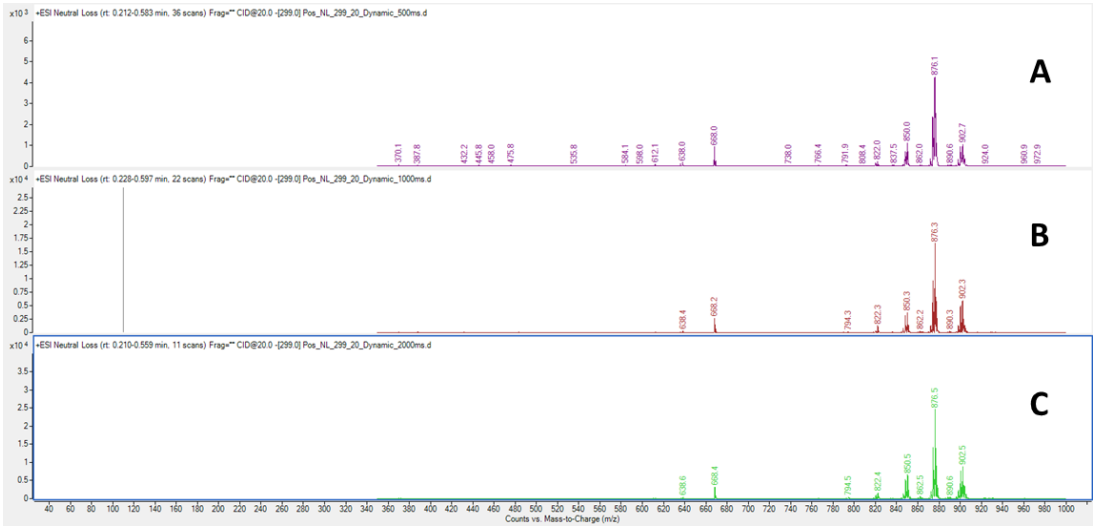

Figure 5.6 Positive mode NL 299 from *m/z* 350-1000 collected with three different scan times: 500 (A), 1000 (B), and 2000 (C) ms. This data was collected with a 200X diluted human plasma extract in solvent B.

In order to collect enough scans at three different CE (5, 20, 35 eV; 5-10 scans/CE) with a 1000 or 2000 ms scan time the length of time sample is sprayed into the MS must be increased. This can be accomplished by slowing down the flow rate to below 0.05 mL/min or by injecting more than 20 µL of sample.

With the 1290 pump, the flow rate cannot be decreased without lowering the pressure to below 30 bar. Slowing down the flow rate was not an option with this configuration but it could be with a nanoLC. A better approach was to inject more sample. Given the sample preparation procedure, this is not an issue for plasma extracts but for projects with more precious sample this may not be possible and nano-infusion or DI might be a better option. Figure 5.7 shows a positive mode NL 299 scan injected with 20, 30, and 40 µL of a 20X dilution of plasma extract. There is a clear increase in the time the sample was sprayed for the larger injection volume. Using 80% absolute intensity (y-axis) as a marker for sample cutoff, it can be approximated the spray times for the 20, 30, and 40 µL injections are approximately 0.3, 0.5, and 0.9 minutes, respectively. The subsequent spectra show no difference in signal intensity or quality of peaks (Figure 5.7, inset). Note the tailing in the signal increases as the sample volume increases suggesting that a larger sample volume may require a longer wash period to prevent carryover.

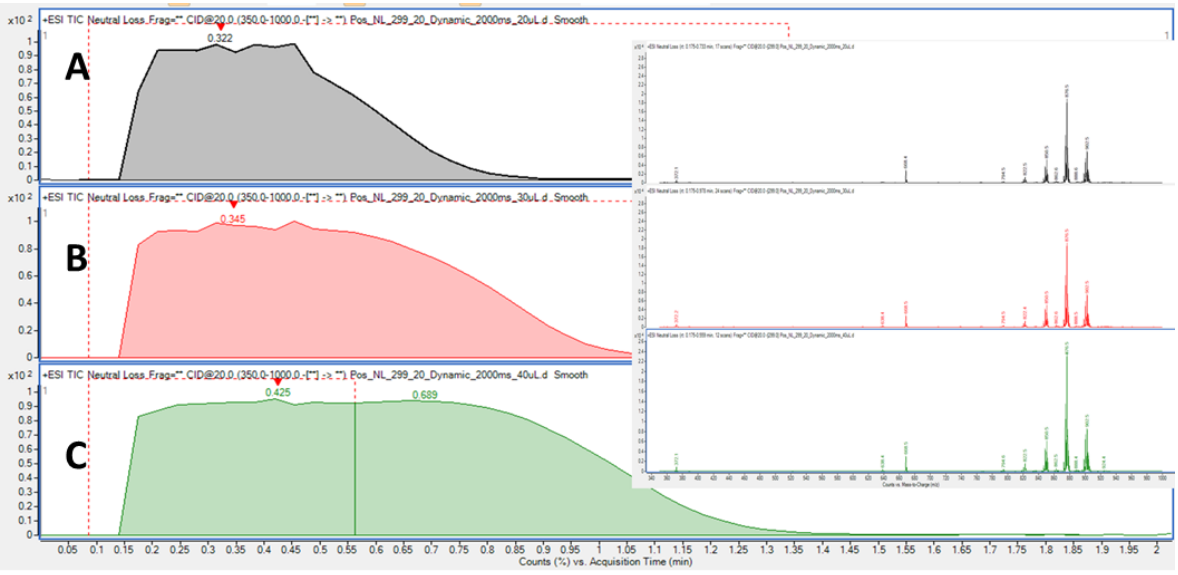

Figure 5.7 Three TICs of a plasma extract (20X dilution) injected at 20 (A), 30 (B), 40 (C) µL volumes. Extreme smoothing parameters were applied to get automatic integration. The spectra (inset) are averaged over the whole TIC integration.

With the larger injection volume it was possible to measure three CE in one injection and record ten scans using a 1000 ms scan speed (Figure 5.8). In order to simplify and automate data analysis, MassHunter Qualitative workflow was used. For each data file, the TICs for individual CE were separated. Next, the TIC signal could be smoothed into a pseudo Gaussian peak (as shown in Figure 5.7) and automatically integrated. Another approach was to alter the acquisition method to measure three different time segments. Segment one was full or product ion scan. Segment two was the Prec or NL scan for that method and it began when the sample is eluting. Segment three was a full or product ion scan and ended at the end of the injection (including the line wash). After the TIC for each CE was extracted, the extracted chronogram appears as a short segment of signal and was easily integrated (Figure 5.8). In all cases, a Qualitative software summation integration feature would benefit the Prec and NL scan data analysis workflow.

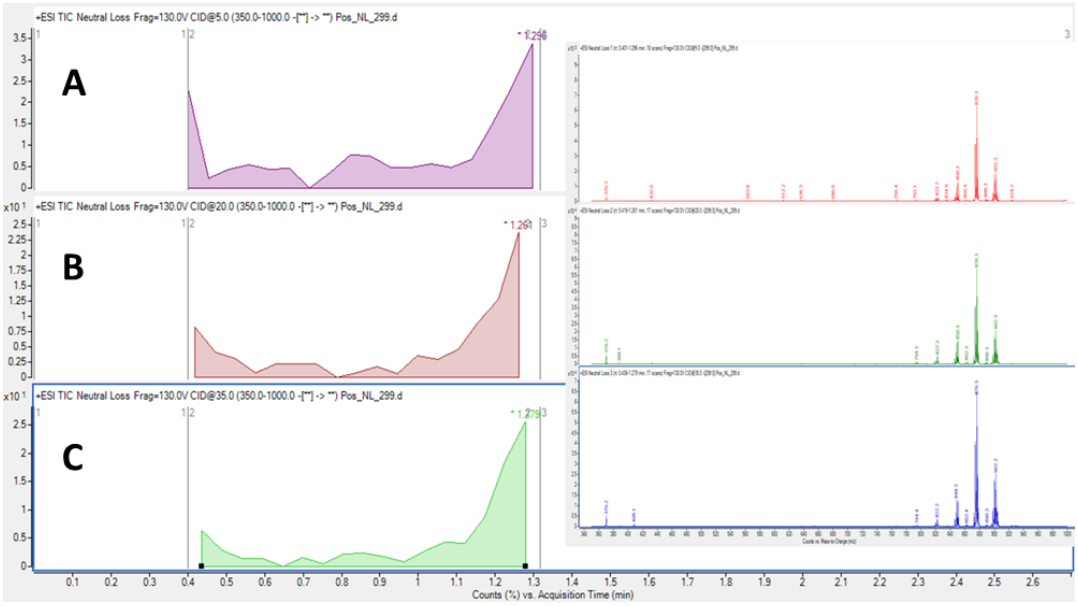

Figure 5.8 Positive mode NL 299 chronogram with three CE extracted and manually integrated. The data starts and stops at discrete points because the NL 299 scan was only set for that time segment. A, B, and C represent 5, 20, and 35 eV, respectively.

The ‘Fragmentor Mode’ in MassHunter Acquisition can be set to either ‘Fixed’ or ‘Dynamic’ mode. This was evaluated using two methods. One method was set to dynamic with a voltage ramp that include three ions: *m/z* 118.0 at 90V, *m/z* 666.5 at 130 V, and *m/z* 874.6 at 210

V. The other method had a fixed fragmentation energy of 130 V. Spectra collected with both methods were compared (Figure 5.9). The signal quality appeared to be better for the fixed methods (Figure 5.9, A and D) and so the fragmentor was fixed in the Prec and NL methods. This may change given a different mass range and should be evaluated if the mass range changes.

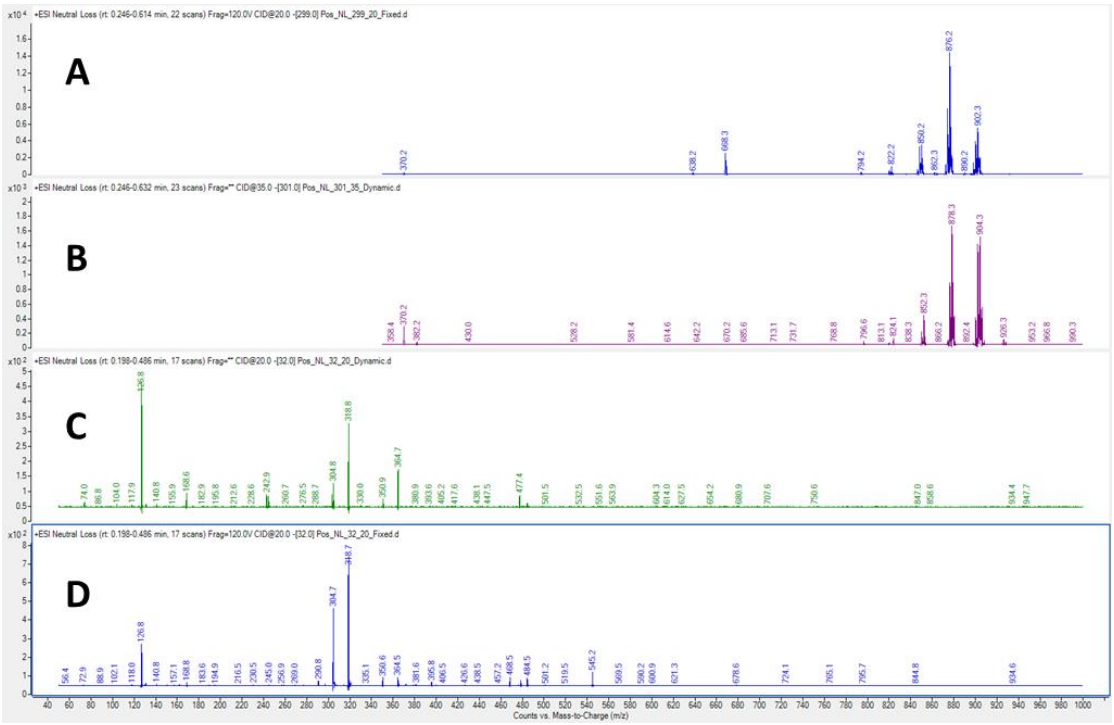

Figure 5.9 Fixed (A and D) and dynamic (B and C) fragmentor voltages for positive mode NL 301 scan (A and B) and positive mode scan (C and D). A 20X dilution of a plasma sample in solvent B was used for both.

A full list of the Prec and NL scans is listed in the Appendix. These scans and their values were taken from literature sources and is continuously growing.[62, 81-90] Note not all Prec and NL scans need to be performed for every experiment. If *a priori* knowledge suggests targeting a group of molecules characterized by a few functional groups then those can be collected. However, if a project aims for independent (unsupervised) discovery, then many or all of the scans should be performed.

Carryover should be initially assessed at this point. Three blanks (solvent B) were analyzed with representative scans. Then, six samples were analyzed followed by three more blanks. The needle wash time or the wash solvent can be changed to remove sample carryover from the well. Removing carryover in the lines with a longer wash period should be avoided because it increases the method time (injection to injection) and decreases throughput of the method. In all of the above experiments a 20X dilution provided high signal for various analytes, did not appear to have carryover, and was chosen as the sample preparation dilution at this stage.

The final list of transitions discovered with Prec and NL scans vary in length (500-6000 transitions) depending on how many scans are tested, the *m/z* range of the scans, the complexity of the sample, and the criteria for 'discovery'. In summary, this Prec and NL experiment optimization aimed to create a scan method that acquired fast and reproducible signal. In the workflow, the data was easily extracted and combined in a final transition list for MRM experiments. See section 7.4.1 below for the final discovery Prec and NL experiments and procedures.

5.3.5 MRM Method Optimization

Many of the parameters optimized in Prec and NL development were carried over to the MRM method. The final parameter to optimize was dwell time. The sample preparation and total MRM method reproducibility were also evaluated at this stage.

The dwell time optimization study used a pooled sample prepared as described in Table 5.1 but with a 20X dilution. Methods with varying dwell times (5-100 ms) were created and each contained the thirty highest and thirty lowest responding transitions. The pooled sample was injected six times for each method. The height of each transition was recorded and the relative standard deviation (RSD) for the height was calculated (Table 5.3).

Table 5.3 Dwell time study summary.[c]

30 Highest Intensity Transitions					
Dwell time (ms)	5	10	20	50	100
Average height (counts)	160,509	161,387	161,677	158,929	131,661
Average RSD	4%	3%	3%	3%	2%
RSD above 10%	0	0	0	0	0
30 Lowest Intensity Transitions					
Dwell time (ms)	5	10	20	50	100
Average height (counts)	768	757	736	723	703
Average RSD	9%	8%	6%	4%	4%
RSD above 20%	1*	0	0	0	0
RSD above 15%	3*	4*	0	0	0

c. MRM methods with different dwell times contained 60 transitions and were measured with a human plasma extract (20X dilution) 6 times. Average height of the transitions and RSD are listed. The number of transitions with RSDs above 10%, 15%, or 20% are reported. The * indicates that the transitions were below 200 counts.

The data showed that the highest responding transitions were very reproducible. All had RSDs below 10% and the average RSD for all the transitions was below 5%. The lowest responding transitions had more error as the dwell time decreased. The average RSD at 5 ms was 9% compared to 4% at 100 ms. However, this seemed to be caused by a few very poorly responding transitions (<200 counts). These transitions were likely noise and when they were removed the RSDs for all transitions and dwell times were below 15%. This data proves that a 5 ms dwell time is very reproducible with on the 6470 QQQ with these transitions and sample. This instrument can collect data even faster (0.5 ms dwell time). However, this is not necessary for our experiments due to a common software limitation; the MassHunter Acquisition software cannot contain more than 500 transitions per segment.

5.3.6 Reproducibility Evaluation

Until this point, sample preparation was performed on an individual sample scale. Testing the reproducibility of a 96-well plate sample preparation method is important to ensure each sample is prepared correctly by the procedure and liquid handler. This also tests the robustness of

the FI-MRM method over many samples and a longer time period. For this study, a pooled sample was pipetted 96 times on a well plate and worked up using the method in Table 5.1 but with a 20X dilution. One injection per well was acquired using the MRM method. The PCA analysis (Figure 5.10) showed separation of the samples over time. The first 48 injections (red) were separating from the last 48 injections (green).

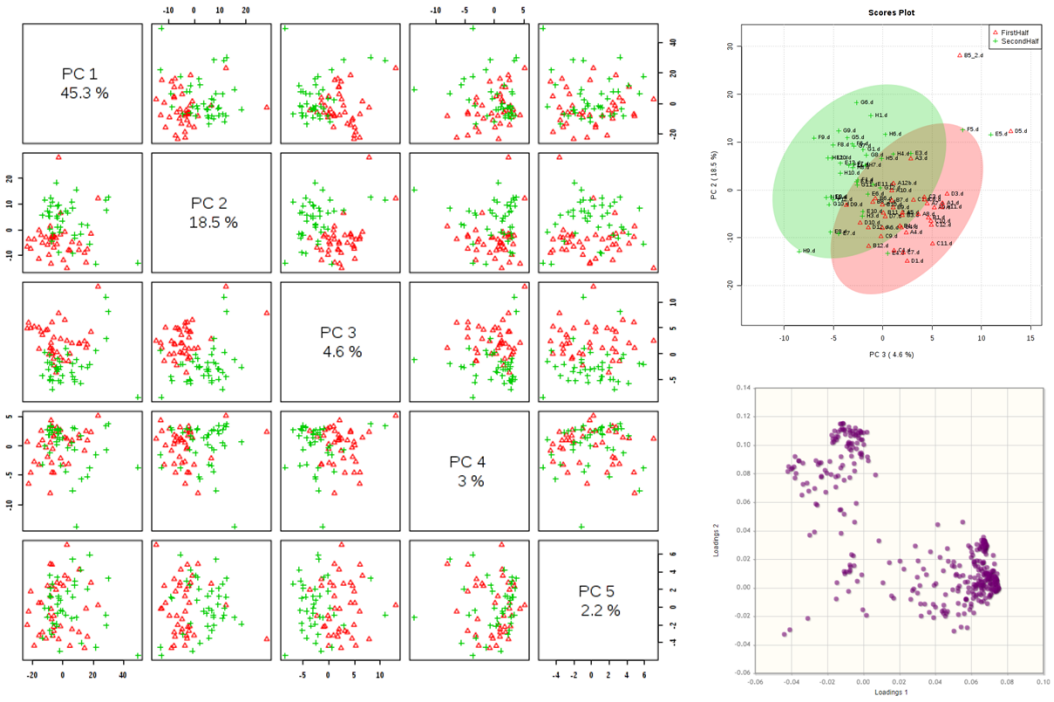

Figure 5.10 PCA plots for the first half (red) and second half (green) of a plate prepared with the same sample and collected using the same MRM method. The loading plot (bottom right) shows separation between identical lipid transitions due to carryover.

After investigating the issue, an increase in lipid signals was causing the separation (Figure 5.10, loading plot). This was due to carryover that was not detected previously. In an earlier study, carryover was evaluated by analyzing before and after solvent blanks with six injections of a 20X diluted sample in between. With Prec and NL scans, this showed no significant carryover. However, if 20 or more samples were injected, carryover was observed on the MRM method. It is hypothesized that lipids began to adhere to the stainless steel tubing and were subsequently observed in the after blanks. Initially, to solve this problem, a number of wash methods and

solvents were tested to clean the lines after each injection. These did not work well enough and a dilution of the sample was ultimately made (200X verses 20X). The final method had a more thorough washing of the lines and a larger dilution (200X) to prevent carryover. The data from four plates of individual samples were not separating significantly and the method was therefore reproducible (Figure 5.11).

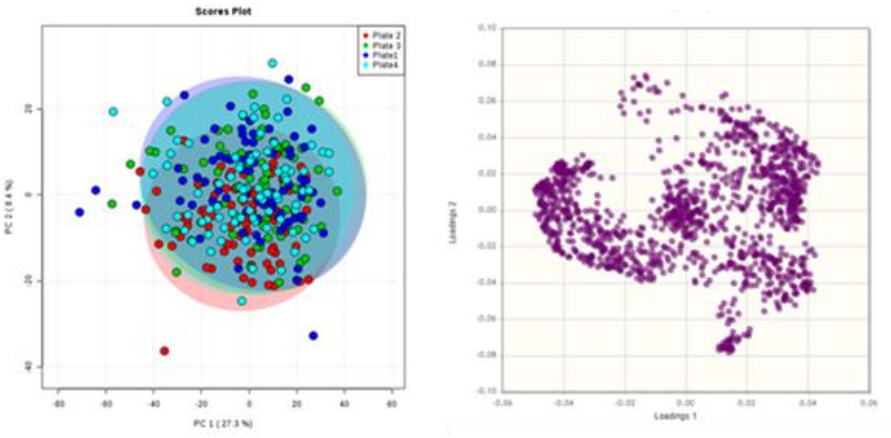

Figure 5.11 PCA plot of four 96-well plates of random samples with data and collected using the same MRM method. The loading plot does not show separation of any one or any group of analytes.

5.3.7 Quality Control Analyte

With this metabolite profiling methodology it is hard to check data for individual quality *e.g.* correct sample preparation, no bubbles in the pump lines, sensitivity of MS, etc. For this reason an inexpensive deuterated drug (alprazolam-D_5) was spiked at 100 ng/mL into the solvent B used for sample dilution. This was a quality control analyte to check for proper sample preparation and performance of the instrument. It was not meant for quantification so any analyte may be used as long as it is not endogenous to the sample studied. This analyte was measured in every time segment and if it was statistically high or low in a sample then the sample was re-prepared and reanalyzed. If the sample was rejected a second time then the sample was eliminated from the study.

5.4 Methods

The sample preparation, solvent, pump, and MS parameters optimized above were used in the experiments described below.

5.4.1 Discovery Phase

An example of the Prec and NL parameters used during MassHunter MS data acquisition is reported in Figure 5.12. The mass range was maximized in each scan by setting ‘MS1 From’ to the lowest possible value but ‘MS1 To’ never exceeded *m/z* 1000.

A

Time segments

#	Start Time	Scan Type	Div Valve	Delta EMV (+)	Delta EMV (-)	Stored
1	0	Product Ion	To MS	0	0	☑
2	0.4	Neutral Loss	To MS	0	200	☑
3	1.3	Product Ion	To MS	0	0	☑

B

Acquisition | Source | Chromatogram | Instrument | Diagnostics

Scan segments

Segment Name	Neutral Loss	MS1 From	MS1 To	Scan Time	Frag Mode	Fragmentor	Collision Energy	Cell Accelerator Voltage	Polarity
	121	150	1000	1000	Fixed	130	35	5	Negative
	121	150	1000	1000	Fixed	130	20	5	Negative
	121	150	1000	1000	Fixed	130	5	5	Negative

Figure 5.12 Example of MassHunter QQQ Acquisition method for Prec and NL scans. A) Time segments were used to measure the Prec or NL from 0.4 min to 1.3 min. B) An example of the acquisition parameters used for Prec and NL scans.

Pooled samples were used in the discovery Prec and NL scans to reduce erroneous signals from biological variability while averaging the signal that is relevant to the sample and the disease state. Pooling also created a large volume of the sample without using all of any one individual sample. This is good for precious samples since the Prec and NL scans require more sample than the screening phase. Pooling can be simple: mix ten disease and ten control samples to make a disease and control pool. Ideally there would be more than ten individual samples in each pool to reduce the variability even more. Additionally, more groupings can be created to emphasize

different biomarkers related to subpopulations of a disease or different severities of disease. Subpopulation pools are good to include so their specific biomarkers will be higher and related transitions will therefore be included in the MRM method. This allows for variants of the analytical procedure to be performed after data collection. For this project, control, high CAD, low CAD and peripheral artery disease (PAD) pools were each created from 30 individual samples. The high and low designations were taken from descriptions in the clinician notes of the diagnosis (*i.e.* severe and mild).

The pooled samples were prepared individually as described in Table 5.1. The solvent B was doped with 100 ng/mL of alprazolam-D_5. Data was acquired for each pool using the Prec and NL scans (Appendix). After data acquisition the spectra were extracted and a list of transitions created. For this, a MassHunter Qualitative workflow was used to work up each data file efficiently. First, chronograms were separated by CE, then integrated, *m/z* peak lists copied to excel. In the Qualitative workflow a noise threshold was applied to the peak list (*i.e.*. 500 counts). To make the transition lists, the following parameters for each *m/z* peak were listed in excel: mode (positive or negative), precursor ion, scan type (Prec or NL), scan value (Prec or NL value), CE (eV), and intensity of the peak (counts). From the precursor ion *m/z* value, scan type, and scan value the product ion was calculated. After the signals for all the transitions were combined, there were overlapping transitions. Filtering was done to leave one unique transition per CE (parameters with the highest intensity were retained). Additional filtering was done to remove overlapping transitions *e.g.* 780.1→ 184.0 vs 780.2→184.0. After this, 1266 usable transitions were found in plasma extracts, 1122 positive mode and 144 negative mode.

5.4.2 Discrimination Study

Because the software does not allow more than 500 transitions per time segment, four injections must be made to collect data for 1266 transitions in two modes; this obviously limits throughput. Given four 1.5 minute injections and additional time to wash the pump lines after each injection (*c.a.* 3 min), the method is over 10 minutes per sample. This large amount of time justifies a discrimination study to reduce the number of transitions. Discrimination studies have been performed with previous MRM-profiling methods [1]. It tests a small representative population of samples and performs univariate statistics with broad parameters (*e.g.* p value=0.1) to reduce the

number of insignificant transitions in the study and in this way to give a final method that is < 5 minutes per sample.

For the discrimination study, a subset of 383 samples was selected randomly from the control, CAD and PAD samples and arranged in four, 96-well plates. These samples were prepared as described in Table 5.1 and diluted into solvent B containing 100 ng/mL alprazolam-D_5. The samples were analyzed using a method with four segments to collect all 1266 transitions in four, 20 µL injections (3 positive mode and 1 negative mode). MassHunter Quantitative software can perform a spectrum summation to quickly integrate a peak using a start and stop time point. This feature was used to integrate the signals for all the transitions. Each time segment (including the negative mode injection) had the alprazolam-D_5 transition (*m/z* 314.1→210.1). This was integrated as well. Each transitions' area under the curve (AUC) was exported to Excel.

Outliers were eliminated so as not to skew the data. The data were analyzed first by principal component analysis (PCA) to check if any of the plates appeared to be an outlier as a result of being prepared incorrectly. One plate did separate so the corresponding data was removed. Next, by plate, alprazolam-D_5 signal was analyzed in individual samples. If the alprazolam-D_5 signal was an outlier then the sample was removed. After outlier removal, 251 samples remained.

To determine which transitions were significant, the samples were analyzed by univariate statistics. In this step, broad, non-strict univariate parameters were used to avoid type two errors, or false negatives. The strategy here was to prefer to include, or keep, unimportant transitions rather than risking the elimination of important ones (type I error, false negative). [91-92]] The univariate statistics were performed with Metaboanalyst 3.0 and included t-test (p=0.1), fold change (FC = 1.5), and receiving operating characteristic (ROC, AUC >0.7). The samples were grouped in several ways to avoid loss of metabolites important to different population. The groups compared to controls were (i) CAD, (ii) PAD, (iii) high low density lipoproteins (LDL), (iv) high triacylglycerides (TAG), (v) low high density lipoproteins (HDL), and (v) 'severe' CAD. Additionally, each of these groups were then separated by gender and filtered again. The transitions found to be significant for each of these studies were combined. Duplicate transitions were eliminated and the final list contained 485 transitions.

5.4.3 Screening Phase

The final MRM method contained 485 transitions measured in three consecutive injections. MassHunter Acquisition parameters are reported in Figure 5.13. Individual samples (N=956) were organized randomly into 96 well plates, prepared no more than twelve hours prior to injection, and kept at 4C before and during data acquisition. The final method was 4.7 minutes injection to injection. Data were collected over four days. Each plate was analyzed for outliers as described in previous section. If any were found, the plate was re-prepared and re-acquired in a later plate.

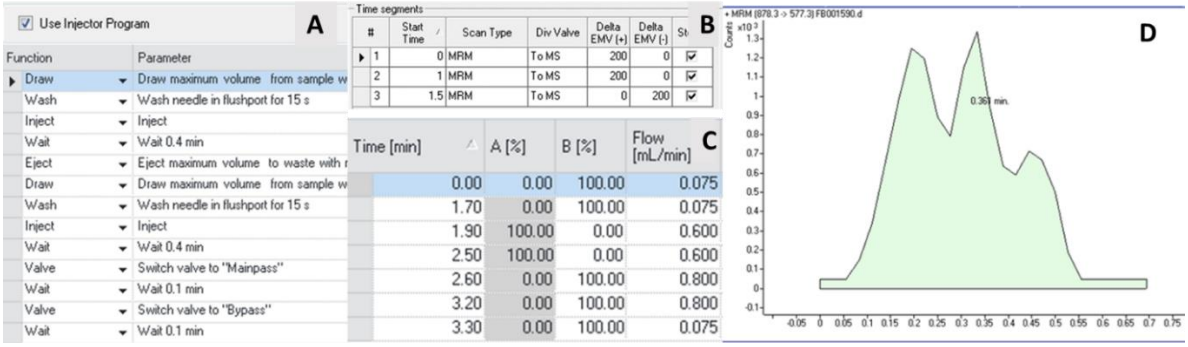

Figure 5.13 The final method utilized an injector program (A) to inject three 20 µL injections per data file. Each injection was analyzed with a different transitions set by defining time segments (B). The pump (C) ran at a 75 µL/min flow rate (Bottle B, solvent B) followed by a wash method to clean the pump lines (Bottle A, 40% Methanol, 40% isopropyl alcohol, 20% chloroform). The data was integrated in MassHunter Quantitative software using spectral summation tool (D).

5.4.4 Data Analysis

In total 956 samples was tested. After, analytical outliers were removed, 800 samples remained for data analysis. The clinical data for the samples, provided by the Fairbanks Institute, described the samples as ‘case’ or ‘control’. The gender and age of the subject was always reported. Additional medical history, laboratory test results, and personal information was sometimes reported. For CAD analysis, biological outliers were removed by using this clinical data so as not to skew the data on the basis of other diseases or habits.[93] Smokers, those with a history of cancer or stroke, and those with PAD were removed and 535 samples remained. A final grouping by age and gender was performed (Table 5.4). The male and female population between 46 and 65 age was analyzed further because it contained significantly more samples than other age groups. The

PAD samples were matched with random controls. No biological outliers were removed and no further grouping was performed with PAD samples because of the small sample set (N=103).

Table 5.4 Table of 535 CAD cases and controls analyzed by age and gender.[d]

	F		M	
	Case	Control	Case	Control
Total Samples:	107	143	223	81
Age Range:	37-84	39-85	22-82	33-78
22-45 year old:	8	12	17	9
46-65 year old:	64	106	150	59
66-85 year old:	34	18	46	12

d. Smokers, those with a history of stroke or cancer, and PAD samples were removed.

Data sets for female and male case and control samples in the 46-65 year old age group were analyzed using Mass Profiler Professional (MPP). Working within each gender group, the significant transitions between case and controls were found with univariate statistics (p=0.05 and FC= 1.25). The following tests and limits were used for all univariate analysis: unpaired t-test, asymptotic p-value computation, Benjamini-Hochberg correction, and 1000 absolute count cutoff. A FC of 1.25 was used because individual transition signals were not expected to alter in an extreme manner in this disease or biofluid. Additionally, with no chromatography, the measured signal might be derived from multiple different analytes while only one may actually be changing in the disease. Thus, FC is not a strict parameter in this study.

After univariate statistics, PLSDA modeling was performed using the significant transitions. In MPP, a validation study was done for each model by leaving one third of the samples out of the model and classifying those left out based on a model made with the two thirds group. This validation was done 100 times for each model and an averaged cross confusion matrix was created to calculate the sensitivity, specificity, and total accuracy of the method. The same analysis was done for PAD samples verses random controls.

5.4.5 LC-MS Methods

An LC method described in an Agilent application note for lipid separation was adjusted for optimal separation of mono- and lyso-lipids, phospholipids, and TAGs in the plasma extract.[94] A ZORBAX Eclipse Plus RRHD C18, 2.1 × 150 mm, 1.8 µm column was used for separating the analytes. IPA/MeOH/water (5:1:4) with 5 mM ammonium acetate and 0.1 % acetic acid (Pump A) and IPA/water (99:1) with 5 mM ammonium acetate and 0.1 % acetic acid (Pump B) were used as mobile phases. The gradient and source conditions are reported in Figure 5.14. A 2 µL injection of the plasma extract in solvent B (no dilution) was used. On the QQQ, data was collected over the whole gradient for the transitions of interest. Using MassHunter Qualitative software a RT for every transition of interest was found.

A

Time [min]	A [%]	B [%]	Flow [mL/min]	Max. Pressure Limit [bar]
0.00	100.0	0.0	0.350	400.00
4.50	100.0	0.0	0.350	---
12.50	85.0	15.0	0.350	---
18.00	82.0	18.0	0.350	---
30.00	30.0	70.0	0.350	---
45.00	23.0	77.0	0.350	---
47.00	2.0	98.0	0.350	---
51.00	2.0	98.0	0.350	---
53.00	100.0	0.0	0.350	---

B

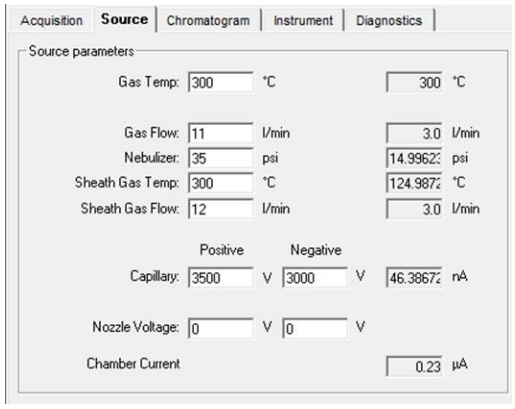

Figure 5.14 LC-ESI conditions for separation of unknown analytes using IPA/MeOH/water (5:1:4) with 5 mM ammonium acetate and 0.1 % acetic acid (Pump A), IPA/water (99:1) with 5 mM ammonium acetate and 0.1 % acetic acid (Pump B), and the gradient reported in (A). The source conditions are reported in (B).

Once a RT had been determined the LC system and pump method were implemented using a QTOF and a full scan high resolution MS method was performed. Using MassHunter Qualitative software the peaks at the known RT were integrated, spectra extracted, and an exact mass for each transition precursor determined. Next, a targeted MS/MS method was performed using a narrow isolation width (~1.7 *m/z*) to collect high resolution product ion data for the given precursor ion. Agilent purine and 922 masses were infused in the dual AJS source at 10 µL/min and used as TOF

calibration masses during data acquisition. This experiment provided the exact mass, RT, and high resolution product ion spectra for many transitions. With this information, Metlin, HMDB, and LipidMaps databases were used to identify the transitions. Some of the transitions were not found with this chromatographic method. Alternative mobile phases or columns may be needed to identify these further.

5.5 Results and Discussion

5.5.1 Modeling, Accuracy, Specificity, and Sensitivity

After the univariate statistics, the female CAD samples between 46 and 65 years old separated between case and control using 62 transitions, the male CAD samples between 46 and 65 years old separated using 44 transitions, and the PAD samples separated using 55 transitions. Many transitions were overlapping between the three models. The samples separated in a total of 104 unique transitions.

The PLSDA models for female and male case verses control samples are shown in Figure 5.15. Females between 46-65 years old had a sensitivity of 95%, specificity of 87% and an accuracy of 90%. Males in the same age group had a sensitivity of 70%, specificity of 96% and an accuracy of 78% (Table 5.5). The PAD model (Figure 5.16) had a sensitivity of 83%, a specificity of 86%, and an accuracy of 85% (Table 5.5). Because of the small sample population biological outliers were not removed from PAD population. However, the separation for this group is good even without removing the outliers.

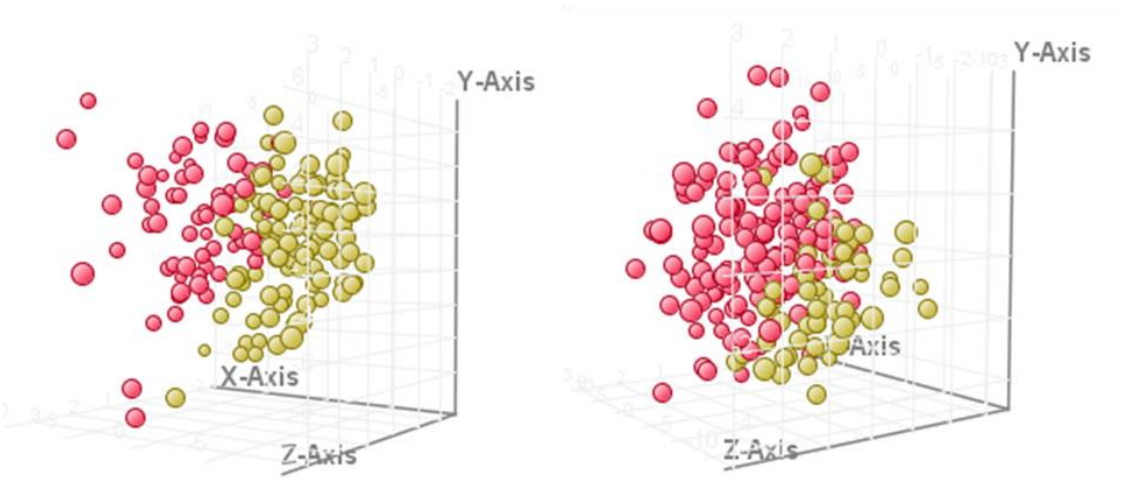

Figure 5.15 CAD PLSDA models of case (red) and control (yellow) samples made with filtered transitions sets in MPP. The female samples (left) between 46-65 years old separated on the basis of 62 transitions and the male samples (right) in the same age group separated on the basis of 44 transitions.

A

		Predicted			
		Case	Control	Accuracy:	91%
Actual	Case	61	3	Sensitivity:	95%
	Control	13	93	Specificity:	88%

B

		Predicted			
		Case	Control	Accuracy:	78%
Actual	Case	106	44	Sensitivity:	71%
	Control	2	57	Specificity:	97%

C

		Predicted			
		Case	Control	Accuracy:	85%
Actual	Case	86	17	Sensitivity:	83%
	Control	14	93	Specificity:	87%

Figure 5.16 Cross confusion matrices for female (A) and male (B) case verses control (age 46 to 65) and PAD verses control (C). Sensitivity, selectivity, and accuracy for the models are reported.

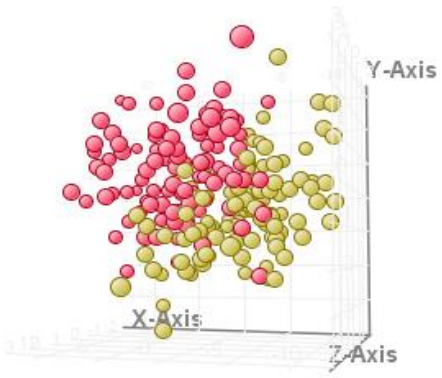

Figure 5.17 PLSDA model showing the separation of PAD samples (red) and control samples (yellow) using 55 transitions.

The MRM-profiling results had good separation with the PLSDA model. The PLSDA plots do not show perfect separation of the groups because the disease is a spectrum. The sensitivity, specificity, and accuracy of the models are highly encouraging. Again, 100% accuracy is not expected because of the nature of the disease. The sample population analyzed consists of patients with different concurrent diseases, varying medical history, and therapies for CAD (and/or other diseases). All of these would cause differences in plasma metabolites. Reducing this variability was the motivation for blocking the population by age and removing biological outliers. Working with a clinician who is more knowledgeable of the disease and patients would likely guide this blocking and improve the results.

5.5.2 Analyte Identification

The signal from the MRM-profile is sufficient for classification of a sample. However, for this project exact chemical identifications were desired to show that the metabolite profile consisted of signal relevant to a plasma sample and important to the disease. Many of the lipid transitions can be identified easily without chromatography because the Prec and NL scans are very specific. But many others cannot be identified by QQQ transitions alone.

The RT and HRMS data revealed that the 104 discriminating transitions consisted of 39 unique compounds (Table 5.6). Many compounds had a number of transitions (same precursor and different product ion) in the method and several of the lipids were represented as both the protonated and sodiated forms. The analytes were separated over a one hour gradient (Figure 5.17). Since the chromatographic method used was intended for lipids and triglycerides, the more polar analytes were not retained but many were analyzed in the solvent front. Another LC method would be needed to separate these better. The mono- and lyso-phospholipids, PCs, sphingomyelin (SM) lipids, and TAGs separated clearly.

Table 5.5 MRM transition parameters for 104 significant transitions in the final method.[e]

ID	Precursor Ion (*m/z*)	Product Ion (*m/z*)	Exact mass (*m/z*)	RT (min)	Adduct Ion	F CAD	M CAD	PAD
No ID	60.9	43.9	Not found in LC method					↑
TMAO	76	58	Not found in LC method			↑	↑	↑
Choline	104	45	104.1071	3	M+H			↑
No ID	114	43	114.0657	1	M+H			↑
Octylamine	130	71	130.1586	0.9	M+H	↑	↑	↑
	130	43	130.1586	0.9	M+H			
	130	56	130.1586	0.9	M+H			
	130	85	130.1586	0.9	M+H			
No ID	144.7	85	144.1017	1	M+H	↑		↑
Carnitine	161.9	85	162.1123	0.9	M+H	↑		↑
	162	103	162.1123	0.9	M+H			
	162	59	162.1123	0.9	M+H			
γ-hydroxy-L-homoarginine	204.9	85	205.1271	1	M+H	↑		↑
	204.9	86	205.1271	1	M+H			
No ID	218	85	218.1084	1	M+H			↑
No ID	229.1	142.1	229.1544	0.9	M+H	↑		↑
No ID	232	85	Not found in LC method			↑		↑
No ID	246.1	85	Not found in LC method					↑
No ID	286	85	Not found in LC method			↑		↑
No ID	288	85	Not found in LC method			↑		↑
	288.1	85.1						
	288.1	85						
No ID	316.1	85	Not found in LC method					↑
Cholesterol	369.1	287.1	369.3511	37.5		↓		↓
	369.2	147.2	369.3511	37.5				
	369.2	119.2	369.3511	37.5				
	369.2	175.2	369.3511	37.5				
	369.2	109.2	369.3511	37.5				
	369.2	121.2	369.3511	37.5				
	369.2	91.2	369.3511	37.5				
	369.2	57.2	369.3511	37.5				
	369.2	193.2	369.3511	37.5				
	369.2	147	369.3511	37.5				
	369.2	85	369.3511	37.5				
	369.2	207.2	369.3511	37.5				
	369.3	41.3	369.3511	37.5				
	369.4	68.4	369.3511	37.5				

Table 5.5, continued

ID	Precursor Ion (*m/z*)	Product Ion (*m/z*)	Exact mass (*m/z*)	RT (min)	Adduct Ion	F CAD	M CAD	PAD
No ID	370.1	147	370.3546	37		↓	↓	↓
	370.1	288.1	370.3546	37				
	370.1	229.1	370.3546	37				
	370.2	69.2	370.3546	37				
	370.2	148.2	370.3546	37				
	370.2	176.2	370.3546	37				
	370.2	149.2	370.3546	37				
	370.2	120.2	370.3546	37				
	370.2	41.2	370.3546	37				
	370.2	122.2	370.3546	37				
	370.2	92.2	370.3546	37				
	370.2	194.2	370.3546	37				
	370.2	97	370.3546	37				
	370.3	97.1	370.3546	37				
	370.3	110.3	370.3546	37				
	370.3	93.1	370.3546	37				
MonoChain-PC	520.1	104	520.3371	2.6	M+H	↓	↓	
MonoChain-PC	521.2	104	521.3427	2.6	M+NH4	↓	↓	↓
MonoChain-PC	542	483	542.3215	2.5	M+H	↓	↓	
	542.1	104	542.3215	2.5	M+H			
No ID	632.3	264.3	Not found in LC method			↓		
20:5 Cholesteryl ester	671.3	303	671.5742	37.5	M+H	↓	↓	↓
SM(34:1)	725.2	542.2	725.5563	19.5	M+Na	↓	↓	
PC(34:2)	758.2	104	758.5691	22.9	M+H	↓	↓	
	758.4	86	758.5691	22.9	M+H			
	780.1	575.1	780.5515	22.9	M+Na	↓	↓	
	780.1	721.1	780.5515	22.9	M+Na			
	780.2	147	780.5515	22.9	M+Na			
	780.2	597.2	780.5515	22.9	M+Na			
	780.2	86	780.5515	22.9	M+Na			
SM(38:1)	759.2	184	759.5731	22.5	M+H	↓	↓	
	759.3	86	759.5731	22.5	M+H			
	781.2	147	781.5527	22.5	M+Na	↓	↓	
	781.2	598.2	781.5527	22.5	M+Na			
	781.2	576.2	781.5527	22.5	M+Na			
	781.2	86	781.5527	22.5	M+Na			
SM(40:2)	785.2	184	785.588	23.8	M+H	↓		
	807.2	624.2	807.6329	23.8	M+Na	↓	↓	
	807.3	147	807.6329	23.8	M+Na			

Table 5.5, continued

ID	Precursor Ion (*m/z*)	Product Ion (*m/z*)	Exact mass (*m/z*)	RT (min)	Adduct Ion	F CAD	M CAD	PAD
PC(36:2)	786.1	104	786.6005	25	M+H	↓		
	786.3	86	786.6005	25	M+H			
	808.2	625.2	808.5829	25	M+Na	↓	↓	
	808.2	603.2	808.5829	25	M+Na			
	808.3	147	808.5829	25	M+Na			
SM(40:1)	787.2	184	787.6041	25.1	M+H	↓		
	809.2	147	809.5863	25.1	M+Na	↓	↓	
	809.2	626.2	809.5863	25.1	M+Na			
PC(37:4)	796.1	737.1	796.5239	26.3	M+H	↓	↓	
	796.2	86	796.5239	26.3	M+H			
PC(38:6)	806.3	147	806.5662	23.6	M+H	↓	↓	
TAG	848.5	549.5	848.7687	37	M+H		↑	
TAG	850.4	577.2	850.7868	38	M+H	↑	↑	
	850.5	551.5	850.7868	38	M+H			
	850.5	577	850.7868	38	M+H			
TAG	851.2	577	851.7101	35.8	M+H		↑	
TAG	874.3	575.3	874.7828	37.3	M+H		↑	
	874.4	601.2	874.7828	37.3	M+H			
TAG	876.3	577.3	876.7995	38.5	M+H	↑	↑	
	876.4	603.2	876.7995	38.5	M+H			
	876.5	577	876.7995	38.5	M+H			
	876.5	603	876.7995	38.5	M+H			
TAG	877.3	578.3	877.803	38.6	M+H	↑	↑	
	877.4	604.2	877.803	38.6	M+H		↑	
	877.5	579	877.803	38.6	M+H			
TAG	878.3	577.3	878.7289	36.2	M+H		↑	
Salicylic acid	136.9	92.9	137.0252	1	M-H	↑	↑	↑
p-cresol sulfate	186.9	106.9	187.0424	1	M-H		↑	↑

e. If known, the exact mass, RT, adduct formed, and compound identification is listed. The up and down arrows in the female CAD, male CAD, and PAD columns indicate if the analyte was up or down regulated in the model.

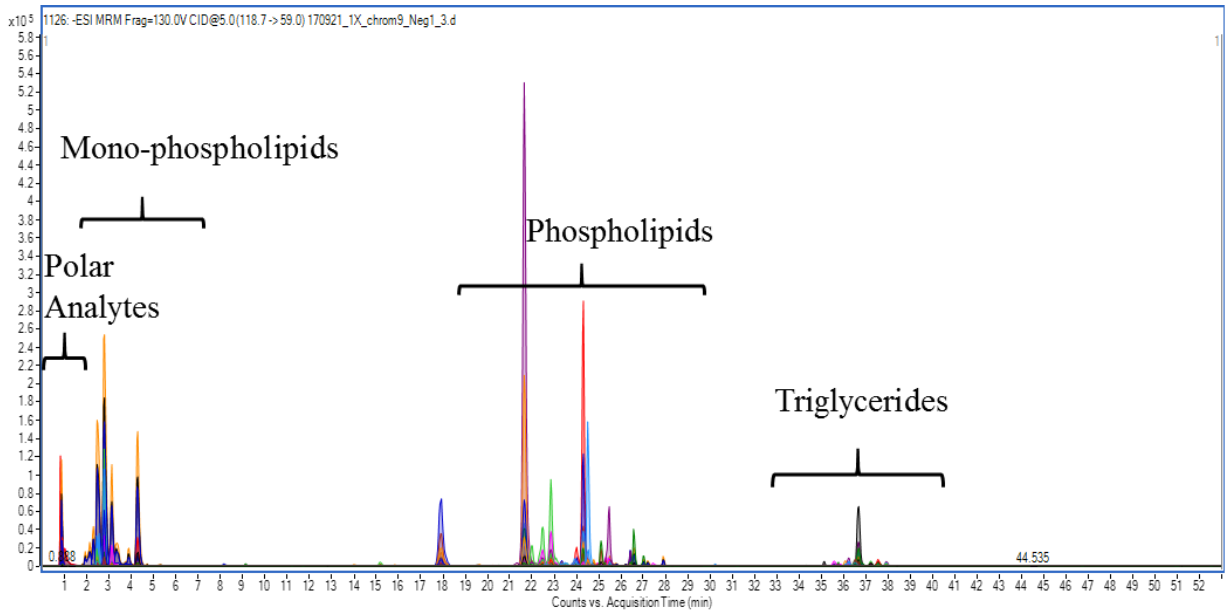

Figure 5.18 Zorbax C18, 150 x 2.1 mm, 1.8µ column was used with the method described in Figure 5.14 Data shown here were collected on a 6470 QQQ using the MRM parameters in the MRM-profiling study. Small polar analytes elute in the first minute followed by mono-chain and lyso-phospholipids, then phospholipids, and finally triglycerides.

One of the most important finding of this study is that the separation of the samples is occurring in signals relevant to the plasma sample and to the disease. Choline and carnitine are upregulated in case samples. These have previously been reported to be altered in CAD populations and are taken as supplements by those with heart disease.[95-96] Another small metabolite, p-cresol-sulfate was also upregulated. This metabolite is found at higher concentrations in CAD patients with renal disease.[97] TAGs are well known to be higher in populations with heart disease and many were upregulated in the disease samples.[98] Mono-chain PCs, SMs, and PC lipids are all down regulated in the disease samples.[68, 99-102] This is indicative of cellular stress and inflammation which can be expected in CAD and PAD populations. Trimethylamine N-oxide (TMAO) was not confirmed by HRMS but its transition matches those found in literature and, just as in other studies, it is up regulated in CAD.[103-104] Interestingly, cholesterol, an upregulated molecular biomarker for heart disease, was found to be down regulated in CAD and PAD populations. This is likely due to medications that the disease population takes and the opposite would be expected for a population that is not taking cholesterol lowering medications.

Salicylic acid was found in the negative mode and was up regulated in PAD and CAD samples. It is the active ingredient in aspirin which is commonly taken by people with heart disease.[105] This is appropriate to include in the transition list and in modeling if the purpose of the MRM-profile is to study the signal profile of a population known to be on drugs (*e.g.* epidemiological studies). When using MRM-profiling for diagnostic purposes, transitions that are known to be or are possibly due to a drug should be removed from the method prior to modeling. When this exogenous analyte was removed, the female group had a sensitivity of 93%, a specificity of 82%, and an accuracy of 86% and the male group had a sensitivity of 70%, a specificity of 91%, and an accuracy of 86%. Removing the exogenous analyte does not alter the classification ability of MRM-profiling significantly in this study. However, it does suggest that MRM-profiling may be helpful for pharmaceutical companies when trying to identify drug metabolites. The metabolite structures could be predicted based on common metabolic pathways and Prec and NL scans targeting them used for discovery with MRM-profiling, although this was not attempted in this study.

5.5.3 Instrumental and Methodological Considerations

This methodology was easy to develop and to use. In a three month period, the workflow for MRM-profiling was integrated on Agilent systems, a method was optimized, and tested on 900+ samples. The flow injection methodology was demonstrated with these samples, the 6470 QQQ mass spectrometer proved to be a fast and reliable instrument for these analyses, and MassHunter and MPP software was highly amenable to the unique analytical requirements of MRM-profiling. Furthermore, the workflow was carried out in a high throughput fashion with eleven 96 sample plates taking less than five days to acquire data for 485 transitions. This is much faster than traditional metabolomics methods of biomarker discovery.

Because of the all-inclusive measurement aim that this methodology embraces, tradeoffs are significant and parameters for every project should be evaluated to ensure that the most diverse signal (in terms of number of analytes) and those of the highest quality are being measured. Fortunately, the development experiments proved to be simple, straight forward, and the sample throughput was fast because of the absence of chromatography.

One major tradeoff, not discussed fully in the method development section above, is the selection of the Prec and NL scans to test. Over 200 scans are reported in the Appendix. For a true discovery methodology these should all be performed. This is an unsupervised methodology and promotes discovery of metabolites with no bias. Many of these scans are highly specific (*e.g.* Prec 184 for PC lipids), however, others are less specific so exogenous analytes, like salicylic acid, might be found. If these less specific scans are not performed then it is possible to miss small metabolites (*e.g.* TMAO, choline, carnitine, and p-cresol-sulfate).

The discrimination study removed transitions thought to be unimportant before the full sample screening. This approach of prescreening a subset of samples and removing those that do not appear informative is intended to save time during the final screening. Depending on the samples studied and the statistical parameters used, this process has the potential to remove important transitions before the final screening. It also takes additional time and materials. It is therefore desirable to avoid it where possible in future MRM-profiling studies. One way to exclude it, while keeping the methodology rapid, would be to use DI instead of FI. DI will continuously spray the sample. All transitions discovered can be measured in different consecutive time segments. No time will be used waiting for the injection to reach the MS or for washing the FI lines. It is estimated that a method containing 1266 transitions with a 5 ms dwell time, and 10 cycles can be measured in under 1.5 minutes per sample with DI verses the 4.5 minutes used here.

Many samples in the final screening were eliminated as analytical outliers. This number could be reduced by performing all the sample preparation pipetting steps with the Bravo liquid handler Furthermore, protein contamination and interference can be minimized by compacting the protein layer better. To do this, less plasma sample could be used and/or centrifuging the plates at a higher speed (20,000 RPM not 4,000 RPM). If less plasma is used, the extract dilution (200X) may need to be reduced.

Those analytes without a RT and exact mass listed were not found with this chromatographic method. This demonstrates that MRM-profiling can measure more analytes in a single injection than traditional LC-MS methods which is advantageous to metabolomics discovery methods.[60, 66] Additionally, a few of the transitions which do have RT and exact mass were not found in the databases. Identification is a weakness of many biomarker methods but MRM-profiling avoids this entirely. This methodology discovers biological relevant signal by functional group and measures it by a single ion transitions. The data from all the biological ion

transitions create a metabolite profile that can classify a sample without ever knowing exactly what analytes contribute to that signal. It can find biological related signal identify the analyte(s) contributing to the signal.

5.6 Conclusion and Future Considerations

MRM-profiling of CAD successfully demonstrated this technique as a high throughput metabolomic methodology. The pooled CAD and control plasma samples were analyzed for biologically relevant signal with Prec and NL scans. Then, over 900 individual samples were screened in under five days for the discovered metabolite signal from the discovery phase. The metabolic profile separated the CAD female, CAD male, and PAD samples from controls with high accuracy: 90%, 78%, and 85%, respectively. Furthermore, LC-MS methods showed that the characteristic signals discovered are related to the disease.

This methodology is fast and simple to develop. Experiments described in the Method Development section are straight forward but are essential for measuring meaningful signal in a high throughput and robust manner. Each MRM project should involve assessment of many of the variables discussed in this chapter. With proper development, a method can be very reproducible and can be used to acquire vast amounts of high quality data without much MS maintenance or data storage concerns normally associated with LC and HRMS workflows.

The Prec and NL scans have a biological purpose and the targeted MRM method only measures that signal so unimportant signal or background noise is not collected. By eliminating noise collection the method can be very fast. This also gives biological specificity to the data collection and results. However, this also means that new analytes cannot be analyzed after screening. For this reason, it is advised that all Prec and NL scans be used and all transitions added to the MRM screening method for an unsupervised and inclusive methodology. Additionally, discrimination studies should be avoided in future studies since signal is removed in this step before the whole sample set is screened.

No libraries or standards are needed for this analysis which reduces the cost of material and aids in the discovery of analytes based on functional groups and not an exact structure. MRM-profiling separates a population without ever needing chromatographic separation of analytes. When trying to identify transitions used in the metabolite profile, the same identification issues

common to HRMS discovery methods were present. That is, if a standard or spectral library didn't exist then an identification could not be made except by ab initio deduction.

MRM-profiling is ideal for quickly identifying a metabolite profile that classifies a population. Thus it should be useful for diagnosis. Also, since drugs which a particular population is using are detected, molecular epidemiological studies can use this as a tool to follow the molecular profile of a population. Drug metabolism of a new drug could also be assessed with this methodology.

In human studies, biological variability is very large and researchers cannot control every aspect of a subject's behavior that might alter their metabolites. Therefore, large samples sets are best studied, and a clinician can guide analysis to remove biological outliers and create subgroups for the discovery phase and analysis models. However, the MRM-profiling methodology is so fast that acquiring data for 1000 samples can be done in less than a week. One outcome of this method could be a metabolite profile that can classify future samples, such as seen in this CAD study, or that can help researchers find transitions for interesting analytes for additional studies (see the PD study in Chapter 8).

Future MRM-profiling studies should test DI or nano-infusion methods. This method is preferred since it uses less sample, provides a continuous spray, should not require a separate discrimination study, has less chance of carryover, and is in principal faster than FI. FI required multiple injections to measure the transition set. Each took time to travel to the source and required additional time to clean solvent lines. If FI is used, the instrument should be set up using the MS switching valve. This would add a negligible amount of time before the sample reaches the MS but the wash step which has a higher flow rate can then be sent to waste preventing any damage to the MS and nebulizer in the course of a large study.

Some bias may be present in this method with the Bligh Dyer sample preparation method. This is a procedure normally used for lipids but a portion of the polar phase was also analyzed to include polar metabolites. The results, however, show many more non polar lipids than polar lipids and metabolites. Future studies should evaluate the sample preparation procedure to ensure optimal extraction and reconstitution of polar metabolites.

CHAPTER 6. CEREBROSPINAL FLUID ANALYSIS FOR PARKINSON'S DISEASE BIOMARKER DISCOVERY

6.1 Introduction

Parkinson's disease (PD) is a neurodegenerative disorder that affects five million people worldwide.[106] Despite its prevalence it has no clear diagnosis or treatment. The disease is systemic, worsens over time, and likely has different metabolomic signatures during its different phases. Initially, during the preclinical stage neurons begin to degrade and symptoms are nonspecific to the disease (*e.g.* visual, sleep, special and/or digestive issues).[107-109] During this phase, diagnosis is approximately 25% accurate. In the clinical stage, symptoms worsen, are heterogeneous, and overlap with other neurological disorders.[107, 110-111] No definitive biomarkers exist for either phase and a diagnosis is often made during the clinical phase after all other diseases have been ruled out and if the patient responds to PD drugs.[108, 112] This diagnosis is not very accurate due to the heterogeneity of the clinical symptoms.[60-61, 110-111, 113]a At this point, treatments are not effective since many of the neurons have degraded and drugs are used in an attempt to manage symptoms. There has been much interest in research for (i) preclinical phase PD biomarkers to diagnose the disease before neurons are destroyed and the patient exhibits clinical symptoms, (ii) for clinical phase biomarkers to indicate if the clinical symptoms are PD related, and (iii) in biomarkers in both phases that might be useful for drug targeting.[107-108, 110, 114-115]

However, PD is a challenging disease to study. Creating a population to study is difficult because of the poor diagnostic accuracy and heterogeneity of the disease. The heterogeneity suggests different subtypes of PD leading clinicians to adopt the term Parkinsonism for a wide variety of clinical indications of PD.[116] Additionally, one third of PD patients in later stages have co-pathologies, or more than one neurological disorder.[110-111, 115] Therefore, researches are often unsure of what population to target or how to differentiate PD biomarkers from other disease markers. This issue leads to studies with underestimated sensitivity and specificity.[106] But, as compared to preclinical phase, studying the clinical phase is slightly more advantageous because subjects can be better defined as 'typical' and may be included more confidently.[114] The Michael J. Fox Foundation for Parkinson's Research BioFIND study helped correct many of the pre-analytical variables but it still suffers from the above issues. It has been reported that 15% of subjects lack clinical or molecular markers for PD which may bias the outcome.[106]

Current biomarker research for PD includes proteomics and metabolomics work.[108-109, 113, 115, 117-119] Protein research is largely based on the use of immunoassays which lack specificity and sensitivity for analytes.[120] Metabolomic MS analysis of samples provides more specificity and sensitivity for analytes that are more closely related to the phenotypes of PD.[113] Given the heterogeneous nature of PD, multiple pathways are likely affected leading to more than one altered biomarker or pathway.[59, 121] The aim of this study was to use MRM-profiling to discover biomarkers in cerebrospinal fluid (CSF) with biological reasoning, while using a minimal amount of sample per injection (<15 µL). This study was first published in 2016.[69] It found an accuracy of 56% and 76% for female and male samples, respectively. The study, however, used a preclinical phase PD sample set for discovery and the BioFIND late stage clinical PD samples for the screening phase. These sample sets do not likely have exactly the same biomarkers. Additionally, the original study used less than twenty Prec and NL scans for discovery, limiting the number of biological signals included in the screening method. In this chapter, a study is described in which only late stage clinical PD and healthy control (HC) samples were investigated. The study used over 100 Prec and NL scans, and significant transitions were identified by conventional LC-MS methods, an approach which lies outside the MRM-profiling methodology.

6.2 Chemicals, Instrumentation, and Software

A Thermo TSQ Quantum Access MAX was used for all MRM-profiling experiments with Xcalibur software. An electrosonic spray ionization (ESSI) source, a Hamilton 500 µL glass syringe, and the TSQ syringe pump were used for DI of samples and ionization. An Agilent 1290 Infinity pump, 6460 QQQ, and 6545 QTOF were used for LC-MS identification studies. Metabolanalyst 3.0 was used for univariate and multivariate statistics (Metabolanalyst.ca, accessed December 2016 to March 2017 and October 2017). Agilent MassHunter Acquisition and Qualitative software were used for QQQ and QTOF experiments. Metlin, PCDL, and HMDB databases were used for identification. Agilent HILIC and ZORBAX Eclipse Plus RRHD C18, 2.1 × 150 mm, 1.8 µm column were used for separation.

HPLC grade methanol, analytical grade acetic acid, lidocaine (137-57-6), arginine-$^{13}C_6$ (Arg-$^{13}C_6$; SKU: 643440), 2-hydroxyglutarate-D_3 (2HG-D_3), 1-amino-3-methoxypropan-2-ol (SKU: CDS009718), 2-dimethylaminoethanol (CAS: 108-01-0), chloromethyl methyl ether

(CAS: 107-30-2), iodomethane (CAS: 74-88-4), and 2-[2-(dimethylamino)ethoxy] ethanol (CAS: 1704-62-7) were purchased from Sigma Aldrich. Commercial human CSF was purchased from Lee BioSolutions (Maryland Heights, MO).

6.3 Sample Sets and Sample Blinding

PD and HC BioFIND samples were provided by the Michael J Fox Foundation. The BioFIND study is described well elsewhere.[114] Briefly, the PD samples were moderate to advanced clinical cases, and to be included, the patients needed three signs of Parkinsonism, be over the age of 50, respond to L-dopa or amantadine therapies, have no incidence of cancer, and take no other medications. The matched HC samples must be over the age of 50, have high cognitive scores, and have the same cancer and medical criteria as the PD group. A breakdown of the age and gender of the PD and HC samples is in Table 6.1.

Table 6.1 The BioFIND samples studied by MRM-profiling separated by gender.

	Female	Male
PD	20	40
HC	33	24
Other/tremor	2	1

The validation of this method was done blinded. Sample status was known to researchers in the discovery phase studies, then they were blinded by a third party scientist, data was acquired blinded, and then half were unblinded for building the multivariate statistical model. The remaining blinded samples were classified by the model and reported prior to unblinding.

6.4 Methods

6.4.1 Discovery Phase

Prec and NL scans (N=144, Appendix) were acquired on a QQQ for 1 min using a 1 second scan speed, three CE (5, 18, 30 eV), and the maximum mass range extended to *m/z* 2000. The positive mode scans used a voltage of 3500 V and the negative mode used 3000 V. CSF samples were pooled to create both male and female PD and HC pools. They were diluted 10X with the solvent system (95% methanol, 5% water, and 0.1% acetic acid) and directly injected at 5 µL/min. This solvent system was not optimized but it was adopted from a previous PD MRM-profiling method.[69] Since the metabolites under investigation were unknown, data for every NL and Prec scan in the library at the time was acquired. For each collision energy the spectrum was exported and transitions above 30% the base peak were kept. If all the signal intensities were greater than 5000 counts than the threshold was dropped to 5000 counts. Duplicate transitions with different collision energies were eliminated so that the transition and collision energy pairs with the higher intensity remained. The tube lens and collision energy for each transitions were optimized to achieve the greatest sensitivity for each transition. Product ion scans were also performed for all precursor masses found in the full scan spectrum above the baseline. This last point was a procedural carry over from the previous PD MRM-profiling study and is not suggested for other MRM profiling methods because there is minimal biological significance to this scan.[69]

6.4.2 Discrimination Studies

All the transitions (N=3252) were included in a MRM method where they were scanned 10 times each with a 100 ms dwell time. A discrimination study was performed using this method to reduce the number of transitions. Eight male and female, HC and PD pools and 32 individual samples were analyzed using the method. Each sample was diluted 16X with solvent, directly injected using a flow rate of 3 µL/min, and ionized with ESSI. Univariate statistics as were used to determine which transitions were important (t-test, p=0.1, FC=2, ROC AUC= 0.7).

6.4.3 Screening Phase

The final method contained 206 transitions. The method was less than 5 min long and used a 100 ms dwell time for 10 number of cycles. A 3 µL/min flow rate was used to spray a CSF sample, diluted 16X into the solvent system doped with 10,000 ng/mL Arg-$^{13}C_6$ and 2HG-D_3. These two standards were also measured in the method to check for correct sample preparation and MS quality. Arginine (Arg) was used as a normalization analyte and was also measured in the positive mode. The transitions used were (+) 175.1→70.3 for endogenous Arg, (+) 181.1→74.3 for Arg-$^{13}C_6$, and (-) 150.0→132.1 for 2HG-D_3.

The blinded samples were randomized and data were acquired over a three day period. QC samples as described below were tested first each day to ensure the MS was operating correctly. Between samples the syringe was rinsed twice with 500 µL of water and methanol and the ESSI line was rinsed once with 500 µL methanol and water. Before beginning the MRM method, a full scan was recorded for each sample to confirm peak stability. Then the MRM method data were collected for each sample dilution (n=3).

6.4.4 QC Procedure

To ensure the performance of the instrument, quality control samples were developed and implemented. Commercially CSF was spiked with serotonin and arginine (10 ppm). The sample was diluted in the doped solvent system and sprayed. The transitions for serotonin, Arg, and Arg-$^{13}C_6$ were acquired with an MRM method in positive mode. The serotonin and Arg signals were normalized to Arg-$^{13}C_6$ and the spiked sample was compared to a blank CSF sample. The baseline sensitivity of the assay was determined by the signal to blank ratio (or signal to noise, S/N) and this sensitivity was the threshold for instrument use. This process ensured that each day the MS performed optimally and any instrument or assay issues were corrected prior to analyzing BioFIND samples.

6.4.5 Data Analysis

Signals for each transition were summed and the three injections averaged. Outliers were determined by the signal of Arg-$^{13}C_6$. If this signal was calculated as an outlier then the sample was re-prepared and data re-acquired. If the signal remained an outlier, the sample was excluded

from the study. Each positive mode signal was normalized with endogenous Arg signal and each negative mode signal with 2HG-D_3.

With data from the unblinded samples (N=55), univariate statistics were performed and a model built to classify the blinded samples. Using Metaboanalyst 3.0, the data were autoscaled and univariate statistics, including t-test (p=0.05), fold change (FC=2), and ROC curve (AUC=0.75), was used to find significant transitions. Linear supporting vector machine (LinSVM) was used for modeling and classification of unknowns.

6.4.6 LC-MS and HRMS

Two HILIC normal phase and one C18 reverse phase LC methods were developed to separate the unknown transitions (Figure 6.1). The C18 sample was diluted 1:2 in water doped with Arg-$^{13}C_6$ and the HILIC diluted 1:2 in acetonitrile doped with Arg-$^{13}C_6$. The mobile phases used for the both methods were water with 5 mM ammonium formate and 0.1% formic acid (Pump A) and acetonitrile with 5 mM ammonium formate and 0.1% formic acid (Pump B). The 17 transitions were recorded for the entire gradient to determine RT(s) for each transition. Then, the LC was coupled to a 6545 QTOF where an MS was used to method determine the exact mass. Then, a targeted MS method with a narrow isolation width (*m/z* 1.7) was used to collet HRMS product ion spectra. If possible the RT, exact mass, and product ion spectra were compared to a standard. If a standard was not available, Metlin and HMDB databases were used to identify analytes.

Some standards for identification were purchased while others had to be synthesized. 1-(Dimethylamino)-3-methoxypropanol was made by mixing one part 1-amino-3-methodypropan-2-ol with two parts iodomethane. The reaction at RT was allowed to progress for 10 minutes before it was diluted into acetonitrile to approximately 10,000 ng/mL. This was mixed 2:1 with either CSF or water then 5 µL was injected onto the column. To make 2-(methoxymethyl)-N,N-dimethylethanamine, one part 2-dimethylamino ethanol was mixed with onD part chloromethyl methyl ether. This was diluted to approximately 10,000 ng/mL before being diluted and injected as stated above.

A

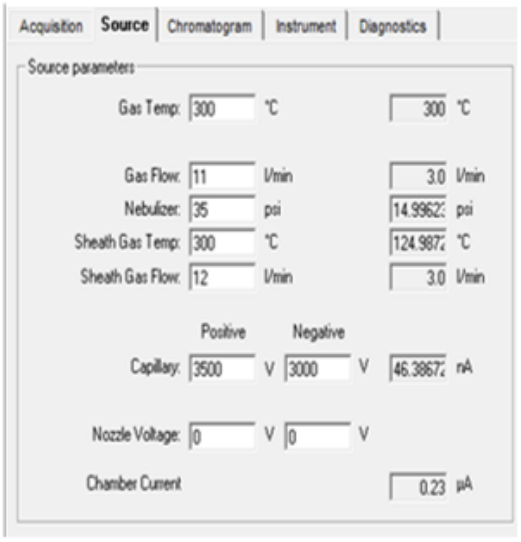

B

HILIC	
Time (min)	% Mobile Phase B
0	95
5	95
40	2
45	2
50	95
55	95

C

C18	
Time (min)	% Mobile Phase B
0	2
5	2
40	45
45	98
55	98
57	2
65	2

Figure 6.1 (A) Source conditions for the LC-QQQ methods. (B) The HILIC and (C) Zorbax C18 methods used a flow rate of 0.2 mL/min with water with 0.1% formate acid and 5 mM ammonium formate as mobile phase A and acetonitrile with 0.1% formate acid and 5 mM ammonium formate as mobile phase B.

6.4.7 DI-MS/MS Quantitation

The quantitation of the unknown analyte used the transitions *m/z* 134.0→72.0. The method used DI, ESSI, and the TSQ QQQ. Since the structure was unknown, analogs not biologically present in CSF were used as a MS/MS calibrator standard and internal standard. The standard, 2-dimethylamino ethanol was measured using the transition *m/z* 90.3→72.4 and the internal standard (IS), 1-amion-3-methoxypropan-2-ol was measured using *m/z* 106.0→88.2. The Cals and QCs were made by mixing Cal stocks (20X in water) to 1X in commercial CSF. The Cal concentrations were 50, 100, 400, 1500, 3000, and 6000 ng/mL and the QCs were 150, 1000, and 5000 ng/mL. The samples were diluted 15 µL CSF into 180 µL 95% acetonitrile with 0.1% formic and 1,000 ng/mL IS. The samples were sprayed 10 µL/min for 30 seconds using a dwell time of 250 ms. A subset of the BioFIND samples were acquired with this method (N=82).

6.5 Results and Discussion

6.5.1 MRM-profiling

The discovery phase found 3252 transitions, 944 from the NL and Prec scans and 2308 transitions from the product ion scans. The product ion scans found significantly more transitions in part due to the high chemical noise in the sample and the use of a methanol based solvent system. This signal is not as biologically specific as the transitions from the NL and Prec scans but remained in the analysis to be consistent with the previous PD MRM-profiling study.

Biological outliers, ‘tremor/other’, were not used in the model or classification statistics. Five analytical outliers existed and were removed from the model and classification. The normalization to endogenous Arg signal was a procedure that remained from the previous MRM-profiling study. The 2HG-D_3 standard was added to normalize negative mode transitions in this study. From the screening method, a total of 17 transitions were found to be significant using univariate statistics (N=55, Table 6.2). The LinSVM model plot shows separation of the HC and PD groups in the modeling sample set using the 17 transitions. Metaboanalyst performed 100 cross validations of the model set and gave a predictive accuracy of 87% and 93% sensitivity and specificity. The ROC curve has an AUC= 0.935 (Figure 6.2).

Table 6.2 17 transitions found to be significantly different by univariate statistics in the modeling set (N=55). The misregulation trend of PD from the modeling boxplots is described and the average signal from HC and PD samples is given.

Mode	Precursor (*m/z*)	Product (*m/z*)	Boxplot PD Trend	Avg HC Signal	Avg PD Signal
Positive	134.0	72.0	downregulated	22,225	6,383
Positive	153.1	136.0	upregulated	1,589	79,969
Positive	222.0	162.0	Slightly up	30,476	37,186
Positive	235.1	86.3	Slightly down	348,169	400,499
Positive	449.9	337.8	No significant fold change	69	69
Positive	459.9	191.1	Slightly up	15,862	17,560
Positive	608.4	495.8	Slightly up	68	75
Positive	613.0	284.7	Slightly down	12,106	10,076
Positive	725.7	680.9	Slightly down	455	259
Positive	740.4	717.2	Slightly down	203	89
Positive	746.3	718.9	No significant fold change	55	87
Negative	255.9	217.8	Slightly down	68	48
Negative	374.9	89.2	Slightly down	50	49
Negative	398.7	294.4	Slightly down	57	51
Negative	398.7	352.8	Slightly down	127	93
Negative	460.8	295.0	Slightly down	51	48
Negative	516.5	471.0	Slightly down	62	47

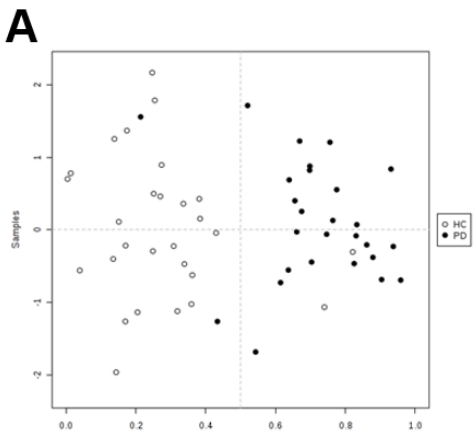

B

All Sample Validation					
		Predicted			
		PD	HC	Accuracy:	93%
Actual	PD	26	2	Sensitivity:	93%
	HC	2	25	Specificity:	93%

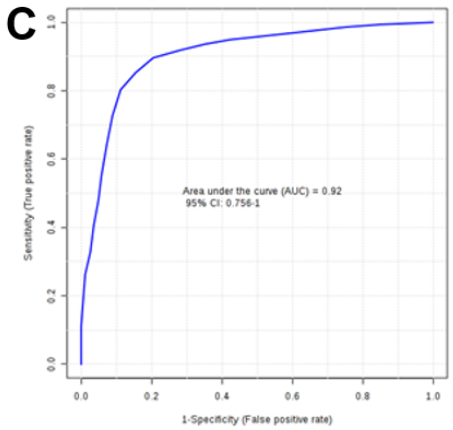

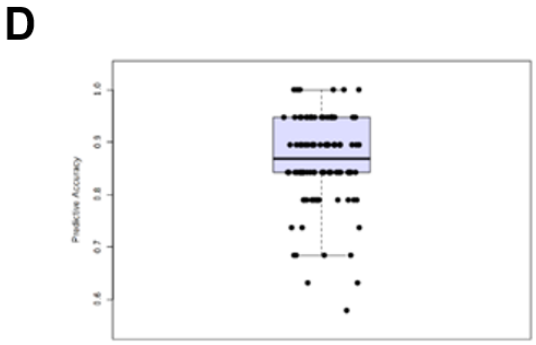

Figure 6.2 (A) 55 modeling samples separated by LinSVM model. (B) 100 permutations of a leave one out LinSVM validation model gave 93% accuracy, specificity, and sensitivity. (C) The ROC curve for the model was 0.92 AUC and (D) the 100 permutations gave an average 87 % predictive accuracy.

Because of the high metrics (Figure 6.2), this model was used for classifying the blinded samples (Table 6.3). The blinded classifications were reported and the samples were unblinded. The blinded set had less separation, sensitivity, and specificity than the modeling set (Figure 6.3). The validation accuracy was 72%, the sensitivity was 74%, and specificity 70%. Compared to the previous reported PD MRM-profiling study, in this study, female and males samples were classifying equally suggesting no gender bias with this assay.

Table 6.3 The BioFIND blinded samples (N=57), gender, classification, and clinical diagnosis.

BioFIND Sample ID	Subject Number	Gender	Classification	Diagnosis
BF0003-2137	1003	Male	HC	PD
BF0003-2215	1055	Male	PD	PD
BF0003-5459	1079	Male	PD	PD
BF0003-6777	1036	Female	PD	HC
BF0004-0806	1178	Female	PD	HC
BF0004-4940	1256	Male	HC	HC
BF0004-6181	1086	Male	HC	PD
BF0004-6196	1091	Male	PD	PD
BF0004-6367	1005	Female	HC	HC
BF0004-6372	1009	Male	HC	HC
BF0004-6382	1012	Female	PD	HC
BF0004-6387	1013	Male	HC	HC
BF0004-6392	1014	Female	HC	HC
BF0004-6397	1017	Male	PD	HC
BF0004-6402	1021	Female	HC	HC
BF0004-6412	1023	Male	HC	HC
BF0004-6442	1033	Female	HC	HC
BF0004-6447	1034	Female	HC	HC
BF0004-6457	1041	Female	HC	HC
BF0004-6467	1045	Male	PD	PD
BF0004-6477	1057	Male	PD	PD
BF0004-6482	1060	Female	PD	PD
BF0004-6497	1070	Female	HC	PD
BF0004-6502	1071	Female	PD	HC
BF0004-6514	1075	Female	HC	HC
BF0004-6529	1083	Male	PD	PD
BF0004-6539	1085	Male	PD	PD
BF0004-6544	1097	Female	HC	HC
BF0004-6549	1098	Male	PD	PD
BF0004-6579	1122	Male	PD	HC
BF0004-6584	1126	Female	HC	HC
BF0004-6589	1127	Male	HC	PD
BF0004-6594	1128	Female	HC	HC
BF0004-6599	1130	Male	HC	PD
BF0004-6604	1131	Male	HC	HC
BF0004-6609	1133	Male	PD	PD
BF0004-6614	1134	Male	HC	PD
BF0004-6619	1135	Male	PD	HC
BF0004-6629	1137	Female	HC	HC
BF0004-6634	1141	Male	PD	PD
BF0004-6639	1144	Male	PD	PD
BF0004-6649	1147	Female	HC	HC
BF0004-6664	1153	Female	PD	PD
BF0004-6669	1155	Male	PD	PD
BF0004-6674	1160	Male	PD	PD

Table 6.3, Continued

BioFIND Sample ID	Subject Number	Gender	Classification	Diagnosis
BF0004-6689	1172	Female	HC	HC
BF0004-6704	1191	Male	PD	PD
BF0004-6714	1195	Male	HC	HC
BF0004-6719	1205	Male	HC	PD
BF0004-6724	1207	Male	PD	PD
BF0004-6734	1210	Male	HC	PD
BF0004-6739	1211	Male	PD	PD
BF0004-6744	1213	Male	PD	PD
BF0004-6759	1220	Male	HC	HC
BF0004-6769	1222	Male	PD	PD
BF0004-6789	1229	Female	PD	PD
BF0004-6794	1238	Female	HC	PD

Male Validation

		Predicted			
		PD	HC	Accuracy:	71%
Actual	PD	18	7	Sensitivity:	72%
	HC	3	7	Specificity:	70%

Female Validation

		Predicted			
		PD	HC	Accuracy:	73%
Actual	PD	3	2	Sensitivity:	60%
	HC	4	13	Specificity:	76%

All Sample Validation

		Predicted			
		PD	HC	Accuracy:	72%
Actual	PD	21	9	Sensitivity:	70%
	HC	7	20	Specificity:	74%

Figure 6.3 LinSVM model was used to classify 57 blinded PD and HC samples. The accuracy, sensitivity, and specificity for all the samples and metrics separated by gender are given.

The lower metrics compared to the modeling set are not unexpected. But the large difference in accuracy could be caused by the heterogeneity of the disease that is difficult to model and predict given only the patients gender and binary (HC/PD) diagnosis. Subpopulations with a larger sample set for the discovery and screening could help the results of this study.

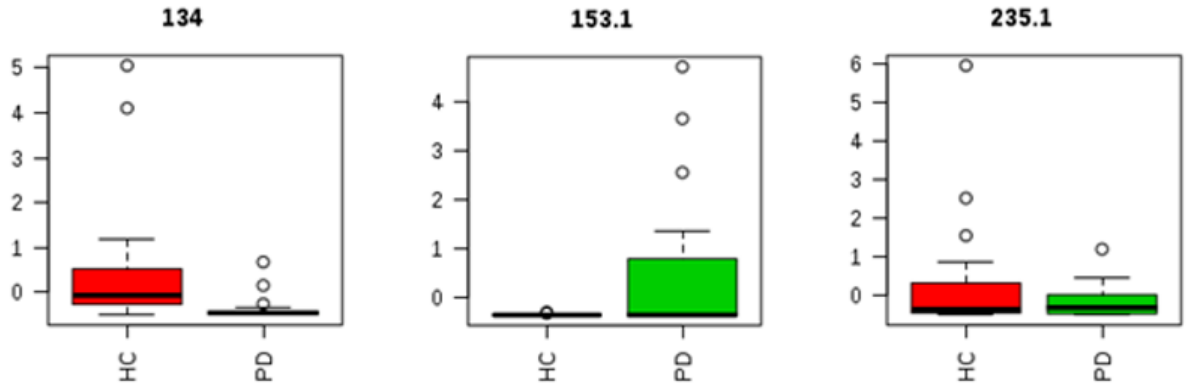

Figure 6.4 Boxplots with the modeling sample sets (N=55) for *m/z* 134.0→72.0, 153.1→136.0, and 235.1→86.3. The signal was normalized by endogenous arginine.

However, several of the analytes had high signal with box plots that showed the individual analytes significance (Figure 6.4). The identification of these and other transitions in Table 6.2 was explored using LC-MS methods.

6.5.2 LC-MS Identification

Fourteen of the analytes did not yield LC signal with either the C18 or HILIC chromatographic methods. This could be caused by their overall low signal or their response with these chromatographic solvents and columns. Three analytes did have high responses. The identification of these are described below.

6.5.2.1 235.1→86.3, Lidocaine

Using the C18 LC-QQQ method the signal for 235.1→ 86.3 was clearly seen in HC and PD pools. The RT of 14.5 minutes was recorded and an exact mass of *m/z* 235.1808 was found at this RT using the QTOF. Product ion scans for this analyte show only one peak in PD and HC pools (Figure 6.5 A and B). This protonated ion has an exact mass which corresponds to the chemical formula $C_{14}H_{22}N_2O$ which matches the formula for lidocaine, a drug used to numb patients for a lumbar puncture procedure. Data on a lidocine standard was acquired. The standard fragmentation (Figure 6.5, inset) and an exact mass match (less than 2 ppm mass error) compared well to the PD and HC analyte. The RT also matched closely, the 0.5 minute difference was from the CSF matrix of the unknown compared to water matrix of the standard. The same RT shift was observed for the Arg-$^{13}C_6$ standard between the CSF and water sample (data not shown). This transition was therefore identified as lidocaine.

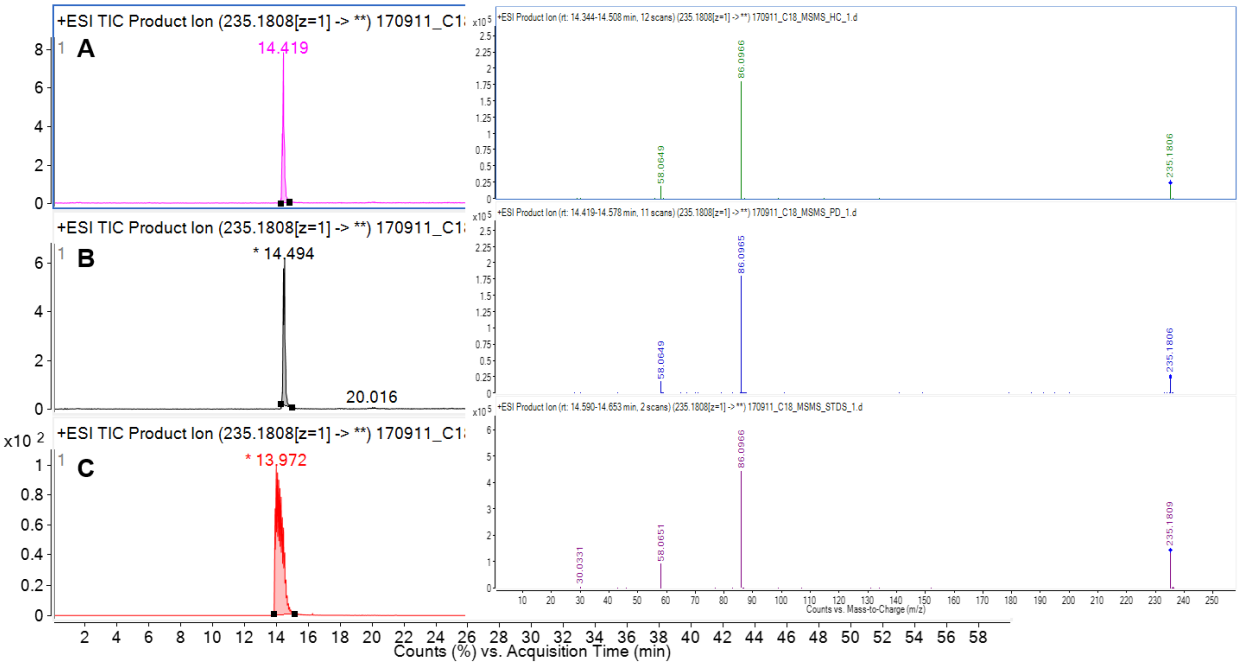

Figure 6.5 LC-QTOF data for a (A) CSF HC pool, (B) CSF PD pool, and (C) lidocaine standard. Using the C18 LC method with a targeted QTOF method for an exact mass of *m/z* 235.1808. The insets are product ion spectra for the respective integrated chromatographic peak.

6.5.2.2 153.1→136.0, Amantadine

The PD and HC pools contained multiple chromatographic peaks for the 153.1→136.0 peak with the C18 method. The absolute counts of the 9.1, 15.7, and 18.0 minute peaks for the LC-QQQ method were not changing significantly (Figure 6.6). The 21.3 minute peak was only present in the PD pool. This analyte was therefore the reason for the upregulation in the MRM data. The exact mass, *m/z* 153.0661, and product ion spectrum (Figure 6.6, inset) from the targeted QTOF method were not identified by Metlin or HMDB. Using PCDL software, the peak was identified as amantadine. This analyte had an exact mass of *m/z* 152.1434. The full scan spectrum (Figure 6.7) had a very high (6 x10^5) *m/z* 152.1434 peak and the *m/z* 153.0661 peak was roughly 10% intensity of it (Figure 6.7, inset). This suggests it is the ^{13}C isotope of amantadine.

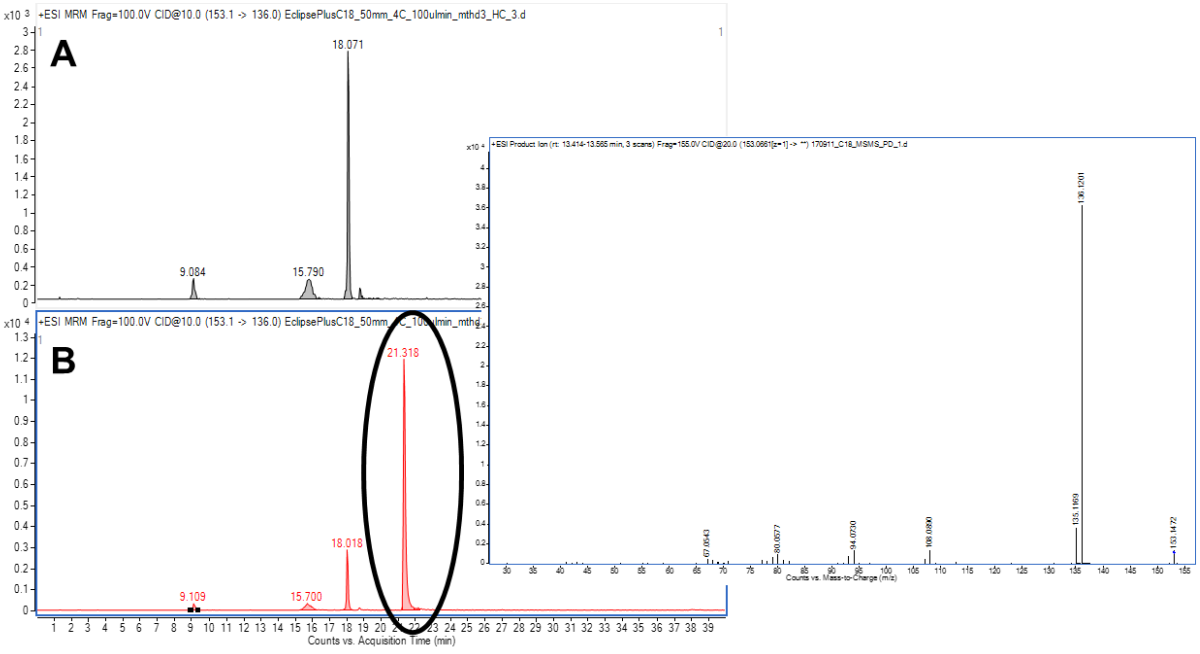

Figure 6.6 LC-QQQ of 153.1→136.0 of (A) a HC pooled sampled and (B) a PD pooled sample using a C18 LC method. Several chromatographic peaks were detected but the only one altered was at 21.3 min. This peak was only detected in PD samples. Its QTOF product ion spectrum is displayed.

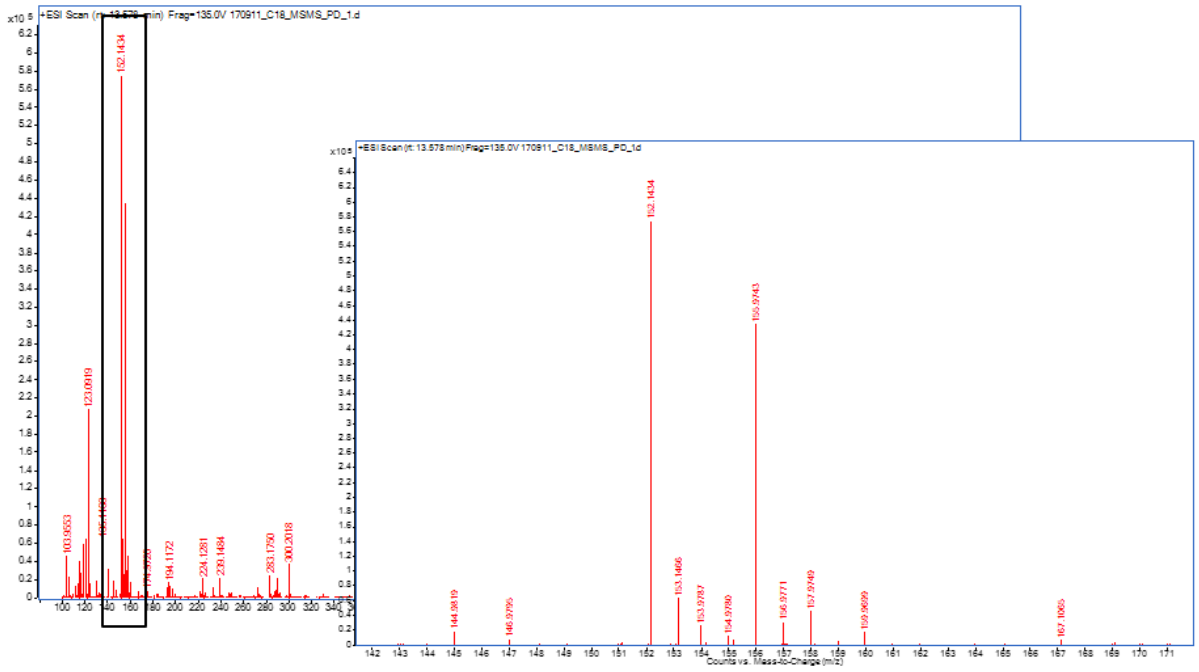

Figure 6.7 Full scan HRMS of PD pool acquired with the C18 LC method. The 21.3 minute chromatographic peak was integrated. The *m/z* 100-1000 region showed a base peak of *m/z* 152.1434 and when the *m/z* 140-170 region was selected (inset) the *m/z* 153.0661 peak was found to be approximately 10% of the *m/z* 152.1434.

Additionally, the fragmentation pattern of the unknown at m/z 153.1 matched those of amantadine but all the unknown mass peaks were one mass unit lower than the amantadine fragments. Amantadine is a PD drug which explains why it is only detected in the PD samples. Both the ^{12}C and ^{13}C isotope for amantadine were discovered by the less selective NL 17 scan and were a part of the original transition list. However, in the discrimination study, the ^{13}C isotope remained in the study while the ^{12}C transition was removed by the univariate statistics.

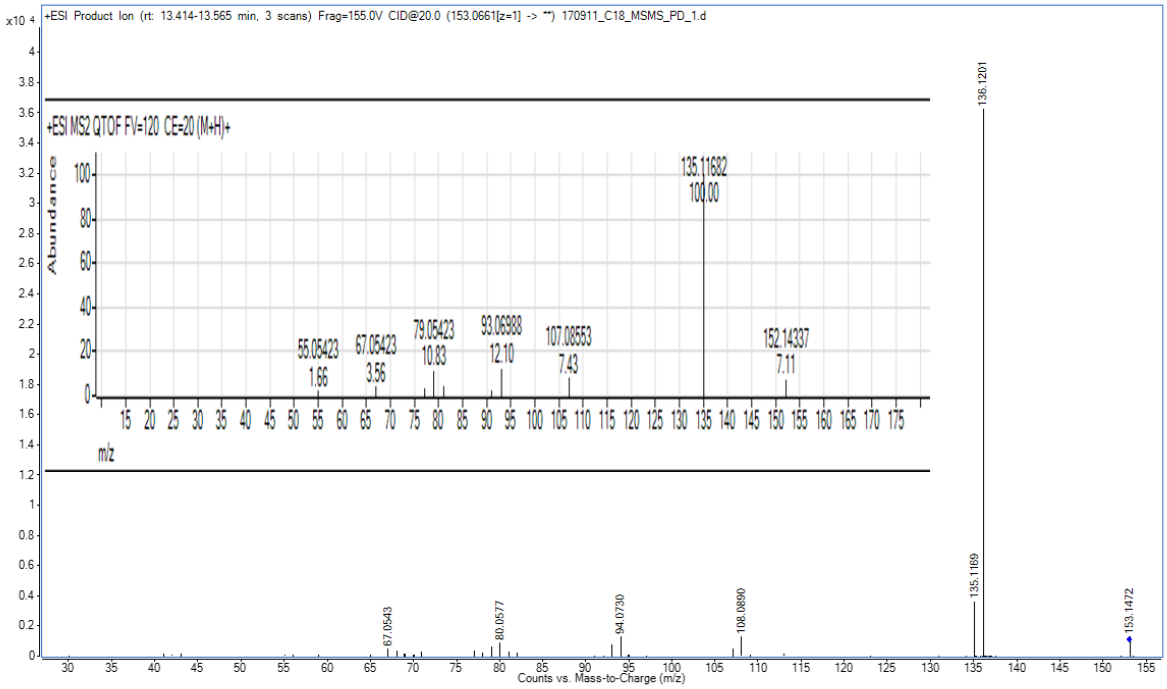

Figure 6.8 HRMS fragmentation spectra of the unknown analyte with precursor *m/z* 153.0661 at 21.3 minutes compared to amantadine fragmentation from the Metlin PCDL library.

This demonstrate that errors in the discrimination study do occur. Additionally, the less specific discovery scans can find drugs related to the populations. This is beneficial for epidemiological studies or metabolism studies but should be avoided for diagnostic assays.

6.5.2.3 134.0→72.0, Unknown

This is the only transition to be included in both the model of this study and the previous MRM-profiling PD study. A HILIC normal phase column was needed to retain this unknown analyte. In a pooled sample, it produced one peak at 21.3 minutes using a long gradient and a 10.9 min peak using a faster gradient. Figure 6.9 shows the peak for a HC (A) and PD (B) pool. There was a 4 times higher absolute signal from the HC pool verses the PD pool. This column produced a small front shoulder that was due to the normal phase column performance with the complex matrix. Both the main peak and shoulder had the same product ion spectra and are the same analyte (data not shown).

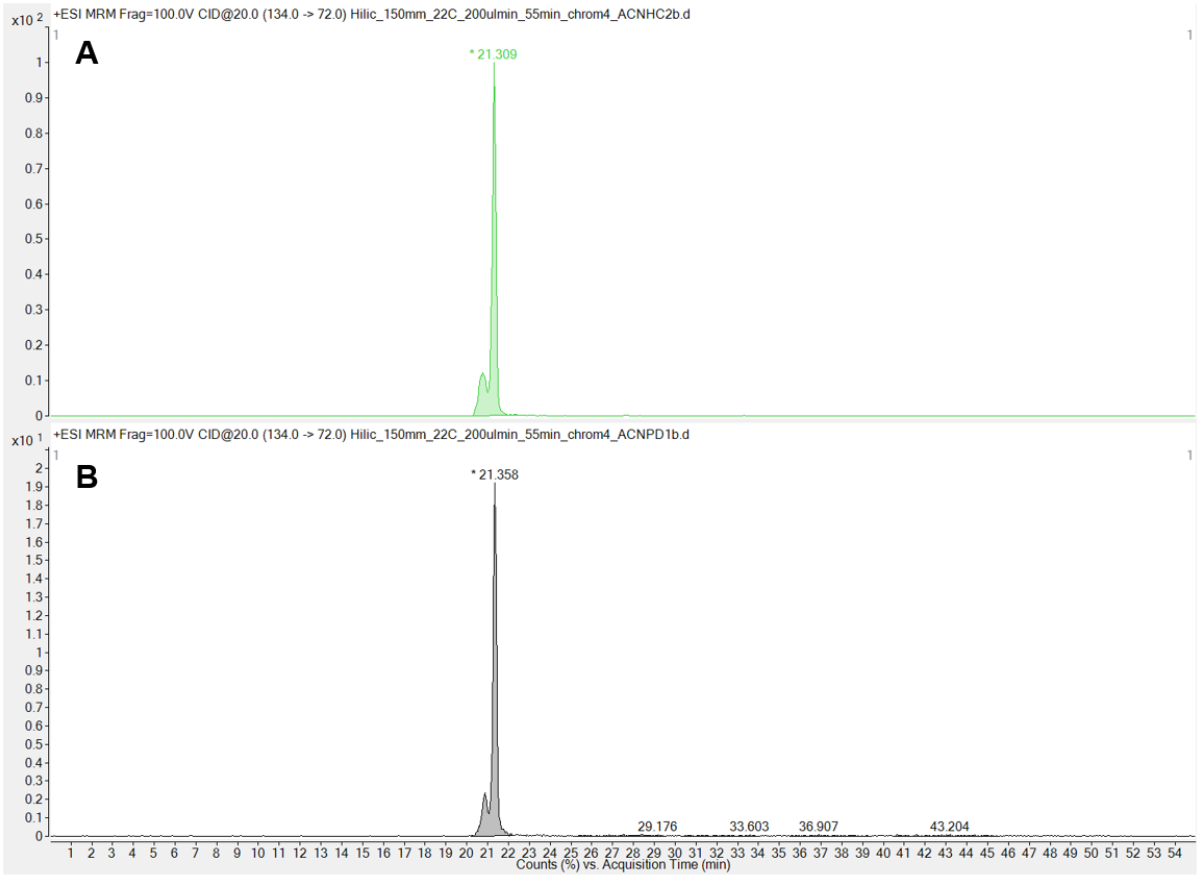

Figure 6.9 LC-MRM for m/z 134.0→72.0 for a (A) HC pool and a (B) PD pool using a HILIC column. The HC pool gave 400,000 counts verses the PD pool which had 70,000 counts.

The LC method on the QTOF (targeted for the *m/z* 134.1172 exact mass) gave several chromatographic peaks but only one had the *m/z* 72.0 fragment which matched the MRM chromatographic results (Figure 6.9). Product ion spectra for this analyte are shown in Figure 6.10. The exact mass measurement corresponded to the chemical formula of $C_6H_{15}NO_2$ (-2.6 ppm error). The *m/z* 105.9536 and 65.9265 mass peaks were background noise from either the column or solvent. These peaks are seen throughout the chromatogram (data not shown). The precursor has an exact mass of m/z 133.9585 and chemical formula of C_4H_3ClOS. This was so close to the unknown peak of *m/z* 134.1172 that the Q narrow isolation width of *m/z* 1.7 was too wide to isolate just the unknown. Developing other normal phase chromatography did not retain the analyte as well. A different MS filter is needed for isolating the precursor better to generate clean product ion spectra.

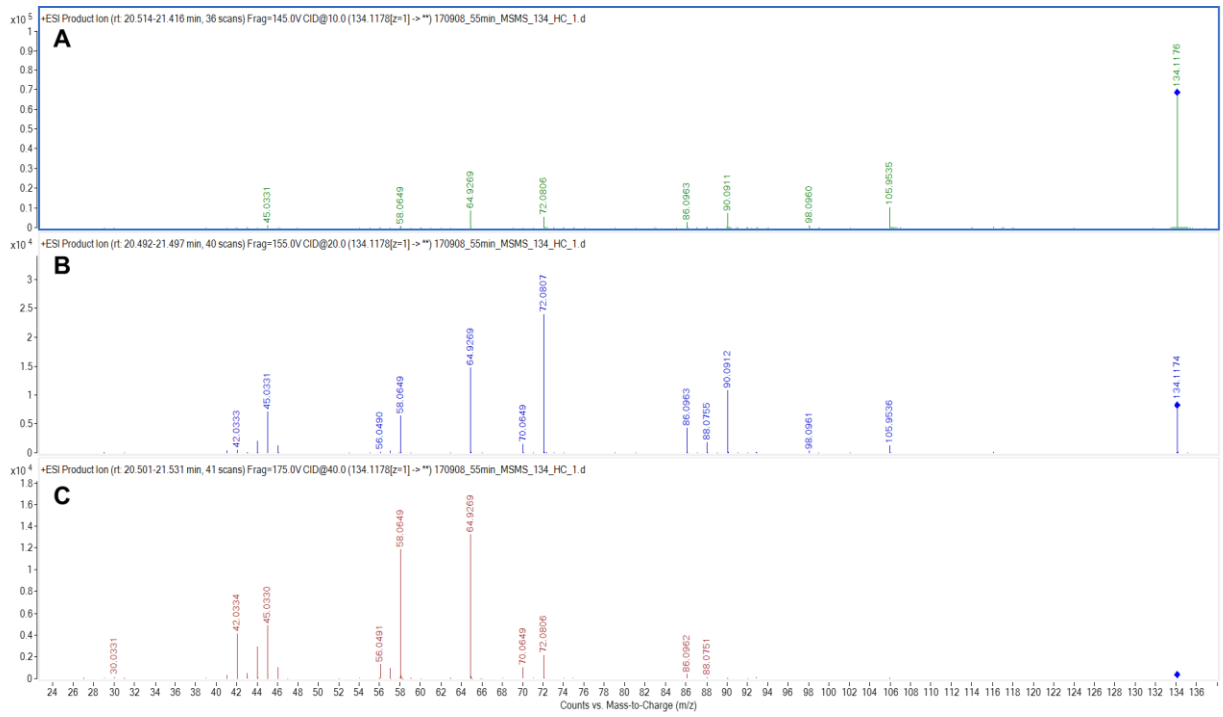

Figure 6.10 LC-QTOF HRMS product ion spectra for the unknown analyte in an HC pool. The QTOF method targeted m/z 134.1178 and used a CE of (A) 10, (B) 20 and (C) 40 eV.

The main fragments are m/z 90.0914 ($C_4H_{11}NO$), 72.0807 (C_4H_9N), 58.0654 (C_3H_7N), and 45.0337 (C_2H_4O). Based on this, the analyte 2-[2-(dimethylamino)ethoxy]ethanol (DMAEE) was considered. The standard was purchased and had a 0.3 min RT shifted from the unknown (when spiked into CSF) and a different fragmentation pattern (Figure 6.11 B). However, the same *m/z* 72 peak was generated and this was suggestive of the dimethylamine structure. The DMAEE spectrum lacked the *m/z* 45 fragment which corresponded to C_2H_4O making it likely that this arises from a terminal ether which was not in DMAEE.

Databases of human metabolites (HMDB, Metlin, and MassIVE) found in the literature did not provide any alternatives for a structure. For this reason, 1-(dimethylamino)-3-methoxypropan-2-ol was synthesized, spiked into CSF and water, acquired with the LC-QTOF method, and spectrum compared to the HC pool (Figure 6.11 C). This structure eluted 0.4 min before the unknown analyte and the fragmentation pattern did not match the unknown. Here, the *m/z* 45 peak was formed but the *m/z* 72 peak was absent, likely due to the placement of the hydroxyl group. Additionally, a water loss was seen, which suggested the hydroxyl group was readily lost and,

therefore, that a hydroxyl was not a part of the unknown structure. The large m/z 58 peak further supports this incorrect hydroxyl placement.

Another analyte, without the hydroxyl group but with the same dimethylamine and terminal ether structure considered was 2-(methoxymethoxy)-N,N-dimethylethanamine. This analyte was synthesized, collected using the LC-QTOF method, and compared to the unknown (Figure 6.11 D). Although this was the closest fragmentation match to the unknown analyte, the RT shift was 0.3 min, lacked the *m/z* 90 peak, and contained a new *m/z* 102 peak. Other structures were proposed but none were synthesized. The chemical structure remains unknown.

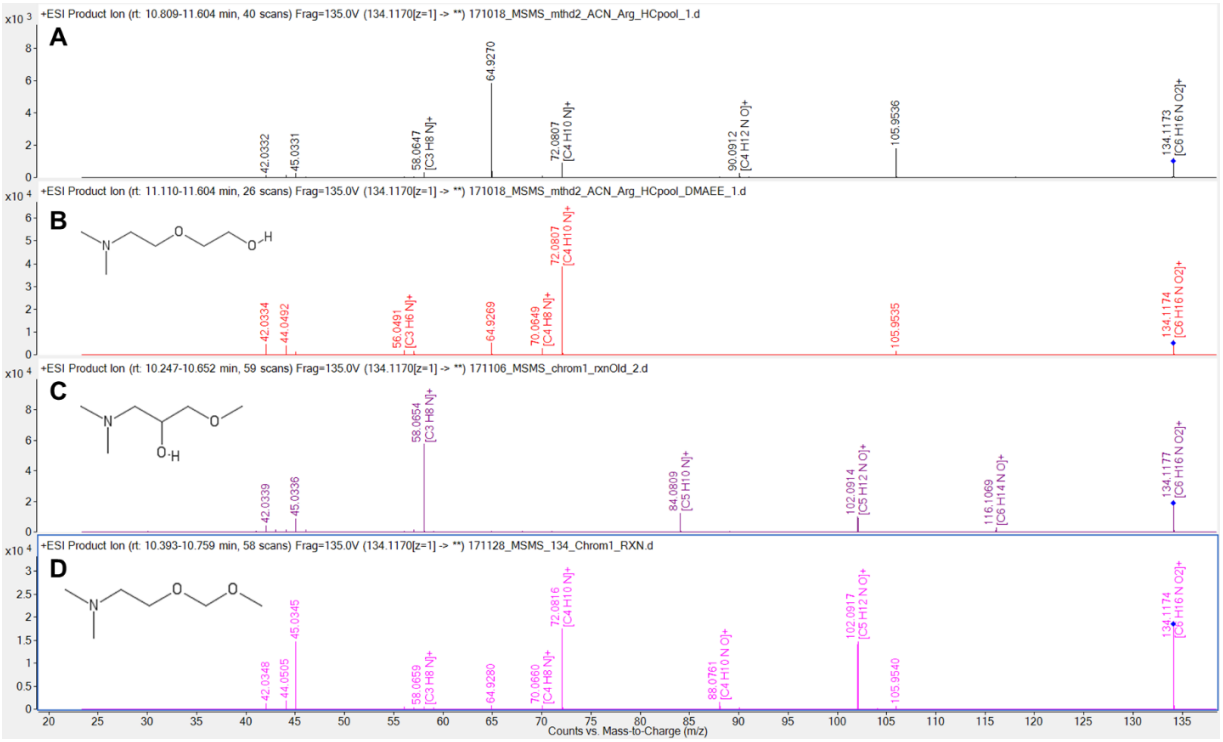

Figure 6.11 LC-QTOF HRMS product ion spectra for (A) the unknown analyte in an HC pool, (B) DMAEE, (C) 1-(dimethylamino)-3-methoxypropan-2-ol, and (D) 2-(methoxymethoxy)-N,N-dimethylethanamine. The QTOF method targeted m/z 134.1178.

6.5.3 DI-MS/MS

The concentration of the unknown (*m/z* 134.0) in the HC pool was estimated to be 200 ng/mL based on the unknown signal intensity compared to dilutions of DMAEE into CSF. This was not enough to purify the unknown for any other type of analysis in the remaining samples (~0.5 mL). Therefore, the analyte was quantified in the individual sample using structural analogs believed not to be present in CSF as a calibration standard and internal standard. This data would validate the trends seen in the MRM-profiling boxplot (Figure 6.4) and show that the signal can be used for PD diagnosis.

A DI-QQQ method was used since the 134.0→72.0 transition in an acetonitrile mobile phase showed only one chromatographic peak (Figure 6.9). Therefore, a LC method is not necessary for quantifying this analyte. Using 1-amino-3-methoxypropan-2-ol as an IS and 2-dimethylaminoethanol as quantitation standard, a quantitative method was developed. The LOD was 10 ng/mL, the calibration curve ($y=0.0002907x+0.0211545$) had an $R^2= 0.99$, three replicates of every standard solution had a RSD below 13%, and the three QCs had a percent error below 16%. Applying the Cal curve fit equation to the unknown signal produced the concentration of the unknown in individual samples. Only 82 of the samples from the original BioFIND study were analyzed with this method.

Original data from the 112 BioFIND samples were replotted and compared to the 82 sample subset (Figure 6.12 A and B). The subset showed the same trend as the full set of samples using the original MRM-profiling data normalized to endogenous arginine. The quantitative data (Figure 6.12 C) boxplots for 134.0→72.0 overlapped more and the analyte, when quantified with this method, and does not appear to be as significant. This difference is likely from the ion suppression correction (IS correction) or from the differences in ionization from the acetonitrile solvent system.

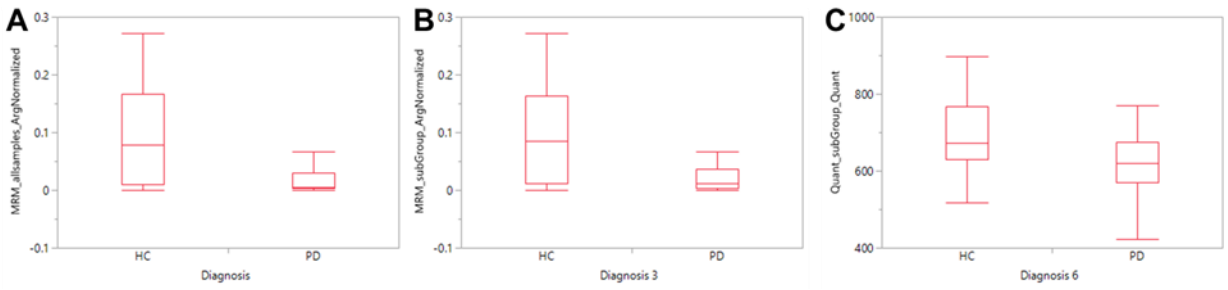

Figure 6.12 Box plots for 134.0→72.0 for MRM-profiling data of (A) 112 samples and (B) a subset of 82 samples. Quantitative data for those same 82 samples is displayed in C.

The LC-QTOF method used acetonitrile based mobile phase and pooled samples. This gave a high signal in HC and low signal in PD. This trend was likely from the pooling so when measuring individual samples by DI-QQQ method the individual sample measurement and corrected ion suppression did not have the same fold change. At this point, this analyte remains unknown and the final quantitative data suggests it might not be significant.

6.6 Conclusions

MRM-profiling is demonstrated as a fast, semi-targeted, metabolomic MS profiling methodology. It uses specific and biologically related functional groups to discover signal for a metabolite profile. In MRM mode, these signals, generated from an ion transition, can be screened very quickly, filtered with univariate statistics, and modeled. Validations on the model are good, but, as shown with the PD study, separate blinded validation sample sets are ideal for testing the model. The PD study improved upon the overall accuracy of previous studies, especially with female samples.[69] The improved performance could be because of use of additional Prec and NL scans, proper blocking of male and female samples in the discrimination study, or from using the BioFIND samples for both the discovery and screening phases.

After investigating the identity of the analytes in the metabolite profile, the analytes separating the samples were not shown to be significant to the biology of the disease. Rather, they were significant to the population of PD patients, *i.e.* PD drugs. Two transitions were identified as drugs related to the disease or the sample collection process (preanalytical). One other transition was not able to be identified but was quantified. The m/z 134.0→72.0 transition does not appear

to be as significant given these values. These results suggest that no endogenous biomarkers for PD exist that separate PD and HC populations. This could be caused by biological or analytical reasons. A root cause could be the nature and challenges of PD. Major variation between the model predicted accuracy and validation set accuracy suggests just such a variation in sample populations, or heterogeneity of the disease. The heterogeneity was not taken into consideration when designing PD pools and analyzing the population. The biomarkers related to a specific form of Parkinsonism could be diluted in a diverse PD sample set and therefore not discovered. Likewise, during the discrimination study or final screening, PD biomarkers may not appear significant and are therefore filtered out in the univariate statistical methods. A larger sample set with more clinical information to support blocking samples based on Parkinsonism or PD subpopulations could benefit future experiments. Other PD studies find similar issues with sample populations and this should be addressed for more meaningful results.[113, 119]

Analytically, this method had more challenges when compared to the CAD study. First, CSF has a low concentration of metabolites and a high salt and sugar content which suppresses the metabolite signal. The ESSI solvent, could be optimized further for small biological metabolites in future CSF studies. In the QC, serotonin and arginine were seen but the LOD was very high. If the LOD was lowered with optimization it is likely to be lower for other endogenous analytes. For this project, the method produced many signals of low abundance that are likely noise. These can be avoided by using a noise filter (absolute counts) on the data in the univariate statistics phase. This was done in the CAD study and the remaining signal could be used for identification with the chromatographic method.

Finding drugs in both the PD and CAD study are from non-specific Prec and NL scans or, in the case of lidocaine, a product ion scan. Product ion scans are not specific and should not be performed in future MRM-profiling experiment. The less specific Prec and NL scans are important for finding small analytes like carnitine and choline but they can also find drugs. If drugs are suspected, they can be measured then removed from the data as was done in the CAD study. This methodology is useful for studying different populations that can be take these drugs or for pharmacological studies trying to identify metabolites and drugged populations. However, they are not helpful in disease diagnostics.

APPENDIX. TABLE OF PREC AND NL SCANS FOR MRM-PROFILING

Mode	Type	Value (amu for NL and *m/z* for Prec)	Functional Group
Negative	NL	27	H_20 - amines, aromatic nitrile, aminosulphonic acids[122]
Negative	NL	28	CO - carboxylic acids, adehydes, H_2CN - nitroaromatics[122]
Negative	NL	30	NO - nitroaromatics, CH2O - aldehydes[122]
Negative	NL	44	CO_2 - carboxylic acids, carbamates[122]
Negative	NL	46	NO_2 - nitroaromatics, CH_2O_2 - carboxylic acids[122]
Negative	NL	62	H_2O and CO_2 [81]
Negative	NL	64	SO_2 - sulfonic acids, sulfonates[122]
Negative	NL	76	Phosphatidylglycerol (PG)[84]
Negative	NL	79	
Negative	NL	80	SO_3 - sulfonic acids[122]
Negative	NL	87	Phosphatydylserine (PS) head group[88]
Negative	NL	98	Steroid conjugate [81]
Negative	NL	121	$C_3H_7NO_2S$ - cysteine conjugates[122]
Negative	NL	131.1	
Negative	NL	132.1	
Negative	NL	146	$C_6H_{10}O_4$ - deoxyhexoside[122]
Negative	NL	153	Phosphoglycerols including phosphatidic acids (PA) and Lysophosphatidylglycerol (LysoPG) [88]
Negative	NL	155.1	
Negative	NL	164	$C_6H_{12}O_5$ - rhamnoside[122]
Negative	NL	176	$C_6H_8O_6$ – glucoronides// steroid conjugate[81, 122]
Negative	NL	183	
Negative	NL	185	
Negative	NL	194	Steroid conjugate[81]
Negative	NL	203	$C_8H_{13}NO_5$ - conjugate with N-acetylglucosamine (benzylic) [122]
Negative	NL	250	$C_8H_{14}N_2O_5S$ - conjugate with gamma-GluCys[122]

Negative	NL	282	Oleic acid; Phosphatidylinositol (PI) [88]
Negative	NL	355	Phosphatidylcholine (PC), alkelnyl-acyl PC (ePC), sphingomyelin (SM) and LysoPC[62]
Negative	NL	357	
Negative	NL	383	
Negative	NL	385	
Negative	NL	444	Oleic acid and inositol; PI[88]
Negative	Prec	59	Arachinonic acid (fatty acid) [81]
Negative	Prec	80	SO_3^-[81]
Negative	Prec	85	
Negative	Prec	97	Sulfatide (ST)// HSO_4^-[62, 81, 84]
Negative	Prec	115	HETE[81]
Negative	Prec	127	HETE[81]
Negative	Prec	135	PA
Negative	Prec	140	Phosphatidylethanolamine (PE)
Negative	Prec	145	HETE[81]
Negative	Prec	151	Leukotrienes[81]
Negative	Prec	153.1	glycerophosphate[62, 87]
Negative	Prec	155	HETE[81]
Negative	Prec	167	HETE[81]
Negative	Prec	168	SM; demethylated headgroup[88]
Negative	Prec	171	PG
Negative	Prec	175	HETE[81]
Negative	Prec	179	HETE[81]
Negative	Prec	184	
Negative	Prec	191	Glucuronide[81]
Negative	Prec	193	Glucuronide[81]
Negative	Prec	195	Leukotrienes[81]
Negative	Prec	196	PE; dilyso-H_2O[88]
Negative	Prec	199	glycerolipids; Dodecanoic acid residue
Negative	Prec	207	HETE[81]

Negative	Prec	219	HETE[81]
Negative	Prec	223	PI
Negative	Prec	225.2	glycerolipids; myristoleic acid residue and Sulfoqunoovosyldiacylglycerol
Negative	Prec	226	prostaglandin[81]
Negative	Prec	227.2	glycerolipids; Myristicacid residue
Negative	Prec	241	PI head group, nositol phosphate[82, 84]
Negative	Prec	253.2	glycerolipids; Palmitoleic/Sapienic acid residue
Negative	Prec	255.2	glycerolipids; Palmitic acid residue
Negative	Prec	264.3	
Negative	Prec	266.4	
Negative	Prec	271.9	
Negative	Prec	275.2	glycerolipids; stearidonic acid
Negative	Prec	277.2	glycerolipids; gama-Linolenic acid residue
Negative	Prec	279.2	GPI 18:2[87-88]
Negative	Prec	281.2	GPI 18:1[87-88]
Negative	Prec	282.2	
Negative	Prec	283.2	GPI 18:3[87-88]
Negative	Prec	292.4	
Negative	Prec	301	glycerolipids; Eicosapentaenoic acid residue
Negative	Prec	303.2	GPI 20:4[87]
Negative	Prec	305.2	glycerolipids; eicosatrienoic residue
Negative	Prec	307.3	glycerolipids; eicosadienoic residue
Negative	Prec	309.3	glycerolipids; Gondoic acid residue
Negative	Prec	311.3	glycerolipids; Arachidicacid residue
Negative	Prec	327.3	glycerolipids; docosahexaenoic DHA residue
Negative	Prec	329.3	glycerolipids; Eicosapentaenoic acid EPA residue
Negative	Prec	331.3	glycerolipids; Docosatetraenoic acid residue
Negative	Prec	333	Leukotrienes[81]
Negative	Prec	335.2	glycerolipids; docosadienoic residue
Negative	Prec	337.3	glycerolipids; Erucic acid residue

Negative	Prec	339.3	glycerolipids; Behenic acid residue
Negative	Prec	355.3	glycerolipids; nisinic acid residue
Negative	Prec	365.4	glycerolipids; nervonic acid residue
Negative	Prec	367.4	glycerolipids; Lignoceric acid residue
Negative	Prec	395.4	glycerolipids; cerotic acid residue
Negative	Prec	423.4	glycerolipids; melissics acid residue
Negative	Prec	451.4	glycerolipids; lacceroic acid residue
Negative	Prec	479.5	glycerolipids; geddicacid residue
Negative	Prec	507.5	glycerolipids; montanic acid residue
Positive	NL	17	NH_3- aliphatic amines (aromatic amines), oximes[122]
Positive	NL	18	H_2O - carboxylic acids, adehydes, ester[122]
Positive	NL	27	H_20 - amines, aromatic nitrile, aminosulphonic acids[122]
Positive	NL	28	CO - carboxylic acids, adehydes, H_2CN - nitroaromatics[122]
Positive	NL	30	NO - nitroaromatics, CH_2O - aldehydes[122]
Positive	NL	32	CH4O - methyl esters[122]
Positive	NL	34.0	H_2S - thiols[122]
Positive	NL	36.0	HCl –chlorides and 2(H_2O) [85, 122]
Positive	NL	44.0	CO_2 - carboxylic acids, carbamates[122]
Positive	NL	46.0	NO_2 - nitroaromatics, CH_2O_2 - carboxylic acids[122]
Positive	NL	48	H_2O and HCHO- sphingosine[85]
Positive	NL	50	Chloromethane- PC[87]
Positive	NL	59.0	Choline species; $(CH_3)_3N$[84]
Positive	NL	64.0	CH_4OS - methionine sulfoxide[122]
Positive	NL	71.0	C_3H_5NO - serine residue[122]
Positive	NL	74.0	C_3H_6S - methionine side chain[122]
Positive	NL	80.0	SO_3 - sulfonic acids, HPO_3 - phosphates[122]
Positive	NL	81.0	HSO_3 - sulfonic acids[122]
Positive	NL	82.0	H_2SO_3 - sulfonate group[122]
Positive	NL	87	Serine; PS[87]
Positive	NL	98.0	H_3PO_4 - phosphates[122]

Positive	NL	103	Lysophospholipid[81]
Positive	NL	115	PA
Positive	NL	121	$C_3H_7NO_2S$ - cysteine conjugates[122]
Positive	NL	128	HI - aromatic iodides[122]
Positive	NL	129	
Positive	NL	130	$C_6H_{10}O_3$ - dideoxyhexoside[122]
Positive	NL	132	$C_5H_8O_4$ - pentoside[122]
Positive	NL	141	PE head group[84, 88]
Positive	NL	146	Pro/anthocyanidins; $C_6H_{10}O_4$ - deoxyhexoside, $C_5H_{10}N_2O_3$ - conjugate with gamma-GluCys or gluthatione[122-123]
Positive	NL	153	
Positive	NL	162	Pro/anthocyanidins; $C_6H_{10}O_5$ - hexoside[122-123]
Positive	NL	163	$C_5H_9NO_3S$ - N-acetylcysteine conjugate[122]
Positive	NL	176	$C_6H_8O_6$ - glucuronides[122]
Positive	NL	179	Glycosylinositolphosphoceramide (GIPC)
Positive	NL	183	Phosphocholine (Li+)[87]
Positive	NL	185	PS head group[84, 88]
Positive	NL	189	PG[124]
Positive	NL	194	$C_6H_{10}O_7$ - glucuronides (benzylic) [122]
Positive	NL	203	$C_8H_{13}NO_5$ - conjugate with N-acetylglucosamine (benzylic) [122]
Positive	NL	205	lysophospholipids[81]
Positive	NL	217	glycerolipids; Dodecanoic acid residue[83]
Positive	NL	221	$C_8H_{15}NO_6$ - conjugate with N-acetylglucosamine[122]
Positive	NL	222	FMOC derivatitized lipids[87]
Positive	NL	228	TAG 14:0[87]
Positive	NL	245	glycerolipids; Myristicacid residue[83]
Positive	NL	248	$C_9H_{12}O_8$ – malonylglucuronides[122]
Positive	NL	250	$C_8H_{14}N_2O_5S$ - conjugate with gamma-GluCys[122]
Positive	NL	254	TAG 16:1[87]
Positive	NL	256	TAG 16:0[87]

Positive	NL	257	glycerolipids; myristoleic acid residue[83]
Positive	NL	260	glycerophosphoserine[81]
Positive	NL	266	$C_9H_{14}O_9$ - malonylglucoronides (benzylic) [122]
Positive	NL	268	TAG 17:1[87]
Positive	NL	271	glycerolipids; Palmitoleic/Sapienic acid residue TAG[82-83]
Positive	NL	273	TAG 16:0[82-83]
Positive	NL	273.2	TAGs; NH_4^+ $CH_3(CH_2)_{14}COOH$[82]
Positive	NL	277	PI[124]
Positive	NL	277.2	TAGS[82]
Positive	NL	278	TAG 18:3[87]
Positive	NL	280	TAG 18:2[87]
Positive	NL	282	TAG 18:1[87]
Positive	NL	284	TAG 18:0[87]
Positive	NL	293	glycerolipids; stearidonic acid
Positive	NL	295	TAG[83]
Positive	NL	297	TAG[83]
Positive	NL	299	TAG[82-83]
Positive	NL	301	TAG[82]
Positive	NL	304	TAG 20:4[87]
Positive	NL	307	$C_{10}H_{17}N_3O_6S$glutathione conjugates[122]
Positive	NL	312	TAG 20:0[87]
Positive	NL	319	glycerolipids; Eicosapentaenoic acid residue[83]
Positive	NL	321	glycerolipids; Arachidonic acid residue[83]
Positive	NL	323.0	glycerolipids; eicosatrienoic residue[83]
Positive	NL	325.0	TAG 20:2[83]
Positive	NL	327.0	TAG 20:1[83]
Positive	NL	328	TAG 22:0[87]
Positive	NL	329.0	TAG 20:0[83]
Positive	NL	341.0	Digalactosyldiacylglycerol (DGDG) and monogalactosyldiacylglycerol (MGDG)[125]
Positive	NL	345.0	glycerolipids; docosahexaenoic DHA residue[83]

Positive	NL	347.0	glycerolipids; Eicosapentaenoic acid EPA residue[83]
Positive	NL	349.0	glycerolipids; Docosatetraenoic acid residue[83]
Positive	NL	353.0	glycerolipids; docosadienoic residue[83]
Positive	NL	355.0	glycerolipids; Erucic acid residue[83]
Positive	NL	357.0	glycerolipids; Behenic acid residue[83]
Positive	NL	375.0	glycerolipids; nisinic acid residue
Positive	NL	383.0	glycerolipids; nervonic acid residue
Positive	NL	385.0	glycerolipids; Lignoceric acid residue[83]
Positive	NL	413.0	glycerolipids; cerotic acid residue
Positive	NL	441.0	glycerolipids; melissics acid residue
Positive	NL	469.0	glycerolipids; melissics acid residue
Positive	NL	497.0	glycerolipids; melissics acid residue
Positive	NL	525.0	glycerolipids; melissics acid residue
Positive	Prec	85	Acylcarnitines[62]
Positive	Prec	86	PC, LPC, SM; $OHCH_2CH_2NMe_3$-H_2O[84]
Positive	Prec	104	PC, LPC, SM; choline[84]
Positive	Prec	147	Lysophospholipids[81]
Positive	Prec	153	Glycerophosphate[87]
Positive	Prec	166	PC/LPC/SM [84]
Positive	Prec	181	Lysophospholipids[81]
Positive	Prec	184	Phosphatidylcholine (PC), alkelnyl-acyl PC (ePC), sphingomyelin (SM) and LysoPC[84, 88]
Positive	Prec	199	
Positive	Prec	227.2	
Positive	Prec	241	
Positive	Prec	256.3	Ceramides 16:0[86]
Positive	Prec	262.3	Ceramides d18:2[86]
Positive	Prec	264	Ceramides[81]
Positive	Prec	264.3	Ceramides (d18:1; sphingosines)/Cerebrosides[86, 90]
Positive	Prec	266	Ceramides[81]
Positive	Prec	266.4	Ceramides (d18:0; sphinganines) [86, 90]

Positive	Prec	275.2	
Positive	Prec	279	Ceramides[87]
Positive	Prec	279.2	
Positive	Prec	280	Ceramides[81]
Positive	Prec	282.2	Ceramides (t18:0 4-hydroxysphinganines) [86, 90]
Positive	Prec	282.4	Ceramides 18:0[81, 86]
Positive	Prec	283	Ceramides[87]
Positive	Prec	284.3	Ceramides 18:0[86]
Positive	Prec	292.3	Ceramides d20:1[86]
Positive	Prec	292.4	Ceramides (d20:1)[90]
Positive	Prec	300.3	Ceramides 18:0(OH) [86]
Positive	Prec	301	Pro/anthocyanidins[123]
Positive	Prec	303	Pro/anthocyanidins[123]
Positive	Prec	307.3	Ceramides [86]
Positive	Prec	310.3	Ceramides 20:0[86]
Positive	Prec	312	Pro/anthocyanidins[123]
Positive	Prec	328.3	Ceramides 20:0(OH) [86]
Positive	Prec	335.2	
Positive	Prec	338.3	Ceramides 22:0[86]
Positive	Prec	340.4	Ceramides 22:0(OH) [86]
Positive	Prec	352.4	Ceramides 23:1[86]
Positive	Prec	354.4	Ceramides 23:0[86]
Positive	Prec	356.4	Ceramides 23:0(OH) [86]
Positive	Prec	366.4	Ceramides 24:1[86]
Positive	Prec	368.4	Ceramides 24:0 or 23:1(OH) [86]
Positive	Prec	369.1	Cholesterol esters[126]
Positive	Prec	370.4	Ceramides 23:0(OH) [86]
Positive	Prec	380.4	Ceramides 25:1[86]
Positive	Prec	382.4	Ceramides 25:0 or 24:1(OH) [86]
Positive	Prec	384.4	Ceramides 24:0[86]

Positive	Prec	423.4	
Positive	Prec	507.5	
Positive	Prec	523	TAG, NH_4 fatty acyl substituent[82]
Positive	Prec	537	TAG, NH_4 fatty acyl substituent[82]
Positive	Prec	549.5	TAG, NH_4 fatty acyl substituent[82]
Positive	Prec	551.5	TAG, NH_4 fatty acyl substituent[82]
Positive	Prec	563.5	TAG, NH_4 fatty acyl substituent[82]
Positive	Prec	565.5	TAG, NH_4 fatty acyl substituent[82]
Positive	Prec	577	TAG, NH_4 fatty acyl substituent[82]
Positive	Prec	579	TAG, NH_4 fatty acyl substituent[82]
Positive	Prec	603	TAG[82]

REFERENCES

1. Wang, H.; Liu, J.; Cooks, R. G.; Ouyang, Z., Paper spray for direct analysis of complex mixtures using mass spectrometry. *Angewandte Chemie International Edition* **2010,** *49* (5), 877-80.
2. Liu, J.; Wang, H.; Manicke, N. E.; Lin, J.; Cooks, R. G.; Ouyang, Z., Development, Characterization, and Application of Paper Spray Ionization. *Analytical chemistry* **2010,** *82* (6), 2463-2471.
3. Espy, R. D.; Manicke, N. E.; Ouyang, Z.; Cooks, R. G., Rapid analysis of whole blood by paper spray mass spectrometry for point-of-care therapeutic drug monitoring. *Analyst* **2012,** *137* (10), 2344-9.
4. Yang, Q.; Wang, H.; Maas, J. D.; Chappell, W. J.; Manicke, N. E.; Cooks, R. G.; Ouyang, Z., Paper spray ionization devices for direct, biomedical analysis using mass spectrometry. *International Journal of Mass Spectrometry* **2012,** *312*, 201-207.
5. Li, A.; Wang, H.; Ouyang, Z.; Cooks, R. G., Paper spray ionization of polar analytes using non-polar solvents. *Chemical communications* **2011,** *47* (10), 2811-3.
6. Espy, R. D.; Muliadi, A. R.; Ouyang, Z.; Cooks, R. G., Spray mechanism in paper spray ionization. *International Journal of Mass Spectrometry* **2012,** *325-327*, 167-171.
7. Manicke, N. E.; Yang, Q.; Wang, H.; Oradu, S.; Ouyang, Z.; Cooks, R. G., Assessment of paper spray ionization for quantitation of pharmaceuticals in blood spots. *International Journal of Mass Spectrometry* **2011,** *300* (2-3), 123-129.
8. Manicke, N. E.; Abu-Rabie, P.; Spooner, N.; Ouyang, Z.; Cooks, R. G., Quantitative analysis of therapeutic drugs in dried blood spot samples by paper spray mass spectrometry: an avenue to therapeutic drug monitoring. *Journal of the American Society for Mass Spectrometry* **2011,** *22* (9), 1501-7.
9. Su, Y.; Wang, H.; Liu, J.; Wei, P.; Cooks, R. G.; Ouyang, Z., Quantitative paper spray mass spectrometry analysis of drugs of abuse. *Analyst* **2013,** *138* (16), 4443-7.
10. Espy, R. D.; Teunissen, S. F.; Manicke, N. E.; Ren, Y.; Ouyang, Z.; van Asten, A.; Cooks, R. G., Paper spray and extraction spray mass spectrometry for the direct and simultaneous quantification of eight drugs of abuse in whole blood. *Analytical chemistry* **2014,** *86* (15), 7712-8.
11. Shi, R. Z.; El Gierari el, T. M.; Manicke, N. E.; Faix, J. D., Rapid measurement of tacrolimus in whole blood by paper spray-tandem mass spectrometry (PS-MS/MS). *Clinica Chimica Acta* **2015,** *441*, 99-104.
12. Guo, T.; Zhang, Z.; Yannell, K. E.; Dong, Y.; Cooks, R. G., Paper spray ionization mass spectrometry for rapid quantification of illegal beverage dyes. *Analytical Methods* **2017,** *9* (44), 6273-6279.
13. Tsai, C. W.; Tipple, C. A.; Yost, R. A., Application of paper spray ionization for explosives analysis. *Rapid Communications in Mass Spectrometry* **2017,** *31* (19), 1565-1572.

14. Liu, J.; Manicke, N. E.; Zhou, X.; Cooks, R. G.; Ouyang, Z., Chapter 16. Paper Spray. **2014**, 389-422.

15. Ren, Y.; Wang, H.; Liu, J.; Zhang, Z.; McLuckey, M. N.; Ouyang, Z., Analysis of Biological Samples Using Paper Spray Mass Spectrometry: An Investigation of Impacts by the Substrates, Solvents and Elution Methods. *Chromatographia* **2013,** *76* (19-20), 1339-1346.

16. Zhang, C.; Manicke, N. E., Development of a Paper Spray Mass Spectrometry Cartridge with Integrated Solid Phase Extraction for Bioanalysis. *Analytical chemistry* **2015,** *87* (12), 6212-9.

17. Duarte, L. C.; Colletes de Carvalho, T.; Lobo-Júnior, E. O.; Abdelnur, P. V.; Vaz, B. G.; Coltro, W. K. T., 3D printing of microfluidic devices for paper-assisted direct spray ionization mass spectrometry. *Analytical Methods* **2016,** *8* (3), 496-503.

18. Zargar, T.; Khayamian, T.; Jafari, M. T., Immobilized aptamer paper spray ionization source for ion mobility spectrometry. *Journal of Pharmaceutical and Biomedical Analysis* **2017,** *132*, 232-237.

19. Sukumar, H.; Stone, J. A.; Nishiyama, T.; Yuan, C.; Eiceman, G. A., Paper spray ionization with ion mobility spectrometry at ambient pressure. *International Journal for Ion Mobility Spectrometry* **2011,** *14* (2-3), 51-59.

20. Tsai, C. W.; Tipple, C. A.; Yost, R. A., Integration of paper spray ionization high-field asymmetric waveform ion mobility spectrometry for forensic applications. *Rapid Communications in Mass Spectrometry* **2018,** *32* (7), 552-560.

21. Chen, S.; Wan, Q.; Badu-Tawiah, A. K., Mass Spectrometry for Paper-Based Immunoassays: Toward On-Demand Diagnosis. *Journal of the American Chemical Society* **2016,** *138* (20), 6356-9.

22. Yannell, K. E.; Kesely, K. R.; Chien, H. D.; Kissinger, C. B.; Cooks, R. G., Comparison of paper spray mass spectrometry analysis of dried blood spots from devices used for in-field collection of clinical samples. *Analytical Bioanalytical Chemistry* **2017,** *409* (1), 121-131.

23. *Analytical Procedures and Method Validation for Drugs and Biologics Guidence for Industry*; Food and Drug Administration: 2015.

24. Long, G. L.; Winefordner, J. D., Limit of Detection A Closer Look at the IUPAC Definition. *Analytical chemistry* **1983,** *55* (7).

25. Jang, S. H.; Yan, Z.; Lazor, J. A., Therapeutic drug monitoring: A patient management tool for precision medicine. *Clinical Pharmacology & Therapeutics* **2016,** *99* (2), 148-50.

26. Cremers, S.; Guha, N.; Shine, B., Therapeutic drug monitoring in the era of precision medicine: opportunities! *British journal of clinical pharmacology* **2016,** *82* (4), 900-2.

27. Momper, J. D.; Wagner, J. A., Therapeutic drug monitoring as a component of personalized medicine: applications in pediatric drug development. *Clinical Pharmacology & Therapeutics* **2014,** *95* (2), 138-40.

28. Oellerich, M.; Kanzow, P.; Walson, P. D., Therapeutic drug monitoring - Key to personalized pharmacotherapy. *Clinical biochemistry* **2017,** *50* (7-8), 375-379.

29. Neef, C.; Touw, D. J.; Stolk, L. M., Therapeutic Drug Monitoring in Clinical Research. *Pharmaceutical Medicine* **2008,** *22* (4), 235-244.

30. Teilmann, A. C.; Kalliokoski, O.; Sorensen, D. B.; Hau, J.; Abelson, K. S., Manual versus automated blood sampling: impact of repeated blood sampling on stress parameters and behavior in male NMRI mice. *Lab Animal* **2014,** *48* (4), 278-91.

31. McGuill, M. W.; Rowan, A. N., Biological Effects of Blood Loss: Implications for Sampling Volumes and Techniques. *ILAR Journal* **1989,** *31* (4), 5-20.

32. Koch, C. G.; Li, L.; Sun, Z.; Hixson, E. D.; Tang, A.; Phillips, S. C.; Blackstone, E. H.; Henderson, J. M., Hospital-acquired anemia: prevalence, outcomes, and healthcare implications. *Journal of hospital medicine* **2013,** *8* (9), 506-12.

33. Acetaminophen. https://labtestsonline.org/understanding/analytes/acetaminophen/tab/test/ (accessed March 25).

34. Rawlins, M. D.; Henderson, D. B.; Hijab, A. R., Pharmacokinetics of paracetamol (acetominophen) after intravenous and oral administration. *European Journal of Clinical Pharmacology* **1977,** *11*, 283-286.

35. Li, L.; Chen, T. C.; Ren, Y.; Hendricks, P. I.; Cooks, R. G.; Ouyang, Z., Mini 12, miniature mass spectrometer for clinical and other applications--introduction and characterization. *Analytical chemistry* **2014,** *86* (6), 2909-16.

36. Zhang, W.; Wang, X.; Xia, Y.; Ouyang, Z., Ambient Ionization and Miniature Mass Spectrometry Systems for Disease Diagnosis and Therapeutic Monitoring. *Theranostics* **2017,** *7* (12), 2968-2981.

37. Wagner, M.; Tonoli, D.; Varesio, E.; Hopfgartner, G., The use of mass spectrometry to analyze dried blood spots. *Mass Spectrometry Reviews* **2016,** *35* (3), 361-438.

38. Li, W.; Tse, F. L., Dried blood spot sampling in combination with LC-MS/MS for quantitative analysis of small molecules. *Biomedical Chromatography* **2010,** *24* (1), 49-65.

39. Wilhelm, A. J.; den Burger, J. C.; Swart, E. L., Therapeutic drug monitoring by dried blood spot: progress to date and future directions. *Clinical Pharmacokinectics* **2014,** *53* (11), 961-73.

40. Demirev, P. A., Dried blood spots: analysis and applications. *Analytical chemistry* **2013,** *85* (2), 779-89.

41. Spooner, N., A Glowing Future for Dried Blood Spot Sampling. *Bioanalysis* **2010,** *2* (8), 1343–1344.

42. Kralj, E.; Trontelj, J.; Pajic, T.; Kristl, A., Simultaneous measurement of imatinib, nilotinib and dasatinib in dried blood spot by ultra high performance liquid chromatography tandem mass spectrometry. *Journal of chromatography. B, Analytical technologies in the biomedical and life sciences* **2012,** *903*, 150-6.

43. De Kesel, P. M.; Capiau, S.; W.E., L., Current strategies for coping with the hematocrit problem in dried blood spot analysis. *Bioanalysis* **2014,** *6* (14), 1871-1874.

44. Cortes, J. E.; Egorin, M. J.; Guilhot, F.; Molimard, M.; Mahon, F. X., Pharmacokinetic/pharmacodynamic correlation and blood-level testing in imatinib therapy for chronic myeloid leukemia. *Leukemia* **2009,** *23* (9), 1537-44.

45. Manicke, N. E.; Bills, B. J.; Zhang, C., Analysis of biofluids by paper spray MS: advances and challenges. *Bioanalysis* **2016**.

46. Gschwind, H. P.; Pfaar, U.; Waldmeier, F.; Zollinger, M.; Sayer, C.; Zbinden, P.; Hayes, M.; Pokorny, R.; Seiberling, M.; Ben-Am, M.; Peng, B.; Gross, G., Metabolism and disposition of imatinib mesylate in healthy volunteers. *Drug Metabolism and Disposition* **2005,** *33* (10), 1503-12.

47. Takyi-Williams, J.; Dong, X.; Gong, H.; Wang, Y.; Jian, W.; Liu, C.-F.; Tang, K., Application of paper spray–MS in PK studies using sunitinib and benzethonium as model compounds. *Bioanalysis* **2015,** *7* (4), 413-423.

48. Abu-Rabie, P.; Denniff, P.; Spooner, N.; Chowdhry, B. Z.; Pullen, F. S., Investigation of different approaches to incorporating internal standard in DBS quantitative bioanalytical workflows and their effect on nullifying hematocrit-based assay bias. *Analytical chemistry* **2015,** *87* (9), 4996-5003.

49. Lin, C.-H.; Liao, W.-C.; Chen, H.-K.; Kuo, T.-Y., Paper Spray-MS for bioanalysis. *Bioanalysis* **2014,** *6* (2), 1-10.

50. Kim, J. H.; Woenker, T.; Adamec, J.; Regnier, F. E., Simple, miniaturized blood plasma extraction method. *Analytical chemistry* **2013,** *85* (23), 11501-8.

51. Pehrsson, A.; Blencowe, T.; Vimpari, K.; Langel, K.; Engblom, C.; and Lillsunde, P., An Evaluation of On-Site Oral Fluid Drug Screening Devices DrugWipe® 5+ and Rapid STAT® Oral Fluid for Confirmation Analysis. *Journal of analytical toxicology* **2011,** *35*, 211-218.

52. Verstraete, A.; Kwong, T. C.; Morland, J.; Vincent, M. J.; de la Torre, R., Oral Fluid Testing: Promises and Pitfalls. 56 ed.; Huestis, M. A., Ed. Clinical Chemistry 2011; pp 805-810.

53. Heltsley, R.; Depriest, A.; Black, D. L.; Crouch, D. J.; Robert, T.; Marshall, L.; Meadors, V. M.; Caplan, Y. H.; Cone, E. J., Oral fluid drug testing of chronic pain patients. II. Comparison of paired oral fluid and urine specimens. *Journal of Analytical Toxicology*, **2012,** *36* (2), 75-80.

54. Heltsley, R.; DePriest, A.; Black, D. L.; Robert, T.; Marshall, L.; Meadors, V. M.; Caplan, Y. H.; and Cone, E. J., Oral Fluid DrugTesting of Chronic Pain Patients. I. Positive Prevalence Rates of Licit and Illicit Drugs. *Journal of analytical toxicology* **2011,** *35*, 529-540.

55. Huestis, M. A.; Verstraete, A.; Kwong, T. C.; Morland, J.; Vincent, M. J.; de la Torre, R., Oral Fluid Testing: Promises and Pitfalls. *Clinical Chemistry* **2011,** *57* (6), 805-810.

56. Pil; Verstraete, A., Current Developments in Drug Testing in Oral Fluid. *Ther Drug Monit* **2008,** *30* (2), 196-202.

57. Drummer, O. H., Drug Testing in Oral Fluid. *The Clinical Biochemist Reviews* **2006,** *27*, 147-159.

58. Jett, R.; Skaggs, C.; Manicke, N. E., Drug screening method development for paper spray coupled to a triple quadrupole mass spectrometer. *Analytical Methods* **2017,** *9* (34), 5037-5043.

59. González-Domínguez, R.; Sayago, A.; Fernández-Recamales, A., Direct infusion mass spectrometry for metabolomic phenotyping of diseases. *Bioanalysis* **2017,** *9* (1), 131-148.

60. Aretz, I.; Meierhofer, D., Advantages and Pitfalls of Mass Spectrometry Based Metabolome Profiling in Systems Biology. *International journal of molecular sciences* **2016,** *17* (5).

61. Wood, P. L., Mass spectrometry strategies for clinical metabolomics and lipidomics in psychiatry, neurology, and neuro-oncology. *Neuropsychopharmacology : official publication of the American College of Neuropsychopharmacology* **2014,** *39* (1), 24-33.

62. Han, X.; Gross, R. W., Shotgun lipidomics: electrospray ionization mass spectrometric analysis and quantitation of cellular lipidomes directly from crude extracts of biological samples. *Mass Spectrometry Reviews* **2005,** *24* (3), 367-412.

63. Sethi, S.; Brietzke, E., Recent advances in lipidomics: Analytical and clinical perspectives. *Prostaglandins & other lipid mediators* **2017,** *128-129*, 8-16.

64. Rath, C. M.; Yang, J. Y.; Alexandrov, T.; Dorrestein, P. C., Data-independent microbial metabolomics with ambient ionization mass spectrometry. *Journal of the American Society for Mass Spectrometry* **2013,** *24* (8), 1167-76.

65. Anand, S.; Young, S.; Esplin, M. S.; Peaden, B.; Tolley, H. D.; Porter, T. F.; Varner, M. W.; D'Alton, M. E.; Jackson, B. J.; Graves, S. W., Detection and confirmation of serum lipid biomarkers for preeclampsia using direct infusion mass spectrometry. *Journal of lipid research* **2016,** *57* (4), 687-96.

66. Garcia-Sevillano, M. A.; Garcia-Barrera, T.; Navarro, F.; Montero-Lobato, Z.; Gomez-Ariza, J. L., Shotgun metabolomic approach based on mass spectrometry for hepatic mitochondria of mice under arsenic exposure. *Biometals : an international journal on the role of metal ions in biology, biochemistry, and medicine* **2015,** *28* (2), 341-51.

67. Prasain, J. K.; Wilson, L.; Hoang, H. D.; Moore, R.; Miller, M. A., Comparative Lipidomics of Caenorhabditis elegans Metabolic Disease Models by SWATH Non-Targeted Tandem Mass Spectrometry. *Metabolites* **2015,** *5* (4), 677-96.

68. Basak, T.; Varshney, S.; Hamid, Z.; Ghosh, S.; Seth, S.; Sengupta, S., Identification of metabolic markers in coronary artery disease using an untargeted LC-MS based metabolomic approach. *Journal of proteomics* **2015,** *127* (Pt A), 169-77.

69. Ferreira, C. R.; Yannell, K. E.; Mollenhauer, B.; Espy, R. D.; Cordeiro, F. B.; Ouyang, Z.; Cooks, R. G., Chemical profiling of cerebrospinal fluid by multiple reaction monitoring mass spectrometry. *Analyst* **2016,** *141* (18), 5252-5255.

70. Vineenti, M.; Schwartz, J. C.; Cooks, R. G.; Wadef, A. P.; Enke, C. G., The Functional Relationship Scan in Tandem Mass Spectrometry. *Organic Mass Spectrometry* **1988,** *23*, 579-584.

71. Gromski, P. S.; Muhamadali, H.; Ellis, D. I.; Xu, Y.; Correa, E.; Turner, M. L.; Goodacre, R., A tutorial review: Metabolomics and partial least squares-discriminant analysis--a marriage of convenience or a shotgun wedding. *Analytica chimica acta* **2015,** *879*, 10-23.

72. Morand, K. L., *High Throughput Flow Injection Analysis- Mass Spectrometry*. Elsevier: 2004.

73. Cordeiro, F. B.; Ferreira, C. R.; Sobreira, T. J. P.; Yannell, K. E.; Jarmusch, A. K.; Cedenho, A. P.; Lo Turco, E. G.; Cooks, R. G., Multiple reaction monitoring (MRM)-profiling for biomarker discovery applied to human polycystic ovarian syndrome. *Rapid Communications in Mass Spectrometry* **2017,** *31* (17), 1462-1470.

74. Dhillon, J.; Ferreira, C. R.; Sobreira, T. J. P.; Mattes, R. D., Multiple Reaction Monitoring Profiling to Assess Compliance with an Almond Consumption Intervention. *Current Developments in Nutrition* **2017,** *1* (9).

75. Benjamin, E. J.; Blaha, M. J.; Chiuve, S. E.; Cushman, M.; Das, S. R.; Deo, R.; de Ferranti, S. D.; Floyd, J.; Fornage, M.; Gillespie, C.; Isasi, C. R.; Jimenez, M. C.; Jordan, L. C.; Judd, S. E.; Lackland, D.; Lichtman, J. H.; Lisabeth, L.; Liu, S.; Longenecker, C. T.; Mackey, R. H.; Matsushita, K.; Mozaffarian, D.; Mussolino, M. E.; Nasir, K.; Neumar, R. W.; Palaniappan, L.; Pandey, D. K.; Thiagarajan, R. R.; Reeves, M. J.; Ritchey, M.; Rodriguez, C. J.; Roth, G. A.; Rosamond, W. D.; Sasson, C.; Towfighi, A.; Tsao, C. W.; Turner, M. B.; Virani, S. S.; Voeks, J. H.; Willey, J. Z.; Wilkins, J. T.; Wu, J. H. Y.; Alger, H. M.; Wong, S. S.; Muntner, P. *Heart Disease and Stroke Statistics 2017 At-a-Glance*; American Heart Association Statistics Committee and Stroke Statistics Subcommittee: 2017.

76. Cardiovascular diseases (CVDs) Fact sheet. http://www.who.int/mediacentre/factsheets/fs317/en/.

77. Coronary artery disease. https://www.mayoclinic.org/diseases-conditions/coronary-artery-disease/diagnosis-treatment/drc-20350619.

78. Beckmann, M.; Parker, D.; Enot, D. P.; Duval, E.; Draper, J., High-throughput, nontargeted metabolite fingerprinting using nominal mass flow injection electrospray mass spectrometry. *Nature Protocols* **2008,** *3* (3), 486-504.

79. Patterson, R. E.; Ducrocq, A. J.; McDougall, D. J.; Garrett, T. J.; Yost, R. A., Comparison of blood plasma sample preparation methods for combined LC-MS lipidomics and metabolomics. *Journal of chromatography. B, Analytical technologies in the biomedical and life sciences* **2015,** *1002*, 260–266.

80. Cajka, T.; Fiehn, O., Increasing lipidomic coverage by selecting optimal mobile-phase modifiers in LC–MS of blood plasma. *Metabolomics : Official journal of the Metabolomic Society* **2016**, 12-34.

81. Murphy, R. C.; Fiedler, J.; Hevko, J., Analysis of Nonvolatile Lipids by Mass Spectrometry. *Chemical Reviews* **2001,** *101*, 479−526.

82. McAnoy, A. M.; Wu, C. C.; Murphy, R. C., Direct qualitative analysis of triacylglycerols by electrospray mass spectrometry using a linear ion trap. *Journal of the American Society for Mass Spectrometry* **2005,** *16* (9), 1498-1509.

83. Li, M.; Butka, E.; Wang, X., Comprehensive quantification of triacylglycerols in soybean seeds by electrospray ionization mass spectrometry with multiple neutral loss scans. *Scientific Reports* **2014,** *4*, 6581.

84. Milne, S.; Ivanova, P.; Forrester, J.; Alex Brown, H., Lipidomics: an analysis of cellular lipids by ESI-MS. *Methods* **2006,** *39* (2), 92-103.

85. Lieser, B.; Liebisch, G.; Drobnik, W.; Schmitz, G., Quantification of sphingosine and sphinganine from crude lipid extracts by HPLC electrospray ionization tandem mass spectrometry. *Journal of lipid research* **2003,** *44* (11), 2209-16.

86. Colsch, B.; Afonso, C.; Popa, I.; Portoukalian, J.; Fournier, F.; Tabet, J. C.; Baumann, N., Characterization of the ceramide moieties of sphingoglycolipids from mouse brain by ESI-MS/MS: identification of ceramides containing sphingadienine. *Journal of lipid research* **2004,** *45* (2), 281-6.

87. Gross, R. W.; Han, X., Lipidomics in Diabetes and the Metabolic Syndrome. In *Lipidomics and Bioactive Lipids: Specialized Analytical Methods and Lipids in Disease*, 2007; pp 73-90.

88. Brugger, B.; Erben, G.; Sandhoff, R.; Wieland, F. T.; Lehmann, W. D., Quantitative analysis of biological membrane lipids at the low picomole level by nano-electrospray ionization tandem mass spectrometry. *Proceedings of the National Academy of Sciences of the United States of America* **1997,** *94*, 2339–2344.

89. Han, X.; Yang, K.; Yang, J.; Cheng, H.; Gross, R. W., Shotgun lipidomics of cardiolipin molecular species in lipid extracts of biological samples. *Journal of lipid research* **2006,** *47* (4), 864-79.

90. Merrill, A. H., Jr.; Sullards, M. C.; Allegood, J. C.; Kelly, S.; Wang, E., Sphingolipidomics: high-throughput, structure-specific, and quantitative analysis of sphingolipids by liquid chromatography tandem mass spectrometry. *Methods* **2005,** *36* (2), 207-24.

91. Banerjee, A.; Chitnis, U. B.; Jadhav, S. L.; Bhawalkar, J. S.; Chaudhury, S., Hypothesis testing, type I and type II errors. *Indian Journal of Psychiatry* **2009,** *18* (2), 127–131.

92. Rothman, K. J., Curbing type I and type II errors. *European Journal of Epidemiology* **2010,** *25* (4), 223–224.

93. Mueller, D. C.; Piller, M.; Niessner, R.; Scherer, M.; Scherer, G., Untargeted metabolomic profiling in saliva of smokers and nonsmokers by a validated GC-TOF-MS method. *Journal of proteome research* **2014,** *13* (3), 1602-13.

94. Sartain, M.; Sana, T., Impact of Chromatography on Lipid Profi ling of Liver Tissue Extracts. Application Note, C. R., Ed. Agilent Technologies: 2015.

95. Wang, Z. Y.; Liu, Y. Y.; Liu, G. H.; Lu, H. B.; Mao, C. Y., l-Carnitine and heart disease. *Life Science* **2018,** *194*, 88-97.

96. Shah, S. H.; Kraus, W. E.; Newgard, C. B., Metabolomic profiling for the identification of novel biomarkers and mechanisms related to common cardiovascular diseases: form and function. *Circulation* **2012,** *126* (9), 1110-20.

97. Meijers, B. J. I.; Claes, K.; Bammens, B.; de Loor, H.; Viaene, L.; Verbeke, K.; Kuypers, D.; Vanrenterghem, Y.; Evenepoelcorresponding, P., p-Cresol and Cardiovascular Risk in Mild-to-Moderate Kidney Disease. *Clinical Journal of the American Society of Nephrology* **2010,** *5* (7), 1182–1189.

98. Austin, M. A., Plasma triglyceride and coronary heart disease. *Arteriosclerosis, Thrombosis, and Vascular Biology* **1991,** *11*, 2-14.

99. Byeon, S. K.; Lee, J. Y.; Lim, S.; Choi, D.; Moon, M. H., Discovery of candidate phospholipid biomarkers in human lipoproteins with coronary artery disease by flow field-flow fractionation and nanoflow liquid chromatography-tandem mass spectrometry. *Journal of Chromatography A* **2012,** *1270*, 246-253.

100. Cui, S.; Li, K.; Ang, L.; Liu, J.; Cui, L.; Song, X.; Lv, S.; Mahmud, E., Plasma Phospholipids and Sphingolipids Identify Stent Restenosis After Percutaneous Coronary Intervention. *JACC Cardiovasc Interv* **2017,** *10* (13), 1307-1316.

101. Sutter, I.; Klingenberg, R.; Othman, A.; Rohrer, L.; Landmesser, U.; Heg, D.; Rodondi, N.; Mach, F.; Windecker, S.; Matter, C. M.; Luscher, T. F.; von Eckardstein, A.; Hornemann, T., Decreased phosphatidylcholine plasmalogens--A putative novel lipid signature in patients with stable coronary artery disease and acute myocardial infarction. *Atherosclerosis* **2016,** *246*, 130-40.

102. Ganna, A.; Salihovic, S.; Sundstrom, J.; Broeckling, C. D.; Hedman, A. K.; Magnusson, P. K.; Pedersen, N. L.; Larsson, A.; Siegbahn, A.; Zilmer, M.; Prenni, J.; Arnlov, J.; Lind, L.; Fall, T.; Ingelsson, E., Large-scale metabolomic profiling identifies novel biomarkers for incident coronary heart disease. *PLOS Genetics* **2014,** *10* (12), e1004801.

103. Wang, Z.; Levison, B. S.; Hazen, J. E.; Donahue, L.; Li, X. M.; Hazen, S. L., Measurement of trimethylamine-N-oxide by stable isotope dilution liquid chromatography tandem mass spectrometry. *Analytical Biochemistry* **2014,** *455*, 35-40.

104. Guasch-Ferre, M.; Hu, F. B.; Ruiz-Canela, M.; Bullo, M.; Toledo, E.; Wang, D. D.; Corella, D.; Gomez-Gracia, E.; Fiol, M.; Estruch, R.; Lapetra, J.; Fito, M.; Aros, F.; Serra-Majem, L.; Ros, E.; Dennis, C.; Liang, L.; Clish, C. B.; Martinez-Gonzalez, M. A.; Salas-Salvado, J., Plasma Metabolites From Choline Pathway and Risk of Cardiovascular Disease in the PREDIMED (Prevention With Mediterranean Diet) Study. *Journal of the American Heart Association* **2017,** *6* (11).

105. Würtz, M., Aspirin in coronary artery disease: an appraisal of functions and limitations. *Danish Medical Journal* **2015,** *2015* (62), 4.

106. Lleo, A.; Cavedo, E.; Parnetti, L.; Vanderstichele, H.; Herukka, S. K.; Andreasen, N.; Ghidoni, R.; Lewczuk, P.; Jeromin, A.; Winblad, B.; Tsolaki, M.; Mroczko, B.; Visser, P. J.; Santana, I.; Svenningsson, P.; Blennow, K.; Aarsland, D.; Molinuevo, J. L.; Zetterberg, H.; Mollenhauer, B., Cerebrospinal fluid biomarkers in trials for Alzheimer and Parkinson diseases. *Nature Reviews Neurology* **2015,** *11* (1), 41-55.

107. Miller, D. B.; O'Callaghan, J. P., Biomarkers of Parkinson's disease: present and future. *Metabolism: clinical and experimental* **2015,** *64* (3 Suppl 1), S40-6.

108. Andersen, A. D.; Binzer, M.; Stenager, E.; Gramsbergen, J. B., Cerebrospinal fluid biomarkers for Parkinson's disease - a systematic review. *Acta neurologica Scandinavica* **2017,** *135* (1), 34-56.

109. Sharma, S.; Moon, C. S.; Khogali, A.; Haidous, A.; Chabenne, A.; Ojo, C.; Jelebinkov, M.; Kurdi, Y.; Ebadi, M., Biomarkers in Parkinson's disease (recent update). *Neurochemistry international* **2013,** *63* (3), 201-29.

110. Delenclos, M.; Jones, D. R.; McLean, P. J.; Uitti, R. J., Biomarkers in Parkinson's disease: Advances and strategies. *Parkinsonism and Related Disorders* **2016,** *22 Suppl 1*, S106-10.

111. Hirsch, L.; Jette, N.; Frolkis, A.; Steeves, T.; Pringsheim, T., The Incidence of Parkinson's Disease: A Systematic Review and Meta-Analysis. *Neuroepidemiology* **2016,** *46* (4), 292-300.

112. Jankovic, J., Parkinson's disease: clinical features and diagnosis. *Journal of Neurology, Neurosurgery, and Psychiatry* **2008,** *79*, 368–376.

113. Gill, E. L.; Koelmel, J. P.; Yost, R. A.; Okun, M. S.; Vedam-Mai, V.; Garrett, T. J., Mass Spectrometric Methodologies for Investigating the Metabolic Signatures of Parkinson's Disease: Current Progress and Future Perspectives. *Analytical chemistry* **2018,** *90* (5), 2979-2986.

114. Kang, U. J.; Goldman, J. G.; Alcalay, R. N.; Xie, T.; Tuite, P.; Henchcliffe, C.; Hogarth, P.; Amara, A. W.; Frank, S.; Rudolph, A.; Casaceli, C.; Andrews, H.; Gwinn, K.; Sutherland, M.; Kopil, C.; Vincent, L.; Frasier, M., The BioFIND study: Characteristics of a clinically typical Parkinson's disease biomarker cohort. *Movement Disorders* **2016,** *31* (6), 924-32.

115. Parnetti, L.; Castrioto, A.; Chiasserini, D.; Persichetti, E.; Tambasco, N.; El-Agnaf, O.; Calabresi, P., Cerebrospinal fluid biomarkers in Parkinson disease. *Nature Reviews Neurology* **2013,** *9* (3), 131-40.

116. Kang, J. H.; Mollenhauer, B.; Coffey, C. S.; Toledo, J. B.; Weintraub, D.; Galasko, D. R.; Irwin, D. J.; Van Deerlin, V.; Chen-Plotkin, A. S.; Caspell-Garcia, C.; Waligorska, T.; Taylor, P.; Shah, N.; Pan, S.; Zero, P.; Frasier, M.; Marek, K.; Kieburtz, K.; Jennings, D.; Tanner, C. M.; Simuni, T.; Singleton, A.; Toga, A. W.; Chowdhury, S.; Trojanowski, J. Q.; Shaw, L. M.; Parkinson's Progression Marker, I., CSF biomarkers associated with disease heterogeneity in early Parkinson's disease: the Parkinson's Progression Markers Initiative study. *Acta neuropathologica* **2016,** *131* (6), 935-49.

117. Johar, I.; Mollenhauer, B.; Aarsland, D., Cerebrospinal Fluid Biomarkers of Cognitive Decline in Parkinson's Disease. *International review of neurobiology* **2017,** *132*, 275-294.

118. Li, S.; Le, W., Biomarker Discovery in Parkinson's Disease: Present Challenges and Future Opportunities. *Neuroscience Bulletin* **2017,** *33* (5), 481-482.

119. Goldman, J. G.; Andrews, H.; Amara, A.; Naito, A.; Alcalay, R. N.; Shaw, L. M.; Taylor, P.; Xie, T.; Tuite, P.; Henchcliffe, C.; Hogarth, P.; Frank, S.; Saint-Hilaire, M. H.; Frasier, M.; Arnedo, V.; Reimer, A. N.; Sutherland, M.; Swanson-Fischer, C.; Gwinn, K.; Fox Investigation of New Biomarker, D.; Kang, U. J., Cerebrospinal fluid, plasma, and saliva in the BioFIND study: Relationships among biomarkers and Parkinson's disease Features. *Movement Disorders* **2018,** *33* (2), 282-288.

120. Moore, C.; Crouch, D., Oral fluid for the detection of drugs of abuse using immunoassay and LC–MS/MS. *Bioanalysis* **2013,** *5* (12), 1555-1569.

121. Kaddurah-Daouk, R.; Krishnan, K. R., Metabolomics: a global biochemical approach to the study of central nervous system diseases. *Neuropsychopharmacology : official publication of the American College of Neuropsychopharmacology* **2009,** *34* (1), 173-86.

122. Ma, Y.; Kind, T.; Yang, D.; Leon, C.; Fiehn, O., MS2Analyzer: A software for small molecule substructure annotations from accurate tandem mass spectra. *Analytical chemistry* **2014,** *86* (21), 10724-31.

123. Delgado de la Torre, M. P.; Ferreiro-Vera, C.; Priego-Capote, F.; Luque de Castro, M. D., Anthocyanidins, proanthocyanidins, and anthocyanins profiling in wine lees by solid-phase extraction-liquid chromatography coupled to electrospray ionization tandem mass spectrometry with data-dependent methods. *Journal of Agricultural and Food Chemistry* **2013,** *61* (51), 12539-48.

124. Taguchi, R.; Houjou, T.; Nakanishi, H.; Yamazaki, T.; Ishida, M.; Imagawa, M.; Shimizu, T., Focused lipidomics by tandem mass spectrometry. *Journal of chromatography. B, Analytical technologies in the biomedical and life sciences* **2005,** *823* (1), 26-36.

125. Isaac, G.; Jeannotte, R.; Esch, S. W.; Welti, R., New mass-spectrometry-based strategies for lipids. *Genetic Engineering* **2007,** *28*, 129-157.

126. Liebisch, G.; Binder, M.; Schifferer, R.; Langmann, T.; Schulz, B.; Schmitz, G., High throughput quantification of cholesterol and cholesteryl ester by electrospray ionization tandem mass spectrometry (ESI-MS/MS). *Biochimica et Biophysica Acta* **2006,** *1761* (1), 121-8.

VITA

Karen Emily Yannell was born in La Grange, Illinois to Barry and Marcia Cesafsky. Her love of science began in elementary school at St. Isaac Jogues. There her favorite class was science lab and her instructor, Mrs. Latto, encouraged her to participate in science competitions. For high school, she attended St. Ignatius College Prep in Chicago, IL where she continued to enter science competitions and she was also goalie for her lacrosse team. After high school, Karen moved to California where she attended the University of San Diego. There, she began her research career under the advisement of Professor Lauren Benz. Her researched focused on developing magnetic levitation methods to teach reaction kinetics to undergraduate students.

After receiving her Bachelor of Arts in Biochemistry, Karen began working as an LC-MS Technician at Millennium Laboratories. After learning how to operate and maintain mass spectrometers, she moved to a Research Associate position in the Research and Development department. There, she learned practical laboratory skills and how to develop mass spectrometry biofluid assays. It was in this laboratory that she realized her love of the sensitivity and specificity of a mass spectrometer and the precision and accuracy of a well-developed method.

In 2013, she decided to continue her education in analytical chemistry at Purdue University. In Aston Labs, Professor R. Graham Cooks taught her that chromatography is not necessary for all measurements and ambient ionization techniques, like paper spray ionization, offers many benefits to biofluid analysis (see above dissertation). Karen's favorite part of her graduate career was showcasing ambient ionization techniques and her methods to visiting scientists, scholars, and professionals. After her defense, she aims to use her method development talents at a major instrument company.

Karen is much more than a chemist. She is a proud mom to Dorothy and Klaus, partner to Michael, endearing sister to Katie, Bobby, Laura, Kevin, Kim, Sarah, Liz, Ian, Crystel, and Sean, and supportive aunt to Olivia, Ellie, Coral, Jack, Abby, Oliver, and Zoe. In her free time, you will find Karen experimenting with new recipes in her kitchen or tackling a challenging Sudoku. She is a longtime Chicago Cubs fan, curtesy of her Dad and Grandpa.

PUBLICATIONS

1) Guo, T., Zhang, Z., Yannell, K., Dong, Y., & Cooks, R. (2017). Paper spray ionization mass spectrometry for rapid quantification of illegal beverage dyes. *Analytical Methods, 9*(44), 6273-6279.
2) Yannell, K., Smith, K., Alfaro, C., Jarmusch, A., Pirro, V., & Cooks, R. (2017). N-Acetylaspartate and 2-Hydroxyglutarate Assessed in Human Brain Tissue by Mass Spectrometry as Neuronal Markers of Oncogenesis. *Clinical Chemistry*, *63*(11), 1766-1767.
3) Cordeiro, F., Ferreira, C., Sobreira, T., Yannell, K., Jarmusch, A., Cedenho, A., Cooks, R. (2017). Multiple reaction monitoring (MRM)-profiling for biomarker discovery applied to human polycystic ovarian syndrome. *Rapid Communications in Mass Spectrometry, 31*(17), 1462-1470.
4) Yannell, K., Kesely, E., Chien, K., Kissinger, R., & Cooks, H. (2017). Comparison of paper spray mass spectrometry analysis of dried blood spots from devices used for in-field collection of clinical samples. *Analytical and Bioanalytical Chemistry, 409*(1), 121-131.
5) Ferreira, C., Yannell, K., Mollenhauer, B., Espy, R., Cordeiro, F., Ouyang, Z., & Cooks, R. (2016). Chemical profiling of cerebrospinal fluid by multiple reaction monitoring mass spectrometry. *The Analyst, 141*(18), 5252-5255.
6) Ferreira, C., Yannell, K., Jarmusch, A., Pirro, V., Ouyang, Z., & Cooks, R. (2016). Ambient Ionization Mass Spectrometry for Point-of-Care Diagnostics and Other Clinical Measurements. *Clinical Chemistry, 62*(1), 99-110.

Anal Bioanal Chem (2017) 409:121–131
DOI 10.1007/s00216-016-9954-5

RESEARCH PAPER

Comparison of paper spray mass spectrometry analysis of dried blood spots from devices used for in-field collection of clinical samples

Karen E. Yannell[1] · Kristina R. Kesely[1] · Huynh Dinh Chien[2] · Candice B. Kissinger[1] · R. Graham Cooks[1]

Received: 16 June 2016 / Revised: 8 September 2016 / Accepted: 16 September 2016 / Published online: 7 November 2016

Abstract Paper spray (PS) is an ambient ionization technique applicable to ionizing analytes from untreated dried biofluid samples. In-field sample analysis could benefit from the capability to use a finger prick of blood to measure drugs in whole blood at low cost and in a short time. Some studies may require specialized blood collection devices that can be used in remote areas. In this study, four different dried blood spot (DBS) devices are used with PS sources and tested for rapid quantification of imatinib and *N*-desmethyl-imatinib. A triple quadrupole mass spectrometer allows analyte detection with high sensitivity. Analytical figures of merit for the four devices are compared, and it is concluded that several of the novel devices successfully deploy DBS with PS and yield similar results to traditional manual PS methods. Clinical samples collected in a remote location were analyzed as a proof of concept for in-field blood collection and subsequent rapid laboratory analysis.

Keywords Paper spray ionization · Multiple reaction monitoring · Therapeutic drug monitoring · Field sample collection · Imatinib

Electronic supplementary material The online version of this article (doi:10.1007/s00216-016-9954-5) contains supplementary material, which is available to authorized users.

✉ R. Graham Cooks
cooks@purdue.edu

[1] Department of Chemistry, Purdue University, West Lafayette, IN 47907, USA

[2] Huế University of Medicine and Pharmacy, Huế, Vietnam

Introduction

Dried blood spot (DBS; for abbreviations see, Electronic supplementary material (ESM) Table S1) analysis by mass spectrometry (MS) is a widely used technique that involves analyte extraction from the blood matrix followed by chromatographic separation and transfer into a mass spectrometer [1–4]. DBS cards are a common way to collect and analyze drugs and exogenous analytes in whole blood while using only microliters of the biofluid [1, 2]. The cards are applicable to point-of-care studies and are easily stored, handled, and shipped [1–3]. Because of their increased popularity, more commercially available DBS devices are being developed which promise better results, improved sample collection, and simpler overall protocols [3].

For clinical trials involving in-field sampling, DBS are appealing because they only require a small sample of blood obtained from a finger prick rather than an intravenous blood draw [3, 5]. This allows multiple replicates to be taken painlessly. Furthermore, storing samples as DBSs facilitates in-field blood collection because the sample is stable, easy to ship, and conventional field requirements such as refrigeration of a liquid sample are unnecessary [3, 5, 6]. However, many DBS methodologies place an unknown amount of blood or blood with varying hematocrit on the DBS, and when the blood spot is removed in the laboratory, some sample is often left on the card. This can cause highly variable results. For quantitative results, an accurate volume of sample should be added to the card using a disposable micropipette or by using a collection device that controls the sample volume and the entire spot should be analyzed [1, 2, 7]. Extracting the entire DBS or a consistent fraction from the card (or related device) is necessary for accurate and precise results [1–3].

Although DBS analysis by MS measures analytes of interest in small samples of blood, traditional DBS-MS methodologies require a significant amount of time and material (e.g., solvent)

for the offline extraction and separation (by liquid chromatography) [1, 2, 4]. This backend sample workup makes DBS-MS relatively time consuming, material consuming, expensive, and thus unsuitable for the analysis of a large number of clinical samples. Paper spray (PS) ionization provides a means of DBS analysis directly from the dried blood spot, with no additional sample preparation, no offline analyte extraction, and no chromatography [8–10]. Liu et al., Ferreira et al., and Manicke et al. discuss PS extensively and emphasize its applicability to the analysis of dried blood spots and to clinical samples [11–13]. Briefly, the PS ambient ionization technique requires a small volume (<10 μL) of blood or other biofluid to be dried on a pointed (typically triangular) cellulose paper substrate. The paper triangle is positioned in front of the MS inlet where a spray solvent (~50 μL) and a high voltage are applied (Fig. 1). The solvent is used to extract the analytes of interest from the blood spot and move them to the tip of the paper. The high voltage is used to create an electrospray from the tip of the paper to entrain and ionize the analytes in the sprayed droplets [8]. This ionization method omits time-consuming chromatographic separations and relies solely on MS for sensitive and selective detection of each analyte. Still, a limitation of PS can be its selectivity; if an isobaric compound is present in the sample and only two stages of mass spectrometry are used (i.e., tandem mass spectrometry), then there may be an interference in the analyte signal. To avoid this, unique fragments should be selected as quantifying transitions in the multiple reaction monitoring (MRM) measurement [14, 15]. Alternatively, ion mobility spectroscopy may be coupled with PS, and this is useful in separating opiate isomers in a complex matrix [16, 17].

PS is a rapid analysis technique that can yield both quantitative and qualitative information from a complex sample [9, 10, 18–23]. In particular, a well-studied application for PS is pharmacokinetic and therapeutic drug monitoring of whole blood [18, 19, 23]. To maintain an appropriate blood concentration and avoid unwanted side effects, therapeutic drug monitoring is necessary for many regularly administered drugs. In the case of the tyrosine kinase inhibitor imatinib (Gleevec®, Novartis), toxicity occurs at relatively low levels so it is particularly important to maintain in vivo concentrations in the narrow therapeutic window [24]. Furthermore, the concentration of the drug and metabolite vary greatly with the individual patient [24]. PS is an excellent method to measure these drugs in a patient using only a finger prick of blood.

Although multiple published studies show the range of PS-MS applications using filter paper, chromatographic paper, or another porous medium, the technology would benefit from an understanding of its performance when using commercially available DBS cards (or other devices) to collect the blood spots and analyzing them with PS-MS [8, 10, 19]. One major requirement for PS is that the blood sample be applied directly to the triangle used as the spray emitter (Fig. 1). However, this limits use of commercially available DBS device to those designed for PS or to those which can be cut to a point. These limited options may not meet the specifications for studies that might require a device with special features such as blood filtration or precise volume measurement of the spotted sample. This restriction can be overcome by either extracting the analyte from the dried blood spot offline, which is time consuming and expensive, or by integrating the DBS device with PS-MS [10]. With this latter approach, the DBS device may be superimposed on a paper triangle to perform PS or the DBS device may be cut to a point and used as the PS source itself. In this way, PS analysis becomes applicable to a wide range of DBS devices including recently marketed collection devices.

In this study, imatinib (Imb) and its major active metabolite, *N*-desmethyl-imatinib (*N*-DM-Imb), were measured in whole human blood by PS tandem mass spectrometry (PS-MS/MS) using multiple DBS devices integrated into the PS platform [25]. Note that only DBSs were analyzed in this study, because agreement between the quantitative results of PS analysis of DBS and whole blood sample analysis by LC-MS/MS has been demonstrated previously [23]. Several commercially available DBS devices, namely Whatman FTA cards, TomTec PDMS-4 cards, Novilytic Noviplex blood filtration cards, and Prosolia Velox Sample Cartridges were tested using unique direct extraction and ionization methods by PS-MS/MS. The data obtained were compared with traditional PS measurements using Whatman 31ET chromatography paper triangles. FTA cards are a commonly used DBS

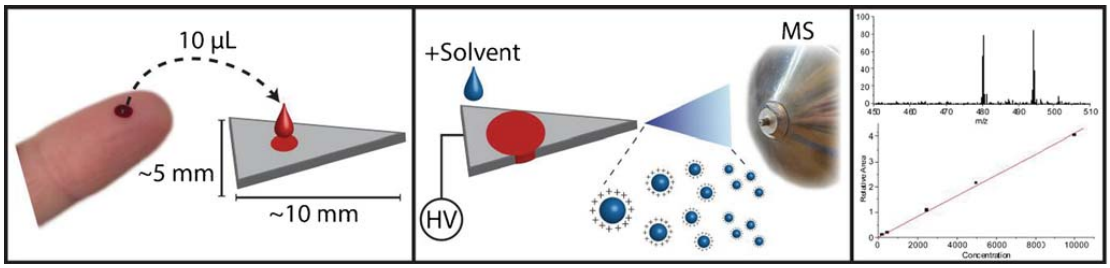

Fig. 1 Paper spray ionization uses a small volume of blood that is pipetted onto a paper triangle (Panel 1). The triangle is placed in front of the MS inlet where a high voltage (3.5 – 5 kV) and solvent are applied to create an electrospray at the tip (Panel 2). Depiction of full scan analysis and targeted quantitative analysis based on MRM are both possible with PS (Panel 3)

collection device that hold up to four DBSs. Among the various FTA cards, the DMPK-C card carries minimal amounts of chemicals from the production process (as seen in the mass spectrum) and is therefore the best choice for PS analysis as interferences and additives causing ion suppression should be avoided [3]. The TomTec card contains nine laser cut circular disks held in place by small bridges of paper that break easily allowing a disk containing the entire blood sample to be removed. The Noviplex device filters a whole blood sample (~25 μL) dispensing just 2.5 μL plasma onto the collection disk. This technology removes the centrifugation step previously required to obtain a dried plasma spot. To be clear, this device only measures the plasma fraction of material in whole blood.

Any of these devices may be used for in-field sample collection, but the DBSs are typically punched out and the analyte is extracted before MS analysis [6]. In this study, the above devices were used with PS for rapid data collection. Although these were not fully validated assays, specific analytical figures of merit were compared between the DBS devices and the success of PS implementation will be discussed. In addition to these comparative measurements of lab samples, capabilities for in-field collection and PS analysis were tested using Whatman 31ET paper to collect field samples from patients dosed with imatinib. These samples were collected in a remote, low resource clinic, shipped back to the lab and measured using the Whatman 31ET methods described below. These preliminary clinical results represent a proof-of-concept test of in-field DBS collection and analysis by PS-MS/MS.

Materials and methods

Chemicals and materials

LC-MS-grade solvents and formic acid (99 %) were purchased from Sigma Aldrich (St. Louis, MO). Imatinib, *N*-desmethyl-imatinib, and their D_8 isotopically labeled internal standards were purchased from AlsaChim (Illkirch-Graffenstaden, France). Whole human blood with K2EDTA was purchased from BioreclamationIVT. SafeTec Microsafe® disposable micropipettes were purchased from SafeTec LLC (Ivyland, PA). Signature™ Ergonomic High Performance Single-Channel Variable Volume Pipettors were purchased from VWR (Radnor, PA).

Instrumentation and DBS devices

A TSQ Quantum Access Max (Thermo Fisher Scientific, Waltham, MA) was used for all MS experiments. Toothless copper clips were purchased from Muller Electric (Akron, OH). Whatman 31ET chromatography paper and Whatman FTA DMPK-C DBS cards were purchased from GE Healthcare Life Sciences (Chicago, IL). Noviplex cards were obtained from Novilytic (West Lafayette, IN), and PDMS-4 cards were obtained from TomTec Life Sciences (Hamden, CT). Velox 360 paper spray ionization source (Prosolia Inc, Indianapolis, IN) and Velox sample cartridges (VSC) were used for the automated PS analysis.

Methodology

Solution preparation

Calibrators (Cal) and quality control (QC) solutions were prepared from separate stock solutions. For each Cal or QC, a 20× concentrated solution of Imb and *N*-DM-Imb was prepared in methanol/water (1:1), then diluted 20× into blank whole human blood and mixed well. If internal standard (IS) was to be incorporated into the liquid sample, it was spiked into the solution at this point. Otherwise, an internal standard stock solution, made in methanol, was spiked directly onto the paper (2 μL). When IS was mixed into the sample, the final concentration was 1500 ng/mL for Imb-D_8 and 500 ng/mL for *N*-DM-Imb-D_8. When the IS was spiked onto the paper, the IS concentration in methanol was 7500 ng/mL for Imb-D_8 and 2500 ng/mL for *N*-DM-Imb-D_8. Calibrator concentrations for Imb were 250, 500, 2500, and 5000 ng/mL with QCs at concentrations of 350 and 2000 ng/mL. The concentrations for *N*-DM-Imb calibrators were 75, 150, 750, and 1500 ng/mL, and the QCs had concentrations of 105 and 600 ng/mL. The calibrator concentrations are a reflection of the therapeutic range and not of the limits of detection, and calibrator one serves as the cutoff value for calculating concentration in unknown samples [3]. The Novilytic calibrators and QCs were higher for *N*-DM-Imb; they were prepared at 300, 600, 3000, and 6000 ng/mL, and the QCs were 420 and 2400 ng/mL in whole blood. Furthermore, for one data set, an additional calibrator (10,000 ng/mL for Imb and 3000 ng/mL for *N*-DM-Imb) and an additional QC (8500 ng/mL for Imb and 2550 ng/mL for *N*-DM-Imb) were added.

Internal standard addition

Three different methods of introducing IS were tested with the drug Imb using Whatman 31ET (W31) paper. First, IS was mixed into the blood sample prior to spotting. Second, IS was prespotted onto the paper and dried before the blood spot was added. When IS was prespotted, a small pencil mark was made onto the W31 paper to indicate the center position. Typically, 2 μL of IS was spotted followed by a 10-μL spot of whole blood sample. With this method, the diameter of the IS spot was approximately half the size of the diameter of the blood spot, ensuring all the IS would be covered by the sample and captured in the analysis. The third method involved spotting 2 μL IS in the center of the DBS after the blood spot was

dried thoroughly onto the paper. Each condition was analyzed in triplicate.

Paper spray ionization

W31 paper is commonly used for paper spray analysis of DBS. In this study, the samples were spotted onto W31 with IS premixed into the sample and with IS prespotted onto the paper. In the first scenario, 10 μL of a blood sample containing IS was spotted onto the W31 paper and allowed to dry. In both cases, the spots dried for 2 h and then the sample was cut from the stock paper manually and attached to a copper clip (ESM Fig. S1a). It is important for efficient analyte extraction that the blood spot be cut out in such a way that the sides of the DBS touch the edges of the PS triangle (ESM Fig. S1a). When IS was prespotted, 2 μL of IS in methanol was first dried onto the paper. As mentioned, a pencil mark is best to note the center of the spot. Next, 10 μL of the blood sample was spotted and allowed to dry for 2 h before being cut out. A voltage of 3500 V was applied via a toothless copper clip, and 45 μL of a spray solvent (95 % methanol, 5 % water, and 0.1 % formic acid) was pipetted to the back of the paper (Fig. 1). This voltage and solvent were used throughout the study unless otherwise noted. An additional experiment tested an in-field blood measurement device. SafeTec Microsafe® disposable micropipettes (10 μL) and a single-channel pipette were used to spike the QC solutions for validation of the micropipette data.

Whatman FTA DMPK-C cards were used in a similar manner to the W31 paper. Internal standard was prespotted on the card followed by a 10-μL blood spot addition. After drying, the spots were manually cut out, attached to a copper clip, and voltage and solvent were applied (ESM Fig. S1c).

The TomTec cards were also prespotted with IS followed by a 10-μL blood spot addition. Once dry, the TomTec disk was punched out and secured to the top of a precut W31 triangle with a copper clip (ESM Fig. S1b). The sample disk was primed with 30 μL of methanol by applying the solvent to the top of the disk and allowing it to flow through the disk onto the W31 paper below. Next, 30 μL of spray solvent was added to the top of the disk and a high voltage was applied. Again, it is important that the top of the disk is in direct contact with the W31 paper surface for efficient extraction of all analyte.

The Noviplex card is a plasma collection device manufactured with multiple layers of filters which are secured on top of a sample disk. The collection disk is covered by the filtration system and therefore does not allow for an application of IS to the collection disk prior to adding the whole blood. Consequently, IS was added to the plasma collection disk after the filtration occurred and when the plasma was dry. The plasma disk spotted with IS was then placed on top of a W31 triangle, primed with 20 μL methanol and sprayed with 20 μL of the spray solvent (ESM Fig. S1d).

A major advantage of the Velox 360 is that it is an automated PS source that may run up to 40 samples in a batch whereas previous techniques required the samples to be analyzed manually, one sample at a time. For the automated analysis, Velox sample cartridges (VSC) were prespotted with IS. Next, 10 μL of the blood sample was spotted on the center of the VSC covering the IS spot (ESM Fig. S1e). It is important to note that the blood must spread horizontally to touch both edges of the VSC. The spots were allowed to dry for 2 h. Cals and QCs were loaded onto the Velox 360 stacker and ran in sequence. Each sample received 9 μL methanol (pump A) as the sample solvent and 120 μL of the 95 % methanol, 5 % water, and 0.1 % formic acid as the cartridge solvent (pump B) and 5000 V.

For all devices, 10 μL of a blank blood sample was applied to the paper to test the background of the card in full scan mode from *m/z* 100–800.

Mass spectrometry

Thermo Fisher Xcalibur software was used for data acquisition and analysis. Multiple reaction monitoring (MRM) in positive ion mode using a TSQ triple quadrupole mass spectrometer was performed for all quantitative analysis. All instrument and method parameters are listed in ESM Table S2. The MRM transitions for Imb were *m/z* 494.3 → 394.1 and *m/z* 494.3 → 217.0 with a tube lens (TL) value of 106 V and nominal collision energies (CE) of 24 and 23, respectively. To quantify Imb, Imb-D_8 was also followed using the MRM transition of *m/z* 502.3 → 394.1 with a CE of 25 and a TL of 129 V. The metabolite, *N*-DM-Imb, was observed with the transitions *m/z* 480.2 → 394.1 and *m/z* 480.2 → 203.1 using CE of 23 and 24, respectively, and a TL of 98 V. Finally, *N*-DM-Imb-D_8 was monitored by *m/z* 488.3 → 394.1 with a CE of 24 and a TL of 100 V. The first fragment is the quantifier while the second fragment is the qualifier. Full scan analysis was performed in positive mode on the TSQ using 0.5 s scan time from *m/z* 100–800.

Data analysis

The relative area for each sample was calculated by dividing the total ion chronogram (TIC) area for the transition used for quantification by the TIC area for the corresponding IS. Limits of detection (LOD) were determined from serial dilutions of the lowest calibrator; where signal to blank (noise) equaled to three. All calibration curves were generated by plotting the concentration of the sample against the relative area using OriginPro software. The calibration curves were not weighted, and the origin was ignored unless noted otherwise.

Matrix effect

Each of the DBS device was spotted with the internal standard solution. On top of the IS spot, blank whole blood or DI water was spotted (10 μL) in triplicate and analyzed with the above methods. The average absolute intensities of the internal standards were compared between the blood and water matrices.

In-field sample collection

A 3 by 4 in. piece of W31 paper was prespotted with four separate internal standard spots. The paper was set between cardboard to maintain the shape and sealed in an aluminum-coated bag containing desiccant and a humidity card. The W31 paper was shipped to field clinics in the Hướng Hóa district of the Quảng Trị province in Vietnam. For five consecutive days, three patients were dosed with 400 mg Imb and one patient with 600 mg. From each patient, a blood sample was taken 5 days in a row, 2 h after the dose was administered. Each sample was taken by cleaning the patient's finger, pricking it with a lancet, discarding the first blood drop, and collecting the second drop with a 10-μL SafeTec Microsafe® disposable micropipette. Each pipette measured precisely 10 μL of blood from the patient then the blood as dispensed onto the W31 paper on top of the internal standard spot. After drying the samples for 2 h, they were sealed with desiccant, stored at room temperature, and shipped back to Purdue University for analysis. The samples were collected over a 1-month period and stored as described above for 3 months before analysis. Calibration curves and QC samples were analyzed using the methods described above followed by the samples collected in field.

Patients provided written, informed consent before entering the study. The study was conducted in accordance with Good Clinical Practice guidelines and the Declaration of Helsinki and was approved by the Vietnamese Ministry of Health and Purdue University (IRB approval: 1507016329; Clinicaltrials.gov identifier: NCT02614404).

Results and discussion

The quality of paper spray mass spectrometry data depends on the method used to introduce the internal standard into the sample [10]. This study, necessitating in-field blood handling, required that the IS be spotted before or after the sample was spotted. The reproducibility and precision of the method was assessed as the relative standard deviation (RSD). The best reproducibly for Imb was achieved when the IS and blood were mixed prior to spotting the sample on paper; the RSD for a QC sample analyzed in triplicate was less than 2 % with this methodology. However, as an acceptable alternative for in-field sample collection, prespotting the IS solution followed by the blood sample yielded a RSD of less than 6 %. The prespotting method was better than spotting the IS to an already dried blood spot, which gave a RSD of greater than 20 %. Additional methods as described by Abu-Rabie et al. may help overcome the poor reproducibility shown when IS was added to a dried blood spot, and they should be investigated in the future [26].

Table 1 summarizes all figures of merit for the DBS devices. Results for all the devices were compared with those for traditional manual PS methodology in which blood and IS were mixed then spotted and dried onto W31 paper. The W31 samples were manually cut out and sprayed. When the IS and blood were premixed, the method yielded a LOD of 5 ng/mL for Imb and 6 ng/mL for *N*-DM-Imb. Linearity was assessed by the R^2 value of the fitted line. Both analytes had linear curves for Imb and *N*-DM-Imb (Fig. 2a; ESM Fig. S2a) with high precision, since the RSDs for the calibrators were less than 3 % for Imb and less than or equal to 6 % for *N*-DM-Imb. The QC samples yielded an accuracy of 106 and 99 % for Imb and 93 and 105 % for *N*-DM-Imb for the low and high QCs, respectively, demonstrating that the method is accurate. Overall, these data suggest a high-performing PS-MS/MS method with good precision, accuracy, and linearity. One reason for this is that the blood and IS are mixed homogenously before spotting. Additionally, any blood sample lost in the cutting process is lost in approximately the same ratio as the IS which allows for highly reproducible and accurate results even if small portion of the sample is removed in the cutting process.

Qualifier ion abundance ratios are an additional step towards positive identification of an analyte in a complex matrix. A qualifier fragment ion intensity was measured along with a quantifier fragment for each analyte. The ratio of the qualifier and quantifier fragments was determined for each calibrator. For Imb, the ratio was between 17 and 20 %, and for *N*-DM-Imb, the ratio was between 19 and 25 %. The variation of both compounds was no greater than 20 % across all calibrators and QC samples, which suggests that these fragmentation processes can be used to positively identify the analytes in blood by PS-MS/MS.

When the internal standard was prespotted to the paper, the performance was similar compared with when the IS was mixed into the sample (Fig. 2b; ESM Fig. S2b). However, the calibrator RSDs of the prespotting method were a little greater: <18 % for Imb and <9 % for *N*-DM-Imb. This additional error was likely due to some of the

Table 1 Summary of figures of merit for the DBS devices investigated

	Device					
	W31 Internal standard	W31	FTA	TomTec	Novilytic	Velox
	Mixed in	Prespotted	Prespotted	Prespotted	Postspotted	Prespotted
Imatinib						
LOD (ng/mL)	5	5	5	2.5	60	10
RSD (%)	3	18	37	16	25	13
QC low accuracy (%)	106	111	79	105	100	108
QC high accuracy (%)	99	90	101	95	110	99
Linearity (R^2)	0.999	0.998	0.996	0.999	0.999	0.999
N-desmethyl-imatinib						
LOD (ng/mL)	6	6	6	6	100	25
RSD (%):	6	9	29	12	27	9
QC low accuracy (%)	93	105	86	89	83	100
QC high accuracy (%)	105	85	89	92	114	110
Linearity (R^2)	0.999	0.999	0.999	0.986	0.999	0.999

blood spot being cut off in sample analysis while the IS remained unchanged. The QC accuracy was still acceptable with 111 and 90 % for the low and high Imb QCs and 105 and 85 % for the low and high *N*-DM-Imb QCs. For one calibration curve, an additional high calibrator and QC were added to assess the linearity and accuracy at higher concentrations (ESM Fig. S3). The RSD of the replicates ($n = 6$) <19 % for Imb and <18 % for *N*-DM-Imb. The low, mid, and high QCs had accuracies of 89, 103, and 118 % for Imb and 85, 100, and 112 % for *N*-DM-Imb, respectively. These acceptable results demonstrate that a greater dynamic range can be used if clinically necessary.

The FTA card had the same LODs as W31, with 5 and 6 ng/mL for Imb and *N*-DM-Imb, respectively. The device also gave a linear response for both analytes (Fig. 2c; ESM Fig. S2c). However, the calibrator reproducibility with this collection device was poor—RSDs were between 9 and 37 % for the Imb calibrators and between 6 and 29 % for *N*-DM-Imb calibrators. The QCs were not as accurate either, 79 and 101 % for Imb QCs and 86 and 89 % for *N*-DM-Imb QCs. The poor reproducibility and accuracy were likely due to a number of factors. First, the full-scan spectra of blank blood showed a higher background signal (10^8 counts) for the FTA cards when compared with the other devices tested (Fig. 3). This background was significantly higher than that observed in other devices. The FTA card paper is also composed of a different material than the W31 paper, and the tip created with the FTA cards is more rounded and not as sharp as the tip made with W31 paper which can also negatively affect the spray quality [27]. Finally, similar to the W31 paper, the RSD was likely increased due to the IS prespotting method combined with sample loss from the cutting process.

The TomTec device was simple and easy to use. The LODs were similar to W31 paper, 2.5 ng/mL for Imb and 6 ng/mL for *N*-DM-Imb. Additionally, the TomTec method yielded curves with linear responses for both analytes (Fig. 2d; ESM Fig. S2d), and the calibrator reproducibility was acceptable with a RSD ≤16 % for Imb and ≤12 % for *N*-DM-Imb. Furthermore, the TomTec device demonstrated good accuracy—105 and 95 % for Imb QC low and high and 89 and 92 % for *N*-DM-Imb. Based on the slopes obtained from the calibration curves and the relative area of the signal, the sensitivity of the TomTec analysis matched that of the W31 analysis (Fig. 2b, c). This suggests that the extraction of the drug and transfer to the triangle paper placed underneath it was as efficient as the extraction of the drug using the traditional W31 PS methodology.

When analyzing plasma with the Noviplex device, the free drug is the only material being measured [28]. Whereas in whole blood analysis by PS, the free and protein-bound fractions contribute to the signal. This study found that, after filtration of the whole blood calibrators, the PS signal using the Noviplex device was linear (Fig. 2e; ESM Fig. S2e). However, this device had a higher LOD, 60 ng/mL for Imb and 100 ng/mL for *N*-DM-Imb, and a smaller slope by an order of magnitude (Fig. 2e; ESM Fig. S2e). The deviation of

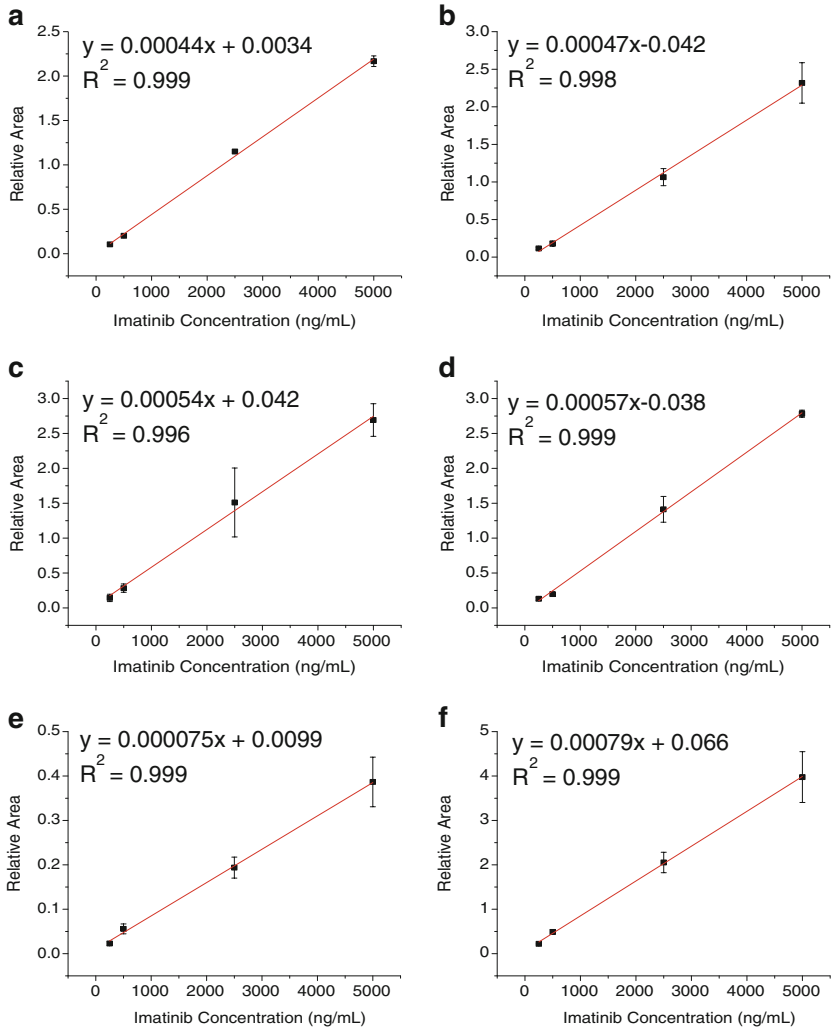

Fig. 2 **a** Imatinib calibration curves for W31 blood spot analysis when IS and blood are premixed, **b** W31 with prespotted IS, **c** FTA cards with prespotted IS, **d** TomTec cards with prespotted IS, **e** Noviplex cards with postspotted IS and **f** Velox cartridges with prespotted IS. Error bars equal 1 sigma ($n = 3$, Velox $n = 6$). The curves are not weighted and the origin is ignored. Fits and *R*-squared values are displayed in the plot

the LOD and sensitivity of the method, when compared with the W31 analysis, can be attributed to two main features of this methodology. First, a smaller sample volume was measured, 2.5 μL plasma versus 10 μL for whole blood. Second, only a fraction of the drug that was spiked into the whole blood calibrator samples was able to contribute to the MS signal. The QC values were accurate with 100 and 110 % for Imb low and high QCs and 83 and 114 % for *N*-DM-Imb QCs. However, the reproducibility of the Noviplex card was poor (between 11 and 25 % for Imb and 9 and 27 % for *N*-DM-Imb calibrators), likely due the addition of the internal standard after the plasma had been filtered, collected, and dried on the disk. As demonstrated earlier, the IS spiking study suggested that the reproducibility suffers when IS is added after the biofluid has been dried. The reproducibility could also be affected by variations in the plasma fraction or variation in the volume measured by the device. Future studies aimed at improving the reproducibility of this method may benefit from spiking the IS onto the plasma collection disk prior to the assembly of the filtration device. Furthermore, plasma Cals and QCs along with whole blood QCs should be utilized in future studies to determine whether the IS addition is the only source of error. Nonetheless, this method could benefit studies that require observation of unbound, available portion of drug in patient plasma and for studies that measure the rate

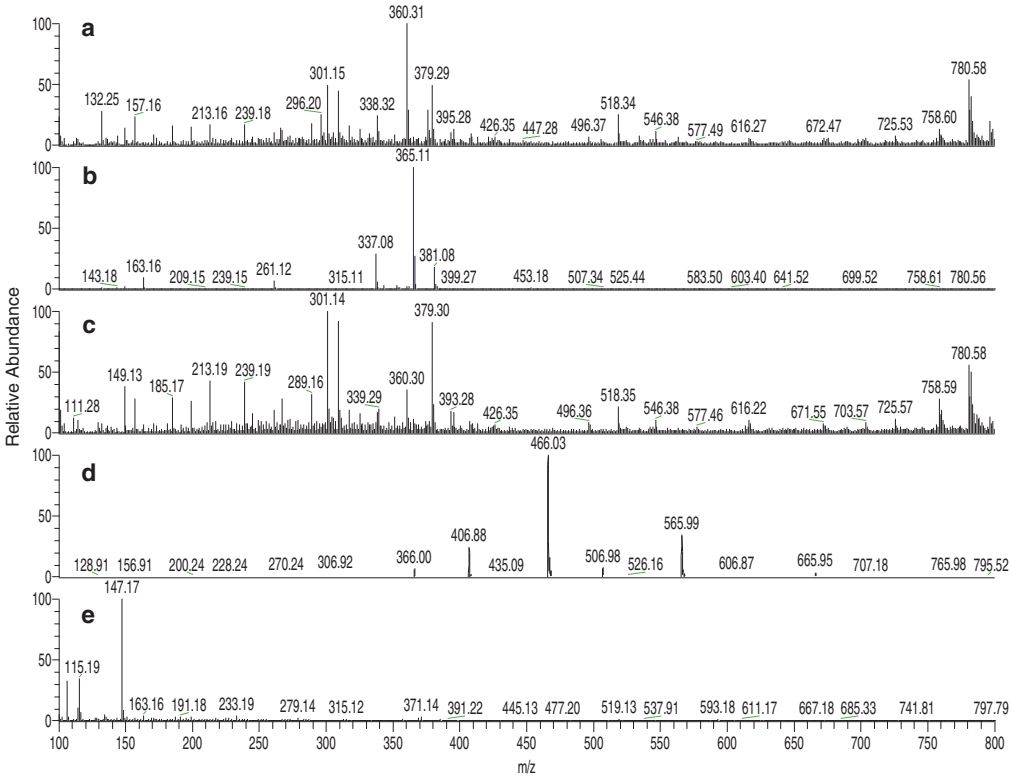

Fig. 3 Full scan spectra of human blank blood on **a** W31, **b** FTA cards, **c** TomTec cards, **d**, plasma from the Novilytic cards and **e** blood using the Velox cartridges. The absolute intensity of W31 is $3x10^6$, FTA is $1x10^8$, TomTec is $3x10^6$, Novilytic is 8 $x10^7$, and 8 $x10^6$ for the Velox

of drug release from the bound form to the unbound form.

The Velox sample cartridge (VSC) allows for automated PS analysis with the Velox 360 ion source, which is convenient to use for high-throughput analysis (ESM Fig. S4). The analytical results from the VSCs were very good, with LODs similar to those of obtained from manual PS, 10 ng/mL for Imb and 25 ng/mL for *N*-DM-Imb. The calibrators produced a linear response (Fig. 2f; ESM Fig. S2f) with Imb calibrators having an RSD <13 % and *N*-DM-Imb RSD of <9 %. The QCs were accurate with 108 and 99 % accuracy for both Imb low and high QCs, respectively, and 100 and 110 % for *N*-DM-Imb QCs. The higher performance of this device is likely a result of the use of laser cut paper rather than the manually cut paper; the later cutting consistently yields the same tip angle and size ensuring optimal ionization. Additionally, pre-cut paper enables the capture and analysis of the entire blood sample with no sample loss from cutting the spot out. The only two drawbacks of the VSCs were related to the cartridge itself. The VSCs are bulkier than other devices, and this must be taken into consideration in field studies. The VSC tip must also remain protected. If it is damaged, it is difficult to obtain stable spray ionization from the paper. Therefore, proper handling and storage is essential with this device. However, the analytical benefits of automated ionization outweigh the drawback of ensuring proper shipping and storage of the cartridges.

To analyze the effect that whole blood matrix has on the Imb signal, the IS signal with a whole blood sample was compared with the IS signal with a water sample. The average absolute intensity of the IS ($n = 3$) was measured for each sample matrices. For W31, FTA, TomTec, Noviyltic, and Velox, the whole blood signal is 9, 91, 30, 88, and 91 %, respectively, compared with the water sample. The lower overall signal for the IS in whole blood is caused by ion suppression and from recovering less sample due to the physical barriers on the paper from the matrix (e.g., dried cells). This, however, is not detrimental to the assay performance because recovery is sufficient and the internal standard normalizes the signal to yield high reproducibility.

For in-field collection of blood samples, a cheap, disposable, and accurate pipette must be used for devices that do not measure the sample volume. Fitting these criteria, SafeTec Microsafe® pipettes were used to measure the blood samples and proved to be as precise and accurate as a single-channel

pipette. QC samples pipetted onto W31 with these micropipettes had RSDs and percent errors comparable with QCs spotted with a single-channel pipette (ESM Table S2). Thus, these micropipettes are acceptable in field devices to collect small blood samples from finger pricks.

To verify this collection method and analysis, 20 patients' whole blood samples were collected on site in Vietnam using the SafeTec Microsafe® pipettes, transferred onto prespotted W31 paper, air dried for 2 h, and then stored under desiccant at room temperature until shipped to the laboratory. As with most drugs, imatinib has been shown to be stable in a DBS under these conditions [6]. The samples were analyzed by manual PS (n=3). Calibration curves were run the day of the clinical sample analysis (ESM Fig. S4), and the curve equation was used to calculate the concentration imatinib and the metabolite *N*-desmethyl-imatininb in each clinical sample (Table 2). The concentrations of the analytes were plotted over a 5-day period to show the blood concentration of Imb and its metabolite in patients throughout the dosing regimen (Fig. 4). Although the IS concentration was fairly consistent between the calibrators and QCs, error was still observed within the replicates of the same sample. The sample RSD was high (average RSD for Imb was 31 %) due to the error associated with manually cutting the paper to remove the DBS coupled with that of prespotting the IS.

An additional source of error was introduced from imprecise dispensing of blood onto the W31 paper. In the laboratory, a clean circle was made over the IS spot but, in the field, the sample was, at times, dispensed in an uneven shape missing part of the IS spot. For this reason, the in-field use of a device like the TomTec cards or the VSCs should reduce error in the future, since they capture the whole sample without introducing manual sources of error. Nonetheless, even with this error, the dosing trend and drug metabolism followed expected results as can clearly be seen in Fig. 4.

Conclusions

A variety of commercially available DBS devices can be used with PS-MS for the quantitation of drugs in human blood. The novel methods of coupling the collection devices to the PS source are easy to implement and optimize, allowing fast turn around and quick determination of figures of merit. In this study, all four devices and the W31 exhibited linear results. All but the Noviplex plasma device yielded the same slope for the calibration curve suggesting the same sensitivity across these devices and coupling strategies. In some cases, e.g., the FTA and Noviplex devices, reproducibility needs to be improved before it can be used in the field.

Table 2 Sample results from manual PS (n = 3)

Patient	Day	Imatinib		*N*-desmethyl-imatinib	
		Concentration (ng/mL)	RSD (%)	Concentration (ng/mL)	RSD (%)
TA005	1	1721	21	214	23
	2	3102	13	666	17
	3	3043	21	652	18
	4	2841	40	708	32
	5	5702	7	1086	6
XY001	1	593	19	90	29
	2	337	52	79	47
	3	1691	17	249	11
	4	915	40	150	32
	5	205[a]	37	64[a]	24
XY003	1	3583	37	374	41
	2	4653	72	1335	90
	3	5513	8	814	15
	4	4376	24	917	27
	5	4392	22	601	18
XY004	1	1145	36	115	38
	2	1672	59	540	62
	3	1462	29	393	26
	4	2020	48	444	50
	5	2259	27	373	20

[a] Values below the cutoff value

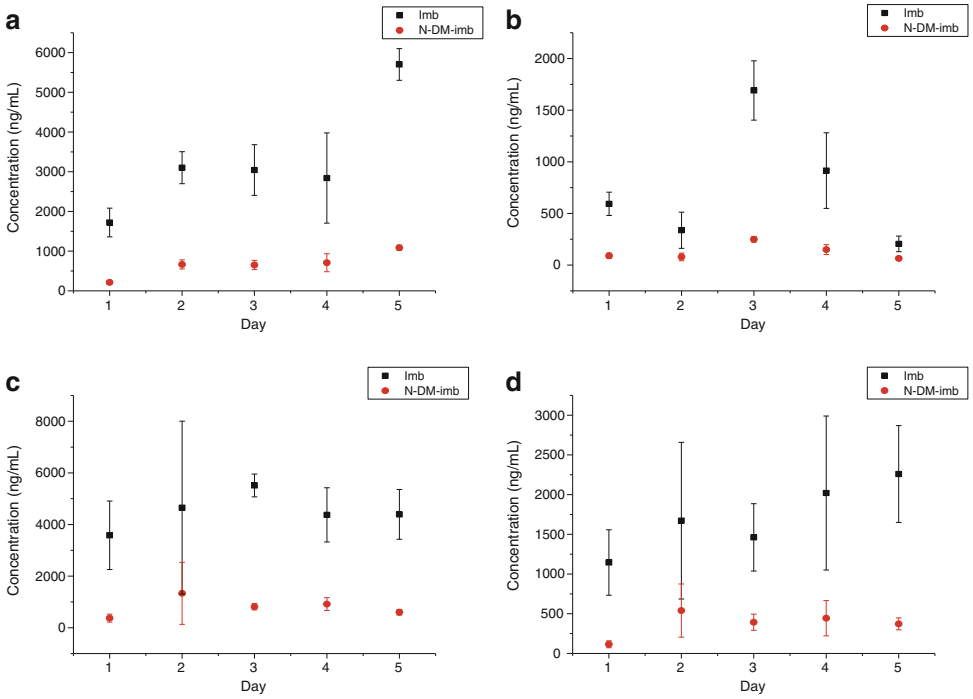

Fig. 4 Longitudinal depiction of drug concentration in patient samples ($n = 3$). Patient TA005 **a** received 600 mg dose, patient XY001 **b** received 400 mg dose, patient XY003 **c** received 400 mg dose and patient XY004 **d** received 400 mg dose. Error bars are 1 standard deviation

As it stands, the most successful devices allow material, such as IS, to be introduced onto the collection device before the addition of the biofluid. The reproducibility is best in devices that can collect and measure the whole sample with no need to tamper with the DBS, such as cutting it out. With the FTA cards and W31, error was introduced with imperfectly spotted DBSs and when cutting the spot from the whole device. On the other hand, the Velox and TomTec cards can capture the whole sample. Automation also improved the analysis; every Velox cartridge is laser cut in a precise shape preventing error introduced with manually cutting paper as required with other types of devices. In addition, the fact that analysis of the Velox cards is part of an automated system reduces human error. Automation would likely improve the PS method for the other DBS devices and should be investigated. However, W31 paper is reasonably priced, simple, and was effective both in the lab and during field studies, for manual PS-MS. In the future, error can be reduced with the field samples by collecting and analyzing the whole samples with a methodology that utilized an automated system.

Overall, drug concentrations present in human biofluids can effectively be quantified using PS ionization with commercially available DBS devices. This method enables more flexibility in the manner of sample collection and analysis which benefits a successful, low-cost clinical study.

Acknowledgments The authors thank Novilytic and TomTec for supplying the blood spot devices for the study. We acknowledge funding from the National Science Foundation (CHE-1307264), the National Institutes of Health (R01 GM24417-37), and the Purdue Center for Cancer Research.

Compliance with ethical standards

Conflict of interest All authors declare that they have no conflict of interest.

References

1. Wagner M, Tonoli D, Varesio E, Hopfgartner G. The use of mass spectrometry to analyze dried blood spots. Mass Spectrom Rev. 2016;35(3):361–438. doi:10.1002/mas.21441.
2. Li W, Tse FLS. Dried blood spot sampling in combination with LC-MS/MS for quantitative analysis of small molecules. Biomed Chromatogr. 2010;24(1):49–65. doi:10.1002/bmc.1367.
3. Wilhelm AJ, den Burger JCG, Swart EL. Therapeutic drug monitoring by dried blood spot: progress to date and future directions. Clin Pharmacokinet. 2014;53(11):961–73. doi:10.1007/s40262-014-0177-7.

4. Demirev PA. Dried blood spots: analysis and applications. Anal Chem. 2013;85(2):779–89. doi:10.1021/ac303205m.
5. Spooner N. A glowing future for dried blood spot sampling. Bioanalysis. 2010;2(8):1343–4.
6. Kralj E, Trontelj J, Paji T, Kristl A. Simultaneous measurement of imatinib, nilotinib and dasatinib in dried blood spot by ultra high performance liquid chromatography tandem mass spectrometry. J Chromatogr B. 2012;903:150–6. doi:10.1016/j.jchromb.2012.07.011.
7. De Kesel PM, Capiau S, Lambert WE. Current strategies for coping with hematocrit problem in dried blood spot analysis. Bioanalysis. 2014;6(14):1871–4.
8. Liu J, Wang H, Manicke NE, Lin J, Cooks RG, Ouyang Z. Development, characterization, and application of paper spray ionization. Anal Chem. 2010;82(6):2463–71.
9. Wang H, Liu J, Cooks RG, Ouyang Z. Paper spray for direct analysis of complex mixtures using mass spectrometry. Angew Chem Int Ed. 2010;49(5):877–80. doi:10.1002/anie.200906314.
10. Manicke NE, Yang Q, Wang H, Oradu S, Ouyang Z, Cooks RG. Assessment of paper spray ionization for quantitation of pharmaceuticals in blood spots. Int J Mass Spectrom. 2011;300(2-3):123–9. doi:10.1016/j.ijms.2010.06.037.
11. Liu J, Manicke NE, Cooks RG, Ouyang Z. Paper spray ionization for direct analysis of dried blood spots. In: Li W, Lee MS, editors. Dried blood spots: applications and techniques. Hoboken, NJ, USA: Wiley; 2014. doi:10.1002/9781118890837.ch23.
12. Ferreira CR, Yannell KE, Jarmusch AK, Pirro V, Ouyang Z, Cooks RG. Ambient ionization mass spectrometry for point-of-care diagnostics and other clinical measurements. Clin Chem. 2015;62(1):99–110. doi:10.1373/clinchem.2014.237164.
13. Manicke NE, Bills BJ, Zhang Z. Analysis of biofluids by paper spray MS: advances and challenges. Bioanalysis. 2016;8(6):589–606.
14. Kondrat RW, McClusky GA, Cooks RG. Multiple reaction monitoring in mass spectrometry/mass spectrometry for direct analysis of complex mixtures. Anal Chem. 1978;50(14):2017–21.
15. Roskar R, Trdan T (2012) Analytical Methods for Quantification of Drug Metabolites in Biological Samples. InTech. doi:10.5772/51676
16. Manicke NE, Belford M (2015) Separation of Opiate Isomers Using Electrospray Ionization and Paper Spray Coupled to High-Field Asymmetric Waveform Ion Mobility Spectrometry. J Am Soc Mass Spectrom. doi:10.1007/s13361-015-1096-z
17. Sukumar H, Stone JA, Nishiyama T, Yuan C, Eiceman GA. Paper spray ionization with ion mobility spectrometry at ambient pressure. Int J Ion Mobil Spectrom. 2011;14(2-3):51–9. doi:10.1007/s12127-011-0069-6.
18. Manicke NE, Abu-Rabie P, Spooner N, Ouyang Z, Cooks RG. Quantitative analysis of therapeutic drugs in dried blood spot samples by paper spray mass spectrometry: an avenue to therapeutic drug monitoring. J Am Soc Mass Spectrom. 2011;22(9):1501–7. doi:10.1007/s13361-011-0177-x.
19. Espy RD, Manicke NE, Ouyang Z, Cooks RG. Rapid analysis of whole blood by paper spray mass spectrometry for point-of-care therapeutic drug monitoring. Analyst. 2012;137(10):2344. doi:10.1039/c2an35082c.
20. Su Y, Wang H, Liu J, Wei P, Cooks RG, Ouyang Z. Quantitative paper spray mass spectrometry analysis of drugs of abuse. Analyst. 2013;138(16):4443. doi:10.1039/c3an00934c.
21. Espy RD, Teunissen SF, Manicke NE, Ren Y, Ouyang Z, van Asten A, et al. Paper spray and extraction spray mass spectrometry for the direct and simultaneous quantification of eight drugs of abuse in whole blood. Anal Chem. 2014;86(15):7712–8. doi:10.1021/ac5016408.
22. Takyi-Williams J, Dong X, Gong H, Wang Y, Jian W, Liu C-F, et al. Application of paper spray–MS in PK studies using sunitinib and benzethonium as model compounds. Bioanalysis. 2015;7(4):413–23. doi:10.4155/bio.14.288.
23. Shi R-Z, El Gierari ETM, Manicke NE, Faix JD. Rapid measurement of tacrolimus in whole blood by paper spray-tandem mass spectrometry (PS-MS/MS). Clin Chim Acta. 2015;441:99–104. doi:10.1016/j.cca.2014.12.022.
24. Cortes JE, Egorin MJ, Guilhot F, Molimard M, Mahon FX. Pharmacokinetic/pharmacodynamic correlation and blood-level testing in imatinib therapy for chronic myeloid leukemia. Leukemia. 2009;23(9):1537–44. doi:10.1038/leu.2009.88.
25. Gschwind HP. Metabolism and disposition of imatinib mesylate in healthy volunteers. Drug Metab Dispos. 2005;33(10):1503–12. doi:10.1124/dmd.105.004283.
26. Abu-Rabie P, Denniff P, Spooner N, Chowdhry BZ, Pullen FS. Investigation of different approaches to incorporating internal standard in DBS quantitative bioanalytical workflows and their effect on nullifying hematocrit-based assay bias. Anal Chem. 2015;87(9):4996–5003. doi:10.1021/acs.analchem.5b00908.
27. Cheng-Huang Lin W-CL, Chen H-K, Kuo T-Y. Paper spray-MS for bioanalysis. Bioanalysis. 2014;6(2):1–10.
28. Kim J-H, Woenker T, Adamec J, Regnier FE. Simple, miniaturized blood plasma extraction method. Anal Chem. 2013;85(23):11501–8. doi:10.1021/ac402735y.